Aus dem Institut für Tumorimmunologie

Direktor: Prof. Dr. Elke Pogge von Strandmann

des Fachbereichs Medizin der Philipps-Universität Marburg

Tumor-associated Natural Killer cells in ovarian cancer ascites: Molecular and functional characterization

Inaugural-Dissertation zur Erlangung des Doktorgrades der Naturwissenschaften

dem Fachbereich Medizin der Philipps-Universität Marburg

vorgelegt von

Nathalie Hoffmann

aus Köln

Marburg, 2020

Angenommen vom Fachbereich Medizin der Philipps-Universität Marburg am: 25.08.2020

Gedruckt mit Genehmigung des Fachbereichs Medizin

Dekan: Prof. Dr. Helmut Schäfer

Referent: Prof. Dr. Elke Pogge von Strandmann

Korreferent: Prof. Dr. Rolf Müller

Table of contents

Abstract

The high-grade serous carcinoma (HGSOC) is the most common ovarian cancer type that, due to late diagnosis, has the highest mortality rate of all gynecological cancers. One third of the patients develop a fluid in the peritoneal cavity called ascites. The ascites contains tumor and immune cells as well as soluble immunomodulatory factors such as cytokines.

NK cells - as a crucial part of the innate immune system - play a major role in tumor immune surveillance. Their effector function is tightly regulated by the balance between activating and inhibitory receptor signaling. However, NK cell function of many tumor patients is restricted and the overall results of NK cell-based immunotherapy are unsatisfying. This is often due to tumor-associated immune escape mechanisms.

One of the best characterized activating receptors of NK cells is NKG2D, which recognizes malignant cells and mediates tumor cell lysis. However, in various tumor entities, the NKG2D/NKG2D-Ligand (NKG2D-L) signaling axis is defective. Shedding of NKG2D-Ls from the surface of tumor cells to a soluble form is one such evasion strategy. The interference mechanisms of the ligands include (1) the downregulation of NKG2D and (2) passive blocking of NKG2D. Subsequently, this leads to dysfunctional NK cells and facilitated tumor growth. However, in mice, (3) they can also inhibit the NKG2D/NKG2D-L macrophage – NK cell crosstalk and thereby support NK cell-mediated tumor cell lysis. The relevance of this mechanism in humans is elusive.

In ovarian cancer ascites, soluble NKG2D-Ls are enriched and negatively correlate with the survival of the patients. Surprisingly, the expression of NKG2D on NK cells and T cells is not reduced. In this thesis, I could show that human macrophages did not express NKG2D excluding a direct interaction of NKG2D-Ls with macrophages. However, NKG2D-Ls were detectable on the surface of macrophages, but the killing of macrophages by NK cells was not NKG2D-dependent. This indicates that, in ovarian cancer, soluble NKG2D-Ls do not influence the NKG2D signaling through the mechanisms described so far in other models. Instead, I provided evidence that soluble NKG2D-Ls have an additional

function – namely the induction of NKG2D signaling and target gene expression upon engagement.

Furthermore, not much is known about the phenotype and differentiation of healthy NK cells to tumor-associated NK cells (TANKs) and in particular about signaling pathways that are involved. In this thesis, I showed that patient-derived NK cells depicted a mixed tumor-associated phenotype, in which NK cells displayed a strong downregulation of most of the activating receptors and an upregulation of the inhibitory receptors PD-1 and TIM-3, indicating a state of exhaustion. These NK cells showed impaired NK cell effector functions, which could be restored upon cytokine activation and blockage of the TGFβ signaling pathway. Moreover, TANKs showed a dysregulation of the natural killer cell-mediated cytotoxicity and the Hippo pathways. I established that proteins suppressed by the Hippo pathway, such as YAP1 and TEAD4, were exclusively expressed in TANKs, while they were absent in healthy donor NK cells. However, if healthy donor NK cells were stimulated with TGFβ, IL-2 and via CD16 crosslinking, expression of TEAD4 was induced. TEAD4-expressing NK cells showed a TEAD4-dependent upregulation of TIM-3. Finally, I provided first evidence that TEAD4-expressing NK cells could acquire a regulatory function, in which they were able to suppress T cell proliferation.

These findings shed more light on the role of NK cells in the tumor microenvironment (TME) of ovarian cancer patients. Based on that, further research will increase our knowledge of NK cell tumor surveillance, paving the way for strategies boosting anti-tumor NK cell functions.

Zusammenfassung

Das seröse Ovarialkarzinom (HGSOC) ist die häufigste Art von Eierstockkrebs, der aufgrund einer späten Diagnose die höchste Mortalitätsrate von allen gynäkologischen Krebserkrankungen aufweist. Ein Drittel der Patientinnen entwickeln eine Flüssigkeit im Peritonealraum, die Aszites genannt wird. Dieser Aszites enthält Tumor- und Immunzellen so wie lösliche, immunmodulierende Faktoren wie etwa Zytokine.

NK-Zellen – als wichtiger Teil des angeborenen Immunsystems – spielen eine wesentliche Rolle in der *tumor immune surveillance*. Ihre Effektorfunktion ist durch das Gleichgewicht zwischen aktivierenden und inhibierenden Rezeptorsignalen streng reguliert. Die NK-Zellfunktion von vielen Tumorpatientinnen ist eingeschränkt und die Ergebnisse von NK-Zell-basierten Immuntherapien sind bislang unbefriedigend. Dies liegt oftmals an Tumor-assoziierten Immunevasions-Mechanismen.

Einer der am besten charakterisierten aktivierenden Rezeptoren von NK-Zellen ist NKG2D, welcher maligne Zellen erkennt und die Tumorzell-Lyse vermittelt. Jedoch ist die NKG2D/NKG2D-Ligand (NKG2D-L)-Signalachse in vielen Tumorentitäten gestört. Das Abspalten („shedding“) von NKG2D-L von der Oberfläche der Tumorzellen zu einer löslichen Form ist eine solche Evasionsstrategie. Die Störungsmechanismen der Liganden beinhalten (1) die Runterregulation von NKG2D und (2) das passive Blockieren von NKG2D. In der Folge führt dies zu dysfunktionalen NK-Zellen und einem begünstigten Tumorwachstum. Allerdings können sie (3) in der Maus auch den NKG2D/NKG2D-L Makrophagen – NK-Zell *Crosstalk*s inhibieren und dadurch die NK-Zell-vermittelte Tumorzell-Lyse fördern. Die Relevanz dieses Mechanismus im Menschen ist bisher unerforscht.

Im Ovarialkarzinom-Aszites sind lösliche NKG2D-L angereichert und korrelieren negativ mit dem Überleben der Patientinnen. Erstaunlicherweise ist die Expression von NKG2D auf NK-Zellen und T-Zellen nicht reduziert. In dieser Dissertation konnte ich zeigen, dass Makrophagen kein NKG2D exprimieren und somit nicht direkt mit löslichen NKG2D-L interagieren. Des Weiteren war die Lyse

von Makrophagen durch NK-Zellen nicht NKG2D-abhängig. Dies weist darauf hin, dass im Ovarialkarzinom die löslichen NKG2D-L die NKG2D-Signalvermittlung nicht durch Mechanismen beeinflussen, die bereits in anderen Modellen beschrieben wurden. Stattdessen konnte ich eine weitere, neue Funktion von löslichen NKG2D-L beschreiben, nämlich die Induktion der NKG2D-Signalvermittlung und damit die Expression von Zielgenen nach ihrer Bindung.

Des Weiteren ist der Phänotyp und die Differenzierung zu Tumor-assoziierten NK-Zellen (TANKs) und insbesondere die involvierten Signalwege noch unvollständig untersucht. In dieser Dissertation konnte ich zeigen, dass NK-Zellen von Patientinnen einen gemischten, Tumor-assoziierten Phänotyp aufwiesen. Bei diesem zeigten die NK-Zellen eine starke Runterregulation der meisten aktivierenden Rezeptoren, sowie eine Hochregulation von PD-1 und TIM-3, was auf einen anergen Status der NK-Zellen hinweist. Diese NK-Zellen zeigten gestörte NK-Zell-Effektorfunktionen, die durch eine Zytokinaktivierung und die Blockierung der TGFβ-Signalvermittlung wiederhergestellt werden konnten. Darüber hinaus zeigten TANKs eine Dysregulation des *kegg pathway*s *natural killer cell-mediated cytotoxicity* und des *Hippo pathway*s. Proteine, die durch den *Hippo pathway* reprimiert werden, wie beispielsweise YAP1 und TEAD4, waren ausschließlich in TANKs exprimiert, während sie in gesunden NK-Zellen nicht nachweisbar waren. Wurden jedoch gesunde NK-Zellen mit TGFβ, IL-2 und durch CD16-*crosslinking* stimuliert, so wurde die TEAD4-Expression induziert. TEAD4-exprimierende NK-Zellen zeigten eine TEAD4-abhängige Hochregulation von TIM-3. Schließlich konnte ich erste Hinweise erbringen, dass TEAD4-exprimierende NK-Zellen eine regulatorische Funktion erlangen können, durch welche sie in der Lage sind, die Proliferation von T-Zellen zu unterdrücken.

Diese Erkenntnisse werfen mehr Licht auf die Rolle von NK-Zellen in der Tumor-Mikroumgebung (*tumor microenvironment*, TME) von Ovarialkarzinom-Patientinnen. Darauf basierend wird weitere Forschung unser Wissen über NK-Zell *tumor surveillance* vergrößern, was den Weg für Strategien, die anti-tumoröse NK-Zell-Funktionen zu verstärken, ebnet.

1 Introduction

The immune system is a powerful tool to control and eliminate tumors. However, in many cancers, the immune system is affected in multiple ways leading to impaired immune surveillance [71]. One of those cancers is ovarian cancer [232]. Therefore, it is essential to understand the molecular and phenotypical changes of the tumor microenvironment in ovarian cancer to improve immunotherapy options and the outcome of the patients.

1.1 Natural Killer cells recognize and eliminate malignant cells

Natural Killer (NK) cells are lymphocytes belonging to the innate immune system. They are classically identified by the expression of the surface markers CD56 and the lack of CD3 expression. They can further be classified into two subsets: $CD56_{bright}$ and $CD56_{dim}$ NK cells. While the $CD56_{dim}$ NK cells express high levels of CD16 and moderate levels of CD56, $CD56_{bright}$ NK cells express low amounts of CD16 and high amounts of CD56. In the peripheral blood of healthy individuals, 90 % of the NK cells are $CD56_{dim}$ NK cells and the remaining 10 % are $CD56_{bright}$ NK cells [51]. $CD56_{bright}$ NK cells are predominantly found within the lymph nodes, produce higher amounts of cytokines, such as interferon gamma (IFNγ) and tumor necrosis factor alpha (TNFα), and represent a more immature status of the NK cells. Conversely, $CD56_{dim}$ NK cells produce low amounts of cytokines but exhibit a higher cytotoxic potential [51] [219].

As part of the innate immune system, NK cells are able to recognize and kill virus-infected or malignant cells. Upon activation, NK cells release cytotoxic granules filled with perforin and granzyme. Perforin integrates into the membrane of the target cells where it forms pores, through which granzymes, belonging to the serine proteases, can enter. Here, granzymes induce the apoptosis of the cell by activation of caspases and the pro-apoptotic BH3-interacting domain death agonist (BID) [3] [193].

Embedded in the membrane of the cytotoxic granules is the lysosomal-associated membrane protein-1 (LAMP-1 or CD107a). CD107a can be detected on the surface of NK cells upon fusion of the cytotoxic granules with the plasma

membrane. A higher expression of CD107a on the surface of NK cells positively correlates with the release of cytokines and the lysis of the target cell. Therefore, CD107a expression can be used as a marker for the cytotoxic activity of NK cells [2] [4].

Moreover, NK cells also kill target cells through the initiation of the extrinsic apoptosis pathway induced by the death ligands TNF-related apoptosis-inducing ligand (TRAIL), CD95L (Fas ligand) or TNFα [104] [130] [152] [243].

1.1.1 Activating and inhibitory receptors of NK cells regulate NK cell function

As NK cells possess a high cytotoxic potential, their regulation needs to be tightly controlled. Therefore, they express a variety of receptors, so-called activating receptors and inhibitory receptors (Introductory Fig. 1). The balance between those receptors is crucial for the activation of the cell and is necessary to distinguish between healthy cells (“self”), virus-infected cells (“missing self”) or malignant cells (“induced-self”).

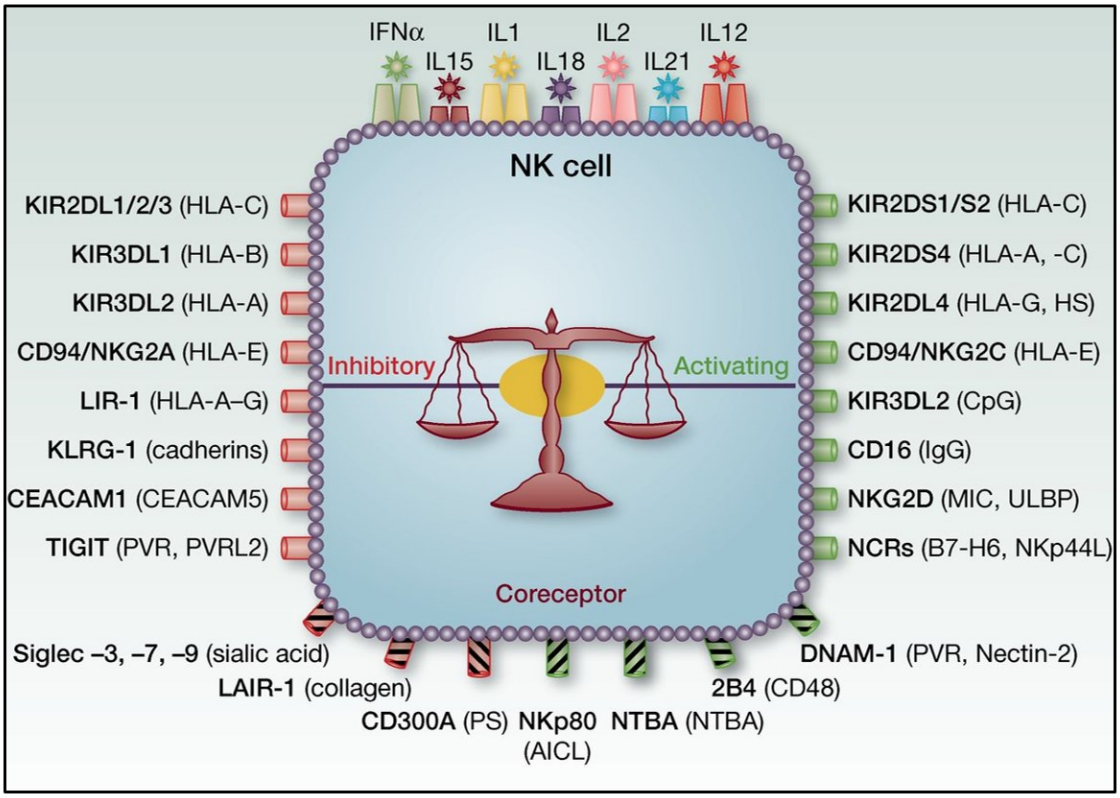

Introductory Fig. 1 (modified from Leung, 2014 [122]): NK cell receptors and their ligands.

Shown are numerous activating (depicted in green) and inhibitory receptors (illustrated in red) expressed on NK cells, as well as cytokine receptors (displayed on the top). Co-receptors are marked with stripes. Ligands of the receptors are shown in brackets.

If the NK cell encounters a healthy cell, the inhibitory receptors will recognize the major histocompatibility complex (MHC) class I molecules expressed on the surface of the healthy cell and an inhibitory signal will be sent to the NK cell, protecting the healthy cell from NK cell-mediated lysis [155] [241].

If the cell is transformed or infected by a virus, MHC class I molecules are downregulated to escape recognition by cytotoxic T cells (CTLs) [31] [170]. However, now NK cells are no longer inhibited by the inhibitory signal of their receptors and solely the activating receptor signal is transmitted. Hence, the NK cell is activated, leading to the lysis of the malignant cell [103]. This phenomenon is called the “missing-self” hypothesis [134].

In addition, if a cell is stressed, activating ligands are upregulated. Hence, the signal of the activating receptor outweighs the inhibitory receptor signal, the NK cell is activated and the target cell is killed – known as the “stress-induced self” hypothesis [39] [220].

Summing up, the NK cell effector function is tightly controlled by the balance between activating and inhibitory receptor signaling.

1.1.1.1 The CD94/NKG2 family modulates NK cell functions

The NK group 2 member (NKG2) family mainly consists of activating receptors but also contains inhibitory receptors. They belong to the C-type lectin-like receptor superfamily and most of the family members (NKG2-A, -B, -C, -E and -H) build disulfide-linked heterodimers with CD94 [16] [22] [116]. They bind the non-classical MHC class I molecule human leukocyte antigen (HLA)-E in humans [20] [25].

NKG2A and NKG2B are inhibitory receptors that are transcribed by the same gene but are alternatively spliced. Furthermore, they contain two immunoreceptor tyrosine-based inhibitory motifs (ITIM) in their cytoplasmic domains [26] [37]. It has been revealed that NKG2A is upregulated on the plasma-membrane of breast cancer patient-derived NK cells, which correlated with a reduced NK cell cytotoxicity [139].

NKG2C, NKG2E, and NKG2H lack the ITIM, but instead have a positively charged residue in their transmembrane domain, which can bind to the immunoreceptor tyrosine-based activating motif (ITAM) of the adaptor protein DNAX-activation protein (DAP) 12. NKG2E and NKG2H are alternatively spliced variants of the same gene. NKG2C, NKG2E, and NKG2H are all described to be activating receptors [16] [114] [215].

One of the most studied activating receptors recognizing malignant cells is NKG2D [10]. NKG2D is expressed on NK cells, all $CD8^+$ T cells and some γδ T cells, NKT cells and $CD4^+$ T cells [179]. Moreover, it does not associate with CD94 [233].

NKG2D forms a homodimer and associates with the adaptor molecule DAP10 in humans and DAP10 and DAP12 in mice [77] [233]. Upon engagement with its ligands, NKG2D recruits DAP10, which contains an Src Homology 2 (SH2) domain-binding site. This then leads to an activation of the phosphatidylinositol-4,5-bisphosphate 3-kinase (PI3K)/Akt signaling cascade triggering cytokine release and killing of the target cell [179] [233].

In humans, eight NKG2D ligands (NKG2D-Ls) exist, which belong to the major histocompatibility complex class I-related chain (MIC) A/B [10] or to the UL16 binding protein (ULBP1-6) family [40] [52] [61] [62]. Those families are MHC class I related glycoproteins. The NKG2D-Ls bind with different avidities to the receptor, but nothing is known about the distinct role of each ligand so far [150] [179]. In mice, NKG2D binds to retinoic acid early inducible gene 1 (Rae-1) proteins (Rae1α, β, γ, δ, ε) [38], members of the histocompatibility 60 (H60) protein family (H60a, b, c) [59] and murine UL16 binding protein-like transcript (MULT-1) [35] [41].

In order to escape immune recognition, malignant cells are able to shed their NKG2D-Ls from the surface via metalloproteases [46] [187] [222] or release them via exosomes [7] [46] [68]. These soluble ligands can bind to NKG2D, induce the internalization of NKG2D and hence impair NK cell function [80] [202]. Elevated levels of soluble NKG2D-Ls are detectable in various tumor entities, resulting in diminished cytotoxicity of NK cells [100] [141] [188]. High levels of soluble NKG2D-Ls were also measured in the ascites of ovarian cancer patients, but the expression of NKG2D was not diminished on patient-derived NK cells [221]. Moreover, the function of NKG2D-Ls on exosomes is still controversially discussed. It is hypothesized that their function rather depends on the type of exosome-releasing cell. While tumor cell-derived exosomes can inhibit the NK cell function, exosomes released by dendritic cells (DCs) can activate NK cells [50] [136] [217].

Finally, to escape immune surveillance, tumor cells can remodel the tumor microenvironment (TME) via the NKG2D/NKG2D-L axis. In mice, Qian *et al.* showed that RAE1ε-expressing tumor cells induce the generation of myeloid-derived suppressor cells (MDSCs) via NKG2D. Those MDSCs secrete IL-10, suppress $CD8^+$ T cell proliferation and thereby promote tumor growth [177].

1.1.1.2 Natural cytotoxicity receptors (NCRs) – an important family for tumor immune surveillance

Another prominent family of NK cell receptors are the NCRs, which are mainly activating receptors and comprises three family members – natural killer cell protein 30 (NKp30), NKp44 and NKp46 [166] [199] [218]. In acute myeloid leukemia (AML) it was shown that NCRs are downregulated resulting in a weak cytotoxic activity of NK cells [53].

NKp30 binds to several ligands, one of them is B7-H6, which is the only known transmembrane protein among them [24]. An intracellular ligand is BCL2-associated athanogene 6 (BAG6) [173], which can be secreted in a soluble form or associated with extracellular vesicles (EVs). When BAG6 is secreted in a soluble form, it exhibits an inhibitory function, while it has an activating function when BAG6 is EV-associated [184] [197]. Another soluble ligand for NKp30, which inhibits NK cell function, is Galectin-3 [226]. Furthermore, NKp30 has three splice variants – NKp30a, b, and c. NKp30a and b are immunostimulatory isoforms, while NKp30c displays an immunosuppressive isoform [57].

NKp44 binds to the activating ligand NKp44L, an isoform of mixed lineage leukemia 5 (MLL5) protein, expressed on the surface of transformed cells [11], and to the inhibitory ligand proliferating cell nuclear antigen (PCNA) [186].

Moreover, NKp46 binds to vimentin, expressed on the surface of mycobacterium tuberculosis-infected human monocytes or activated $CD4^+$ T cells [47] [75]. NKp46 is selectively expressed on NK cells, making it a good marker for NK cells [72] [168].

Finally, all NCRs bind to heparan sulfate on malignant cells [89].

1.1.1.3 The killer cell immunoglobulin-like receptor (KIR) family has diverse functions in NK cell regulation

KIRs are transmembrane glycoproteins, which are expressed by NK cells and a subset of T cells. The KIR family consists of 14 highly polymorphic genes and the receptors can transmit either activating or inhibitory signals. Activating KIRs have a short cytoplasmic domain, which associates with DAP12 to transfer an activating signal. Conversely, all inhibitory KIRs have a long cytoplasmic domain, which contains an ITIM needed to transmit the inhibitory signal. Examples of activating receptors are KIR2DL4 (CD158d), KIR2DS1 (CD158h) and KIR2DS2 (CD158j), and inhibitory receptors are KIR2DL1 (CD158a), KIR2DL2 (CD158b1), KIR2DL3 (CD158b2) and KIR3DL1 (CD158e1). The ligands of KIRs are MHC class I molecules (Table 1) [34] [74]. However, the avidity of inhibitory KIRs is higher than the avidity of activating KIRs [34] [206].

Table 1: KIRs and their ligands.

KIRs	HLA ligands	Signaling
KIR2DL1	HLA-C2	Inhibitory
KIR2DL2	HLA-C1	Inhibitory
KIR2DL3	HLA-C1	Inhibitory
KIR2DL4	HLA-G	Activating
KIR2DS1	HLA-C2	Activating
KIR2DS2	HLA-C1	Activating
KIR3DL1	HLA-Bw4	Inhibitory

1.1.1.4 Other receptors involved in modulating NK cell activity

One of the most important activating receptors on NK cells is CD16, the low affinity Fc receptor FcγRIII, which is responsible for the antibody-dependent cell-mediated cytotoxicity (ADCC) response of NK cells. Here, the Fc part of the immunoglobulin G (IgG) binds to CD16 triggering the cytotoxic response of NK cells [227]. It was shown that CD16 is strongly downregulated on NK cells of ovarian cancer patients, thus preventing a strong NK cell-mediated anti-tumor response [221].

DNAX Accessory Molecule-1 (DNAM-1; also called CD226) is an activating receptor of human NK cells, belonging to the Ig superfamily [115]. It is also expressed by a subset of B cells, monocytes, T cells and platelets [195]. DNAM-1 binds to polio virus receptor (PVR) (also called CD155) and nectin-2 (also known as CD112). Upon engagement of DNAM-1 with its ligands, NK cells are activated, leading to the killing of the target cell and a release of cytokines such as IFNγ [23] [209]. PVR and nectin-2 are frequently overexpressed on tumor cells, such as lung adenocarcinoma [157], colorectal carcinoma [143], pancreatic cancer [161] or melanoma [18] and correlate with tumor progression and a poor prognosis [18] [157] [162]. However, in AML, PVR and nectin-2 are downregulated in order to escape recognition by NK cells showing that the tumor-associated NK cells (TANKs) are shaped by the TME [105]. Moreover, it was observed that DNAM-1 is downregulated on patient-derived NK cells in ovarian cancer [36], myeloma [63] and breast cancer [139].

T cell immunoglobulin and ITIM domain (TIGIT), an immunosuppressive receptor, is expressed by T cells, T regulatory cells (T_{regs}) and NK cells and just like DNAM-1 it binds to PVR and nectin-2. Engagement of PVR on DCs with TIGIT-expressing T cells leads to a release of interleukin 10 (IL-10) and a decreased secretion of proinflammatory cytokines. Furthermore, the ITIM of TIGIT is important for the inhibition of NK cell-mediated cytotoxicity [131] [204] [242]. Besides the inhibition of T cells by DC-released IL-10, TIGIT can also directly inhibit the T cell's function via cell-intrinsic signaling [102]. TIGIT binds PVR with much higher affinity than DNAM-1 and thus outcompetes DNAM-1 [5]. Moreover,

TIGIT can directly interact with DNAM-1 in *cis* and prohibits the homodimerization of DNAM-1 and its function [101]. TIGIT is upregulated on tumor patient-derived T cells and NK cells, leading to an exhaustion of the cells and tumor progression. Blockage of TIGIT seems to be a promising therapeutic option to restore the cytotoxic function of the immune cells [44] [247].

2B4 was initially described as an activating receptor of NK cells in human and mice, but it is also expressed on a subset of $CD8^+$ T cells, γδ T cells, monocytes, basophils and eosinophils [162]. 2B4 is activated by the engagement with CD48, which is broadly expressed on hematopoietic cells [27]. In IL-2-activated NK cells, it can signal on its own, but it can also support the signaling of other activating receptors, such as the NKp46, NKG2D and DNAM-1, as a co-stimulatory receptor [30] [49] [200]. However, it was also described, that 2B4 can act as a negative regulator of murine NK cells, through binding of non–major histocompatibility complexes [118].

Taken together, NK cells express a variety of activating and inhibitory receptors and their signaling is altered in different tumor entities. In order to escape immune recognition, tumor cells shed activating ligands form their surface. Moreover, activating receptors on tumor-associated NK cells are downregulated, while inhibitory receptors are upregulated.

1.1.2 The exhaustion phenotype of NK cells

Exhaustion is a state of immune cells, in which their effector function is dampened and inhibitory receptors are expressed. This leads to a diminished recognition of virus-infected and malignant cells [230]. In NK cells, activating receptors, such as NKG2D, DNAM-1, CD16 and the NCRs are downregulated and inhibitory receptors, such as programmed death receptor 1 (PD-1), NKG2A and T cell immunoglobulin- and mucin-domain-containing molecule-3 (TIM-3) are upregulated [13] [17] [19].

Expression of PD-1 is associated with low cytokine production, diminished degranulation and reduced proliferation in response to cytokines [13] [167]. Blockage of PD-1 enhances NK cell effector function [17].

As a sign of exhaustion, NKG2A expression was increased on NK cells from hepatocellular carcinoma patients and was associated with a poor prognosis [208].

Moreover, TIM-3 was expressed on NK cells of lung adenocarcinoma patients leading to a poor prognosis of the patients and a blockage of TIM-3 could increase NK cell functions [235].

Summing up, PD-1 and TIM-3 expression on NK cells mark a state of exhaustion, in which the NK cell effector function is impaired and patients displaying exhausted NK cells have a poor prognosis.

1.2 Characteristics of ovarian cancer: Incidence, genetic landscape and treatment

Ovarian cancer has the highest mortality rate of all gynecological cancers worldwide [98] [121]. Every seventh reported cancer case in women is epithelial ovarian cancer (EOC) with a 5-year survival rate of 46 % due to the late diagnosis. Since the course of EOC is mainly asymptomatic, it is diagnosed at an advanced stage in 75 % of the cases [124]. The median age of patients at the diagnosis is 63 years [97].

Depending on their histology, EOC can be subdivided into high-grade serous ovarian cancer (HGSOC), endometrioid ovarian cancer, clear-cell ovarian cancer, low-grade serous ovarian cancer and mucinous ovarian cancer [78].

HGSOC is the most common type of EOC (75 % of the cases) and over 90 % of the patients have a gain-of-function mutation in *TP53*. Furthermore, 15-20 % of the HGSOC patients have a germline mutation of *BRCA1* or *BRCA2*. HGSOC is further characterized by chromosomal instability, *e.g.* insertion and deletion mutations. Homologous recombination is defective in half of the cases [15] [124].

The first-line treatment of HGSOC is the removal of the tumor by primary debulking surgery, followed by platinum-based chemotherapy [169]. However, over time the tumor cells eventually develop a resistance against platinum leading to a relapse in most of the patients. Loss of function of the tumor suppressor

genes *RB1, NF1, RAD51B,* and *PTEN* play a role during the acquisition of chemoresistance, and *CCNE1* amplification contributes to primary resistance and refractory disease progression [165]. Furthermore, homologous recombination is also responsible for platinum-sensitivity in HGSOC [124]. In the SOLO1 trial, patients receiving olaparib, a poly (ADP-ribose) polymerase inhibitor, had a 70 % lower risk of disease progression or death in comparison to the placebo group. Here, patients carrying a BRCA mutation with platinum-sensitive, advanced HGSOC were included in the study [154]. Therefore, in 2018, olaparib was approved by the US Food and Drug Administration (FDA) for the maintenance treatment of patients carrying the BRCA mutations [124]. Conversely, if the cells are resistant to platinum, patients are treated with cytotoxic drugs like gemcitabine, paclitaxel, topotecan or PEGylated lyposomal doxorubicin, but the response rate is low (10-30 %) [140]. Therefore, more trials are run to develop new drugs that overcome resistance. In a phase 3 trial (AURELIA) it was reported that chemotherapy in combination with bevacizumab (an angiogenesis inhibitor, targeting vascular endothelial growth factor (VEGF)) treatment could increase the progression-free survival of the patients [176].

1.2.1 Ascites of ovarian cancer patients have a unique tumor microenvironment

EOC is characterized by rapid growth, spreading into the intraperitoneal site and by an accumulation of an effusion, called ascites, in the peritoneal cavity. The ascites creates a unique tumor-supportive microenvironment, which consists of soluble and cellular components [107] [174] [232] (Introductory Fig. 2).

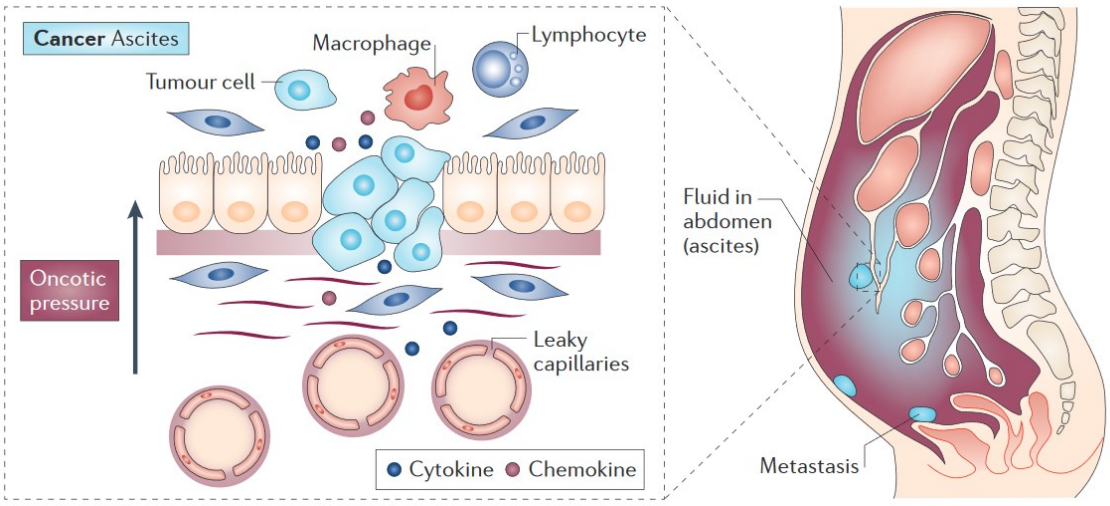

Introductory Fig. 2 (modified from Kipps *et al.*, 2013 [108]): Composition of ovarian cancer ascites.

The ascites is a malignant fluid in the peritoneal cavity of ovarian cancer patients. It consists of soluble factors, such as cytokines and chemokines, and of different cell types, such as tumor cells, stroma cells, and immune cells.

1.2.1.1 Soluble factors in the tumor microenvironment of ovarian cancer

Soluble factors in ascites are cytokines, chemokines, metabolites, proteins, and exosomes [107].

Significantly elevated levels of the pro-tumorigenic cytokines and chemokines IL-6, IL-8, IL-10, macrophage inflammatory protein 1 beta (MIP-1β), C-X-C motif chemokine ligand 10 (CXCL10), CC-chemokine ligand 2 (CCL2), and VEGF were found, while the pro-inflammatory cytokines IL-2, IL-5, IL-7, and IL-17 were reduced [107]. IL-6 and IL-10 levels have been reported to correlate with a poor prognosis [112] [180]. Furthermore, VEGF expression correlates with a poor prognosis due to increased metastasis [189] [244]. In addition, VEGF promotes the accumulation of ascites [32]. Moreover, high levels of the immune-suppressive cytokine transforming growth factor beta 1 (TGFβ1) are associated with reduced relapse-free survival (RFS) [181]. TGFβ induces the expression of VEGF in tumor-associated NK cells and thereby remodels the TME [28].

Regarding metabolites, changes in the levels of fatty acids, cholesterol, ceramide, glycerol-3-phosphate, glucose, and glucose-3-phosphate were found. For example, 2-hydroxyisovalerate was reduced, while glucose-1-phosphate was increased [107]. Furthermore, levels of lysophosphatidic acid (LPA) are elevated and correlate with short RFS [182].

In proteomic studies, Finkernagel *et al.* identified 779 proteins in the ascites, which clustered into groups associated with metastasis and a short RFS (*e.g.* HSPA1A, BCAM, and DKK1), or with immune regulation and a favorable RFS (*e.g.* the protein kinase LCK). Interestingly, most of the proteins that strongly associated with the clinical outcome of the patients are components of EVs [70].

EVs are small particles, which consist of nucleic acids, proteins, and lipids. Exosomes are a special form of EVs, which are released by the fusion of multivesicular bodies with the plasma membrane. EVs can transmit miRNAs, which can influence the outcome of the patients [174]. Au Yeung *et al.* showed that EV-associated miR-21 transmits chemoresistance to ovarian cancer cells. Here, cancer-associated adipocytes and fibroblasts release miR-21 containing EVs which are taken up by ovarian cancer cells, in which miR-21 binds to apoptotic peptidase activating factor 1 (APAF1) and thereby suppresses apoptosis [8]. Moreover, miR-506 is associated with a good prognosis, while miR-433 mediates paclitaxel resistance [228] [238].

1.2.1.2 Cellular components of the ovarian cancer microenvironment

Ascites contains tumor cells and heterogeneous stromal cells. The stromal cells consist of endothelial or mesothelial cells, fibroblasts, adipocytes, bone marrow-derived stem cells, adipose tissue-derived stromal cells, and immune cells [107].

Tumor cells are either present as single cells or as multicellular aggregates, known as spheroids. It is proposed, that tumor spheroids are less susceptible to chemotherapy in comparison to single cells [196].

The TME contains various types of immune cells, including effector cells like $CD4^+$ and $CD8^+$ T cells, and NK cells. However, the effector cells are inhibited by tumor cells, but also by immune-suppressive T_{regs}, MDSCs, immature DCs and tumor-associated macrophages (TAMs) by secretion of immune-suppressive chemokines and cytokines [232]. The presence of high numbers of $CD3^+$ intratumoral T cells correlates with an improved clinical outcome of the patients [246], while high numbers of T_{regs} are associated with reduced survival [54]. Furthermore, a high $CD8^+$/ forkhead box P3 $(FoxP3)^+$ ratio was associated with an enhanced disease-specific survival [119].

Taken together, the composition of the TME plays a critical role in tumor progression and is crucial for the prognosis of the patients. Therefore, it is important to investigate the function of immune cells in the TME.

1.2.2 Therapeutic potential of NK cells in HGSOC

It was observed, that high numbers of NK cells in ascites of HGSOC lead to increased overall survival [90]. However, NK cells from HGSOC patients are dysfunctional. They show a reduced proliferation potential, diminished cytotoxic capacity and a decreased cytokine production, which is a result of secreted factors by the tumor cells and the TME [159]. For example, overexpression of TGFβ can suppress CD16-mediated IFNγ production [213]. Moreover, together with IL-10, it inhibits the cytotoxic capacity and cytokine release of NK cells through downregulation of activating receptors, such as 2B4, NKp30 and DNAM-1 [36] [83] [159]. Macrophage migration inhibitory factor (MIF) has been shown to negatively correlate with the RFS [221] and it leads to a downregulation of NKG2D [111].

In order to restore NK cell function, various therapeutical options are being tested. The first option is to boost the effector function of NK cells by treatment with cytokines. As one example, the effect of IL-15 is elucidated in the clinic. IL-15 is less toxic than IL-2, but the dose required shows severe side effects. Therefore, IL-15 “superagonists” are developed, which exhibit an increased *in vivo* half-life and reduced toxicity [81] [159]. An example of an IL-15 “superagonist” is ALT-803, which has been shown to increase the degranulation and IFNγ release of NK cells [66] [92]. The use of ALT-803 is currently tested in clinical trials [185].

Furthermore, checkpoint inhibitors, such as anti-PD-1, are used to restore not only T cell function but also NK cell function [159]. Nevertheless, the outcome was disappointing so far, since only 11-24 % of the patients responded to the treatment [64]. Clinical trials are currently testing the combined treatment of anti-PD-1 with anti-NKG2A (monalizumab) antibody, anti-KIR2D antibody (lirilumab) or anti-TIGIT (BMS-986207) antibody. The idea behind this co-treatment is to restore the effector functions of NK cells and T cells [6] [159] [201].

Finally, adoptive NK cell transfer is investigated as a treatment option. For this, modified cell lines, such as NK92, or NK cells from third-party donors that have been expanded *ex vivo* can be used. Moreover, the use of engineered NK cells, so-called chimeric antigen receptor (CAR)-NK cells, are currently evaluated. Like

CAR-T cells, they can target a specific antigen, but they show a lower risk of long-term toxicity and autoimmunity, probably due to the relatively short lifespan of CAR-NK cells. Moreover, they should not cause graft-versus-host disease (GVHD) [159] [148]. Currently, CAR-NK cells are analyzed targeting CD24 (a stem-cell marker) [109] and mesothelin (the receptor for CA-125) [126]. CA-125 seems a promising target since it is overexpressed in over 80 % of ovarian cancer patients [95].

Conclusively, NK cells are able to recognize and kill malignant cells. However, their effector function in various cancers is impaired. Therefore, different approaches to restore the NK cell effector functions are tested in the clinic, such as activation with cytokines, usage of checkpoint inhibitors (*e.g.* anti-PD-1) or adoptive NK cell transfer. Nevertheless, the results are still disappointing. Thus, the medical need to detect novel mechanisms to reactivate NK cells is strong.

1.3 The Hippo pathway and its role in cancer

In ovarian cancer, many pathways are dysregulated and one of them is the Hippo pathway [97] [205] [250]. This thesis provides evidence that components of the Hippo pathway are dysregulated in tumor-associated NK cells of ovarian cancer patients, but their functions are potentially Hippo-independent.

The Hippo pathway is responsible for the control of organ size, but its dysregulation also plays a role in tumor development [60]. It is dysregulated at high frequency in a broad range of cancers, such as lung cancer, colorectal cancer, ductal carcinoma and ovarian cancer [205], correlating with a poor prognosis in most of the cases [82] [236] [250].

The Hippo signaling pathway consists of a cascade of multiple serine/threonine kinases and is regulated by contact inhibition, cell-cell adhesion, apicobasal polarity, and mechanotransduction. It can be activated by LPA and sphingosine-1-phosphate (S1P) through their engagement to the G protein-coupled receptors (GPCRs) – LPA receptors (LPAR) and S1P receptors (S1PR) [88].

When the Hippo pathway is turned on, mammalian STE20-like protein kinase (MST) 1 and MST2 are activated and recruit the adaptor protein salvador

homologue 1 (SAV1), leading to the phosphorylation of large tumor suppressor (LATS) 1 and LATS2 [42]. Moreover, LATS1 and LATS2 can also be activated by MOB kinase activator 1 (MOB1, encoded by *MOB1A* and *MOB1B*) [48] [91] (see Introductory Fig. 3). Next, yes-associated protein (YAP, encoded by *YAP1*) and transcriptional co-activator with PDZ-binding motif (TAZ, also known as WWTR1) are phosphorylated by LATS1 and LATS2 at Ser 127 [87] [120] [253]. Then, the 14-3-3 protein can bind to phosphorylated YAP and TAZ, sequestering them in the cytoplasm [251]. In addition, YAP and TAZ can be further phosphorylated at Ser 381, marking them for ubiquitination by SCF$^{\beta\text{-TRCP}}$ E3 ubiquitin ligase and ubiquitin-mediated degradation [253] (Introductory Fig. 3).

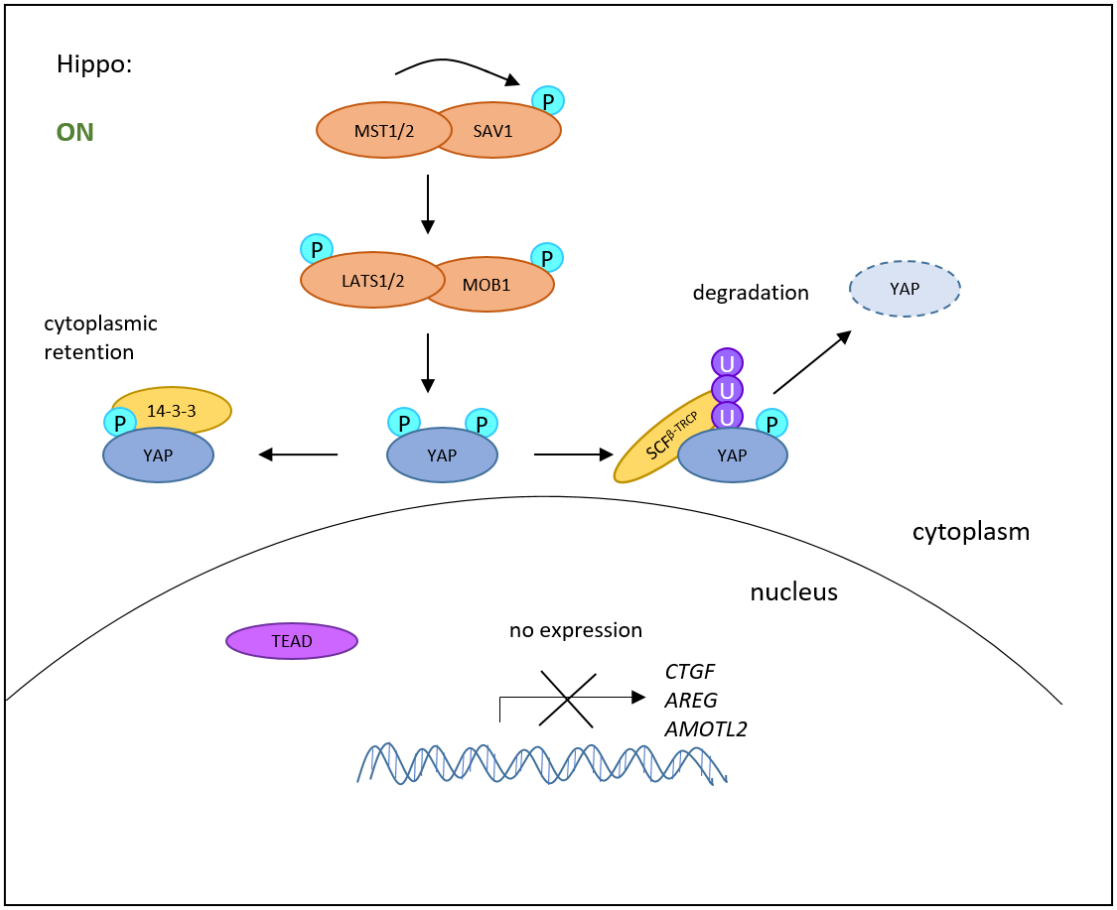

Introductory Fig. 3: "ON-state" of the Hippo pathway.

MST1/2 phosphorylates and recruits SAV1 and then phosphorylates LATS1/2 and MOB1. LATS1/2 then phosphorylate YAP to which 14-3-3 can bind, leading to cytoplasmic retention of YAP. TEAD no longer binds to the DNA and hence, does not induce Hippo target gene transcription. YAP1 can be further phosphorylated marking it for ubiquitination by the E3 ubiquitin ligase SCF$^{\beta\text{-TRCP}}$. Finally, YAP is proteasomally degraded.

Conversely, when the Hippo pathway is turned off, YAP and TAZ are not phosphorylated and can translocate into the nucleus where they bind to the TEA domain transcription factors (TEADs) and activate the transcription of target genes [252]. The target genes are involved in cell survival, proliferation and migration, for example, connective tissue growth factor (CTGF) [252], angiomotin-like protein 2 (AMOTL2) [55] and amphiregulin (AREG) [245] (Introductory Fig. 4). Besides, AMOTL2 has been shown to inhibit YAP as a negative feedback loop [55] [254].

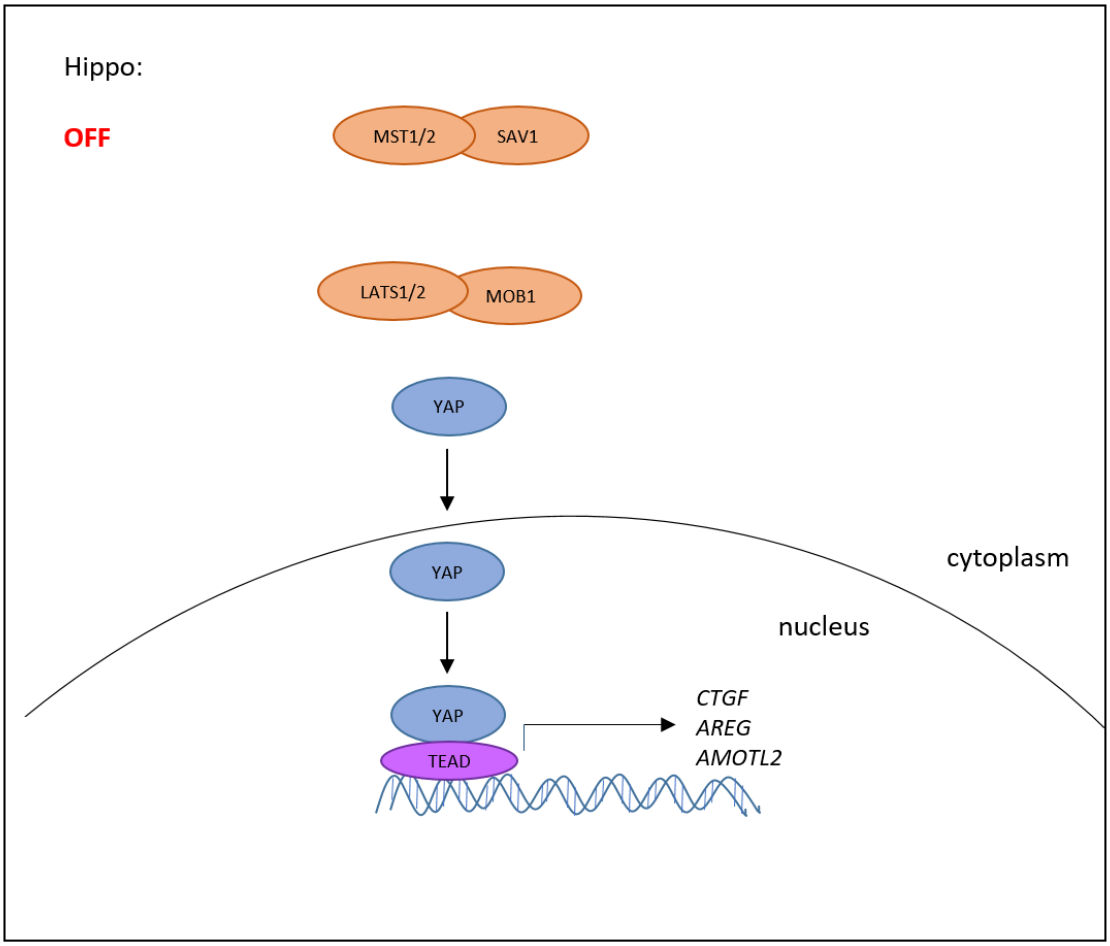

Introductory Fig. 4: "OFF-state" of the Hippo pathway.

If MST1/2 are not activated, LATS1/2 are not phosphorylated and cannot phosphorylate YAP in turn. Hence, YAP translocates into the nucleus, binds to TEAD and activates the transcription of the Hippo target genes *CTGF, AREG*, and *AMOTL2*.

YAP is frequently amplified or overexpressed in human tumors and epigenetic silencing of *MST1, MST2, LATS1,* and *LATS2* have been commonly reported [88]. It has been described that YAP is located within the nucleus in 14 % of

ovarian cancer cases and increased nuclear location of YAP is associated with a poor prognosis. Furthermore, YAP overexpression can transmit chemoresistance in ovarian cancer [250]. In small cell lung cancer (SCLC), WW domain binding protein 5 (WBP5) was shown to induce the nuclear accumulation of YAP1, probably through the inhibition of MST1/2 and thereby inducing multidrug resistance and decreased apoptosis [210]. In addition, it was demonstrated that S1P as well as LPA turn off the Hippo pathway and thereby reduce the phosphorylation of YAP in ovarian cancer cells [33] [65]. Moreover, the YAP-TEAD complex in ovarian cancer cells can be suppressed by usage of verteporfin, which inhibits the interaction of YAP with TEAD [67].

Expression-profiling studies have demonstrated that YAP, TAZ and TEAD transcription factors are expressed in multiple types of stem cells and that YAP plays a role in maintaining stem cell pluripotency [127] [178] [216]. Hence, hyperactivity of YAP and TEAD may influence tumor growth by conveying stem cell properties [88].

Taken together, the Hippo pathway is dysregulated in a broad range of tumor entities. Here, mutations in MST1/2 and LATS1/2 are found, while YAP is amplified and located in the nucleus. YAP overexpression can transmit chemoresistance and high nuclear location of YAP was associated with a poor prognosis. In the nucleus, YAP forms a complex with TEAD to induce Hippo target gene transcription.

1.3.1 The Hippo pathway protein TEAD and its coactivators

In mammals, four TEADs exist (TEAD1-4) [128]. Due to their important function during embryonic development, TEAD1 and TEAD4 knockouts are embryonically lethal in mice [45] [237].

At the N-terminus, TEADs contain a TEA/ATTS domain, necessary to bind to DNA as a homeodomain. This domain is highly conserved among the TEAD family members and recognizes the sequence motif 5′-GGAATG-3′ [128]. It was shown that mutations of Ser 100 and Gln 103 residues completely block binding of TEAD4 to the DNA [194]. Furthermore, at the C-terminus, TEADs have a transactivation domain, which binds to coactivators and is needed to induce target gene transcription. This domain is also highly conserved [128].

TEADs are mainly known to interact with their coactivators YAP and TAZ to induce transcription of Hippo target genes. However, they can also bind to vestigial-like (VGLL) proteins. This family consists of four family members – VGLL1-4. VGLLs share the same binding sites on TEADs as YAP and TAZ and therefore compete with them for TEAD binding [128]. For example, if VGLL4 binds to TEAD, it inhibits the target gene expression of YAP/TAZ-TEAD and therefore inhibits tumor growth [248]. Strikingly, overexpression of VGLL1 upregulates insulin-like growth factor binding protein-5 (IGFBP-5) expression and facilitates cell growth, like the YAP/TAZ-TEAD4 complex [171].

However, TEAD not only induces the transcription of Hippo target genes, but it was also described that TEAD4 plays a role in the regulation of the Wnt/β-catenin signaling. Here, TEAD4 directly interacts with transcription factor 4 (TCF4) to promote TCF4 transactivation and thereby the expression of Wnt target genes. VGLL4 inhibits TEAD4-TCF4 binding, although it does not compete with TCF4 for TEAD binding. It rather represses the TEAD4-TCF4 target gene expression, by a conformational change of the TEAD4-TCF4-VGLL4 complex [99].

Another coactivator family that binds to TEADs is the p160 family of steroid receptors which was identified using yeast-two hybrid screens in which the domain of steroid receptor coactivator 1 (SRC1) bound to TEAD [12].

In several cancers, high expression of TEADs was observed and is associated with poor clinical outcomes. For example, TEAD1 expression was increased in prostate cancer [110], while the expression of TEAD4 was increased in breast cancer [84] [223], head and neck squamous cell carcinoma (HNSCC) [249], and metastatic melanoma [146]. In colorectal cancer, TEAD4 was mainly expressed in the metastatic tissue and a knockout of TEAD4 decreased cell migration and metastasis *in vitro* and *in vivo*. Interestingly, this effect seemed to be YAP-independent as the metastatic potential could be restored with a YAP-binding-deficient Y429H TEAD4 mutant [133].

Summing up, TEADs mainly interact with their coactivators YAP and TAZ, but can also bind to VGLL and p160 proteins. VGLLs and YAP/TAZ share the same binding site on TEAD and therefore compete for TEAD binding. TEADs are frequently upregulated in various cancers and are associated with a poor clinical outcome. Nevertheless, TEAD do not only play a role in the Hippo pathway, but also in other pathways, such as the Wnt/β-catenin signaling pathway.

1.3.2 Hippo signaling and immune cells

The Hippo pathway in cancer is mainly known for its role in tumor cells. However, it has been described to play a role in modulating immune cell responses, too. YAP can induce the expression of cytokines in tumor cells, which modify the TME. Wang *et al.* showed that YAP1-driven CXCL5 secretion led to the recruitment of C-X-C motif chemokine receptor 2 (CXCR2)-expressing MDSCs. Furthermore, blocking of the CXCL5-CXCR2-axis led to an inhibited tumor progression [224]. In a mouse model for HGSOC, it was demonstrated, that *YAP1* is downstream of the oncogene protein kinase C iota (PRKCI) and induces TNFα expression, which recruits MDSCs and suppresses CTLs and thereby promotes tumor growth [190]. Moreover, TAM polarization towards an immunosuppressive M2-phenotype was induced by YAP1-expressing colon cancer cells, but not if YAP1 was knocked out in these cells [93]. It was reported that YAP and TAZ enhance the expression of programmed death-ligand 1 (PD-L1) in breast and lung cancer cell lines which represses T cell function, while the expression of MST1/1 and LATS1/2 inhibited the expression of PD-L1 [96]. Further, binding of YAP1 to the PD-L1 promoter in lung adenocarcinoma cells [117] and to the PD-L1 enhancer in melanoma cells was revealed [106]. Conversely, a double knockout of LATS1/2 was highly tumorigenic *in vitro*, but surprisingly poorly tumorigenic *in vivo*. This can be explained by the secretion of EVs by the double knockout cells, which bind to toll-like receptors (TLRs) and thereby inducing a type I IFN response. This provokes CTL clonal expansion and maturation of DCs and hence mediates tumor destruction [156].

So far, little is known about the intrinsic function of the Hippo pathway in immune cells. It is known that MST1 regulates the transcription factor TEAD2, which then binds to the consensus motif in the 3′ untranslated region of *CD19* and hence induces the expression of CD19 in murine B cells [9].

MST1-deficiency in T cells leads to a reduced expression of forkhead box O1 (FOXO1), the IL-7 receptor, and B-cell lymphoma 2 (BCL2), while FAS was upregulated. In this state of immunodeficiency, naïve T cells were lost due to the MST1/FOXO induced apoptosis of the cells [158]. Moreover, *Mst1*$^{-/-}$ CTLs

depicted an increased T-box transcription factor 21 (T-bet) expression, associated with enhanced levels of IFNγ and granzyme B. These *Mst1*$^{-/-}$ CTLs were able to suppress tumor growth in a mouse lymphoma (E.G7-OVA) tumor model [239].

Furthermore, YAP is highly expressed in T_{regs} and facilitates FOXP3 expression and T_{reg} function *in vitro* and *in vivo* [160]. TAZ expression in $CD4^+$ T cells promotes the T_h17 differentiation and dampens the T_{reg} differentiation, while TEAD1 overexpression induced T_{reg} differentiation [76].

Activation of $CD8^+$ T cells by antigen-stimulation together with IL-2 induces the expression of Hippo pathway components (such as SAV1, LATS1, MOB1, TEAD1, and TEAD3), resulting in YAP degradation and Blimp-1 expression, which is required for terminal differentiation of the T cells [211].

YAP also plays a role in the antiviral response of macrophages. TANK-binding kinase 1 (TBK1) is activated by viral DNA or RNA and further activates the transcription factor interferon regulatory factor 3 (IRF3) by phosphorylation of IRF3. IRF3 then induces a type I IFN response [147]. However, YAP can bind to IRF3 and prohibit its dimerization and translocation to the nucleus and hence, block the antiviral immune response. Though, YAP can be phosphorylated by the inhibitor of nuclear factor κ-B kinase subunit epsilon (IKKε) at Ser 403 leading to degradation of YAP in lysosomes [225].

So far, nothing is known about the expression of the Hippo pathway in NK cells. Nevertheless, in natural killer T-cell lymphoma (NKTCL) tissue and cell lines, it was described, that MST1 was downregulated, while YAP was upregulated [43].

Taken together, the Hippo pathway not only plays a pivotal role in tumor cells but also has an impact on immune cells. Driven through the Hippo pathway, tumor cells can secret immunosuppressive cytokines, can upregulate PD-L1 to inhibit CTLs, or recruit tumor-promoting MDSCs and TAMs. However, little is known about the intrinsic function of the Hippo pathway in immune cells.

1.4 Aims of this thesis

Ovarian cancer has the highest mortality rate of all gynecological cancers worldwide. However, the therapeutic options within the last thirty years have not improved and the overall perspective of the patients is disappointing. As part of the innate immune system, NK cells play a crucial role in the recognition and elimination of malignant cells. The aim of this study was to characterize molecular and phenotypical alterations of TANKs, leading to dysregulation of NK cell effector function. Unraveling dysregulations of TANKs is essential to identify novel therapeutic options to restore impaired effector functions and immune surveillance. Furthermore, the crosstalk between NK cells and TAMs was investigated. To this end, the following specific questions were addressed:

1. What is the function of sNKG2D-Ls?
    a. Do soluble NKG2D-Ls influence NK cells, TAMs or the crosstalk between these two?
    b. What are the specific target genes of membrane-bound NKG2D-Ls vs. soluble NKG2D-Ls when engaged to the NKG2D receptor?
2. What are the molecular and functional alterations of TANKs and which factors are responsible for these changes?
    a. Which receptors are expressed on the surface? Do they show signs of exhaustion?
    b. What is the cytotoxic potential of patient-derived NK cells and which receptors are important for the recognition of ovarian cancer cells?
    c. Which factor within the ascites is responsible for the reduced DNAM-1 expression?
3. What are the molecular mechanisms directing a tumor-associated NK cell phenotype?
    a. Which signaling pathways are dysregulated in patient-derived NK cells?
    b. What induces the expression of the Hippo pathway component TEAD4 in healthy donor-derived NK cells and which function do TEAD4-expressing NK cells display?

2 Material and Methods

2.1 Material

2.1.1 Solutions, chemicals, and buffers

Table 2: Solutions, chemicals, and buffers.

Solutions/chemicals/buffers	Supplier/composition
7-AAD Viability Staining Solution	Biolegend, Koblenz
Absolute qPCR SYBR Green Mix	Thermo Fisher Scientific/Life Technologies, Darmstadt
Accutase	Sigma-Aldrich, Steinheim
Aqua ad iniectabilia	Braun, Melsungen
Annexin V Binding Buffer, 10x Concentrate	BD, Heidelberg
Blasticidin S HCl	Fisher Scientific, Schwerte
Blotting Buffer, 1x	25 mM Tris-HCL, 192 mM Glycine, 20 % (v/v) MeOH
CellTracker™ Violet BMQC	Invitrogen/Life Technologies/Thermo Fisher Scientific, Darmstadt
Coating buffer, 1x	100 mM $NaHCO_3$, 33.5 mM Na_2CO_3, pH 9.5
DPBS, without calcium and magnesium	Thermo Fisher Scientific/Life Technologies, Darmstadt
Dynabeads human T-Activator CD3/CD28	Thermo Fisher Scientific/Life Technologies, Darmstadt; dissolved in PBS with 0.1 % (w/v) BSA
RBC lysis buffer	155 mM NH_4Cl, 10 mM $KHCO_3$, 0.1 mM EDTA pH 7.2-7.4
Ethanol	Roth, Karlsruhe
FACS buffer	PBS, 0.2 % (w/v) BSA, 0.2 % (w/v) sodium azide
FACS Clean solution	BD, Heidelberg

FACS Flow	BD, Heidelberg
FACS Rinse solution	BD, Heidelberg
FACS Shutdown solution	BD, Heidelberg
FastDigest Buffer, 10x	Thermo Fisher Scientific/Life Technologies, Darmstadt
FBS	Thermo Fisher Scientific/ Life Technologies, Darmstadt Sigma-Aldrich, Steinheim
Ficoll (LSM 1077, Lymphocyte Separation Medium)	Capricorn Scientific, Ebsdorfergrund
Human AB serum	Sigma-Aldrich, Steinheim
Immobilon Forte Western HRP Substrate	Merck Millipore, Darmstadt
Isopropanol	Carl Roth, Karlsruhe
LB medium	1 % (w/v) Peptone, 1 % (w/v) NaCl, 0.5 % (w/v) Yeast extract
MACS buffer	PBS, 0.5 % (v/v) FBS, 2 mM EDTA, pH 7.2
Monensin solution (1000x)	Biolegend, Koblenz
PBS	137 mM NaCl, 10 mM Na_2HPO_4, 2.7 mM KCl, 2 mM KH_2PO_4, pH 7.4
peqGOLD TriFast	VWR, Darmstadt
Penicillin Streptomycin solution (100x)	10000 U/ml Penicillin, 10000 µg/ml Streptomycin Sigma-Aldrich, Steinheim
Phosphatase Inhibitor Cocktail	100 mM NaPP, 100 mM ß-glycerophosphate, 100 mM Na_3VO_4, 100 mM NaF
Protease Inhibitor Cocktail	Sigma-Aldrich, Steinheim
RIPA buffer	50 mM Tris-HCL pH 8.0, 150 mM NaCl, 0.1% SDS (w/v), 0.5 % (v/v) TritonX-100, 0.5 % (w/v) DOC (Deoxycholic acid)
RPMI 1640 with GLUTAMAX-I	RPMI 1640 with GLUTAMAX-I + 5 % (v/v)

(R5 medium macrophages)	human AB serum + 1 % (v/v) sodium pyruvate
RPMI 1640 with GLUTAMAX-I	Thermo Fisher Scientific/Life Technologies, Darmstadt
Schneider's Drosophila Medium	Thermo Fisher Scientific/Life Technologies, Darmstadt + 10 % (v/v) FBS + 1 % (v/v) Penicillin/Streptomycin
SDS running buffer, 1x	25 mM Tris-HCL, 192 mM Glycine, 0.1 % (w/v) SDS, pH 8.3
Sodium pyruvate solution (100 mM)	Sigma-Aldrich, Steinheim
TBS-T	150 mM NaCl, 50 mM Tris-HCl, 0.1 % (v/v) Tween-20, pH 7.5
Trypan Blue Solution, 0.4 %	Gibco/Life Technologies/Thermo Fisher Scientific, Darmstadt
Trypsin-EDTA Solution, 10x	Sigma-Aldrich, Steinheim
Tween20	Applichem, Darmstadt

All chemicals were purchased from Merck or Carl Roth, if not stated otherwise.

2.1.2 Cytokines, inhibitors, and proteins

Table 3: Cytokines, inhibitors, and proteins.

Cytokine/inhibitor/protein	Supplier
FastDigest EcoRI	Thermo Fisher Scientific/Life Technologies, Darmstadt
FastDigest XhoI	Thermo Fisher Scientific/Life Technologies, Darmstadt
LPS (100 ng/ml) of *E.coli* 0111:B4 L4391	Sigma-Aldrich, Steinheim
Recombinant human, Interleukin-2 (rhuIL-2, 11340025, 200 U/ml or 10 U/ml)	Immunotools , Friesoythe
Recombinant human, Interleukin-15 (rhuIL-15, 11340153, 10 ng/ml)	Immunotools , Friesoythe
Recombinant human, ULBP2-His (12143-H08H-100, 200 nM)	Sino Biological, Eschborn

SB-431542 (TGFβ receptor kinase inhibitor, 13031, 10 µM)	Cayman chemical/Biomol, Hamburg
T4 Ligase	Thermo Fisher Scientific/Life Technologies, Darmstadt
TGF-β1, human platelets (616450-1UG, 5 ng/ml)	Merck, Darmstadt
YAP-TEAD inhibitor 1 (Peptide 17) (SEL-S8164-1MG, 40 nM)	Selleckchem/Biozol, Eching

2.1.3 Vectors

Table 4: Vectors.

Vector	Function
pAc5.1/V5-His	Expression plasmid for S2 cells
pAc5.1_ULBP2	Overexpression of human ULBP2 in S2 cells
pCoBlast	Plasmid carrying Blasticidin resistance

2.1.4 Kits

Table 5: Kits.

Kit name	Supplier
Calcium Phosphate Transfection Kit	Thermo Fisher Scientific/Life Technologies, Darmstadt
DNA-free™ DNA Removal Kit	Invitrogen/ Life Technologies, Darmstadt
Human IFN-γ ELISA MAX™ Standard	Biolegend, Koblenz
NK Cell Isolation Kit, human	Miltenyi Biotec, Bergisch Gladbach
Pierce™ BCA protein assay Kit	Thermo Fisher Scientific, Darmstadt
RevertAid RT Reverse Transcription Kit + Oligo(dT)18 primers	Thermo Fisher Scientific, Darmstadt

2.1.5 Antibodies and immunoglobulins

Table 6: Antibodies and immunoglobulins.

Antigen	Label	Isotype	Species	Application and concentration	Supplier	Clone	Order no.
Actin	HRP	IgG	Goat	WB; 20 ng/ml	SCBT, Heidelberg	-	sc-1616
Annexin V	AF647	-	Human	FACS; 50 ng	Biolegend, Koblenz, Koblenz	-	640912
Anti-human IgG Fc	AF647	IgG2a	Mouse	FACS; 300 ng	Biolegend, Koblenz	HP6017	409320
Anti-mouse IgG	FITC	IgG	Goat	FACS; 250 ng	Biolegend, Koblenz	-	405305
Anti-mouse IgG	HRP	-	Horse	WB; 15.3 ng/ml	CST, Frankfurt	-	7076 S
Anti-rabbit IgG	HRP	-	Goat	WB; 9.2 ng/ml	CST, Frankfurt	-	7074 S
CCR7	PE	IgG2a	Rat	FACS; 1 µg	BD, Heidelberg	3D12	552176
CD3	V500	IgG1κ	Mouse	FACS; 50 ng	BD, Heidelberg	UCHT1	561417
CD8	APC	IgG1κ	Mouse	FACS; 25 ng	Biolegend, Koblenz	SK1	344721
CD8	PerCP-Cy5.5	IgG1κ	Mouse	FACS; 250 ng	Biolegend, Koblenz	SK1	344709
CD16	-	IgG1κ	Mouse	Blocking; 10 µg/ml	Biolegend, Koblenz	3G8	302014
CD16	APC-Cy7	IgG1κ	Mouse	FACS; 100 ng	Biolegend, Koblenz	3G8	302018
CD45-RA	APC	IgG2b	Mouse	FACS; 11.2 ng	eBioscience/Invitrogen/	HI100	17-0458-42

					Thermo Fisher Scientific, Darmstadt		
CD56	BV421	IgG1κ	Mouse	FACS; 60 ng	Biolegend, Koblenz	HCD56	318328
CD56	FITC	IgG1κ	Mouse	FACS; 50 ng	eBioscience/Invitrogen/ Thermo Fisher Scientific, Darmstadt	TULY56	11056642
CD56	PerCP-Cy5.5	IgG1κ	Mouse	FACS; 150 ng	Biolegend, Koblenz	5.1H11	362506
CD69	PE-Cy7	IgG1κ	Mouse	FACS; 50 ng	Biolegend, Koblenz	FN50	310912
CD107a	PE	IgG1κ	Mouse	FACS; 400 ng	Biolegend, Koblenz	H4A3	328608
CD158a (KIR2DL1)	BV421	IgM	Mouse	FACS; 125 ng	BD, Heidelberg	HP-3E4	564318
CD158b (KIR2DL2/3)	BB515	IgG2b	Mouse	FACS; 50 ng	BD, Heidelberg	CH-L	564678
CD158e (KIR3DL1)	APC	IgG1κ	Mouse	FACS; 12.5 ng	BD, Heidelberg	DX9	564103
CD159a (NKG2A)	APC	REA Control	Recombinant human	FACS; 0.5 µl	Miltenyi Biotec, Bergisch Gladbach		130-098-809
CD159c (NKG2C)	PE-Vio770	REA Control	Recombinant human	FACS; 1 µl	Miltenyi Biotec, Bergisch Gladbach		130-103-702
DNAM-1	-	IgG1κ	Mouse	Blocking; 10 µg/ml	Miltenyi Biotec, Bergisch Gladbach	DX11	130-092-479
DNAM-1	FITC	IgG1κ	Mouse	FACS; 62.5 ng	BD, Heidelberg	DX11	559788

DNAM-1	PE-Cy7	IgG1κ	Mouse	FACS; 200 ng	Biolegend, Koblenz	11A8	338315
IgG1κ	-	IgG1κ	Mouse	Blocking, Crosslink.;10 µg/ml	Biolegend, Koblenz	MOPC-21	400102
rhIgG1-Fc	-	-	Human	FACS; 500 ng	R&D/Bio-Techne, Wiesbaden	-	110-HG-100
Recombinant human IgG (REA Control (S))	APC		Human	FACS; 0.5 µl	Miltenyi Biotec, Bergisch Gladbach	REA293	130-104-614
Recombinant human IgG (REA Control (S))	PE-Vio770		Human	FACS; 1 µl	Miltenyi Biotec, Bergisch Gladbach	REA293	130-104-616
Mouse Gamma Globulin	-		Mouse	FACS; 5.8 µg	Jackson ImmunoResearch Europe Ltd, USA		015-000-002
MICA/B	AF647	IgG2a	Mouse	FACS; 100 ng	Biolegend, Koblenz	6D4	320914
NCOA1	-	IgG1	Mouse	WB; 0.2 µg/ml	SCBT, Heidelberg	1135/H4	sc-32789
NKG2D	-	IgG1κ	Mouse	Blocking; 10 µg/ml	Biolegend, Koblenz	1D11	320802
NKG2D	FITC	IgG1κ	Mouse	FACS; 100 ng	Biolegend, Koblenz	1D11	320820
rhNKG2D-FC	-	-	Human	FACS; 500 ng	R&D/Bio-Techne, Wiesbaden	-	1299-NK-050
NKp30	Purified	IgG1κ	Mouse	Blocking; 10 µg/ml	Biolegend, Koblenz	p30-15	325204

NKp30	BV421	IgG1κ	Mouse	FACS; 125 ng	BD, Heidelberg	p30-15	563385
NKp44	AF647	IgG1κ	Mouse	FACS; 25 ng	Biolegend, Koblenz	P44-8	325112
NKp46	AF647	IgG1κ	Mouse	FACS; 25 ng	Biolegend, Koblenz	9E2	331910
NKp46	PE	IgG1κ	Mouse	FACS; 25 ng	Biolegend, Koblenz	9E2	331908
NKp46	PE-Cy7	IgG1κ	Mouse	FACS; 25 ng	Biolegend, Koblenz	9E2	331916
PD-1	PE	IgG1κ	Mouse	FACS; 50 ng	Biolegend, Koblenz	EH12.2H7	329906
pERK1/2	-	IgG2a	Mouse	WB; 200 ng/ml	SCBT, Heidelberg	E-4	sc-7383
pYAP1 (Ser 127)	-	-	Rabbit	WB; 184 ng/ml	CST, Frankfurt	-	4911
TEAD4	-	-	Rabbit	WB; 5.25 µg/ml	Abcam, Berlin	-	ab97460
TGF-beta 1, 2, 3	-	IgG1	Mouse	Blocking; 5 µg/ml	R&D/Bio-Techne, Wiesbaden	1D11	MAB1835-SP
TIM-3	BV421	IgG1κ	Mouse	FACS; 100 ng	Biolegend, Koblenz	F38-2E2	345008
TIGIT	APC	IgG2a	Mouse	FACS; 30 ng	Biolegend, Koblenz	A15153G	372706
ULBP2	-	IgG1	Mouse	FACS; 250 ng	BamOmaB	BUMO1	BUMO1-100
ULBP2	PE	IgG2a	Mouse	FACS; 5 ng	R&D/Bio-Techne, Wiesbaden	165903	FAB1298P

Suitable isotype controls were purchased at Biolegend or BD Bioscience.

2.1.6 qRT-PCR oligonucleotides

Oligonucleotides were purchased from the company Sigma-Aldrich and were dissolved with ddH_2O at a concentration of 100 pmol/µl.

Table 7: Transcript name and sequence of qRT-PCR oligonucleotides.

Transcript	Sequence (5' → 3')
hACOD1_qfor	ATATGCTGCTTTTGTGAACGGTG
hACOD1_qrev	GCTAAAGCTGTGAGGACAGGAA
hAMOTL2_qfor	GACAGCCTTCTGGGGTGCAGCAGTA
hAMOTL2_qrev	GCTCAGAGTCCTGAAGCACCACCTCCT
hAREG_qfor	ACTCGGCTCAGGCCATTATGCTGCT
hAREG_qrev	TGTGGTCCCCAGAAAATGGTTCACG
hC2_qfor	CCTGAACATCAACCAGAAGAGGA
hC2_qrev	CTCACCATCCTTCTTGGACCC
hC3_qfor	CGGATCTTCACCGTCAACCA
hC3_qrev	GCTGGTTCTGAGAAGACAAGGA
hCD226_qfor	TACCCACAGGGAACTTGGCA
hCD226_qrev	GTGGCTATTTGATGGCACAGC
hCFB_qfor	CAACTTCACAGGAGCCAAAAAGT
hCFB_qrev	AAACCATGCCACAGAGACTCA
hCFI_qfor	GTCCCCTGGTCTCCTTACCT
hCFI_qrev	ACCCCACTGAAGTGAAAAGACTC
hCLEC4E_qfor	TTTCACAGAGCTCTCCTGCTAC
hCLEC4E_qrev	GCCCAGGAAATGGTGTCAGTA
hCTGF_qfor	TGCGAAGCTGACCTGGAAGAGAACA
hCTGF_qrev	TCGGCCGTCGGTACATACTCCACA
hFCGR3A_qfor	AAGGAAATTGGTGGGTGACAGA
hFCGR3A_qrev	GGTCTTCCTCCTTGAACACCC
hGAPDH_qfor	GGAAGGTGAAGGTCGGAGTC
hGAPDH_qrev	TGAAGGGGTCATTGATGGCA

hHLA-E_qfor	GGCTCAGATCTCCGAGCAAA
hHLA-E_qrev	AGTAGCTCCCTCCTTTTCCAC
hKLRK1_qfor	AGCCATGGGAATCCGTTTCA
hKLRK1_qrev	AGGACATGGGCCACAGTAAC
hMICA_qfor	CTGCAGGAACTACGGCGATA
hMICA_qrev	CCCTCTGAGGCCTCGCT
hMICB_qfor	AGAAGAAAACATCAGCGGCAG
hMICB_qrev	CATCCCTGTGGTCTCCTGTC
hNCOA1_qfor	GCTACCCTCTGGAACTCAAGATT
hNCOA1_qrev	GATGAACTGTCCCCGAGGC
hPLA2G7_qfor	GTGGTTTATCCTTTTGACTGGCA
hPLA2G7_qrev	AGCAGCCATCAGTACTTGTATTTTG
hRPL27_qfor	AAAGCTGTCATCGTGAAGAAC
hRPL27_qrev	GCTGTCACTTTGCGGGGGTAG
hTBX21_qfor	CCACCTGTTGTGGTCCAAGT
hTBX21_qrev	CCCGGCCACAGTAAATGACA
hTEAD1_qfor	GCCCTGGCTATCTATCCACC
hTEAD1_qrev	CGTCTTGCCTGTCCTGAGTT
hTEAD2_qfor	GTTTTGGTCTGGAGGATCTGGG
hTEAD2_qrev	GAGGTCAGTAGATGGGGGAGT
hTEAD3_qfor	CGAAATGAGTTGATTGCACGC
hTEAD3_qrev	GCACCTTCTTCCGAGCTAGA
hTEAD4_qfor	GAGCTGATTGCCCGCTACAT
hTEAD4_qrev	TTTAGCTTGGCCTGGATCTCG
hULBP2_qfor	GCCGCTACCAAGATCCTTCT
hULBP2_qrev	GCAAAGAGAGTGAGGGTCGG
hVAV1_qfor	CAGAGTATGACAAGCGCTGC
hVAV1_qrev	GCAGGGGCTTCAAGAAATGC
hVGLL1_qfor	GTATCTCGTGGATCTGCCAGT
hVGLL1_qrev	CCAGTGGTTTGGTGGTGTAA

hYAP1_qfor	TGTCTTCTCCCGGGATGTCT
hYAP1_qrev	CATCTCGAGAGTGATAGGTGCC
hYY1_qfor	CGGGCAACAAGAAGTGGGA
hYY1_qrev	TCAACCACTGTCTCATGGTCAATA

2.1.7 Primary cells

Healthy donor NK cells and monocytes were isolated from either buffy coats or LRS chambers from the University Hospital of Gießen and Marburg. When buffy coats were used, only female and age-matched donors were employed. Donors from LRS chambers were mainly male. Buffy coats were used in figures 1, 2, 3, 6, 7, 8, 9 and 10. The remaining experiments were conducted with LRS chambers. For the experiment of table 1, the donors of the LRS chambers were female.

Moreover, the TAMs and lymphocytes from ascites or peripheral blood, as well as the cell-free ascites of ovarian cancer patients from the university hospital of Gießen and Marburg was used. The study was approved by the institutional ethics committee (reference number AZ 205_10).

2.1.8 Cell lines and competent cells

Table 8: Cell lines and competent cells.

Cell line/competent cells	Origin	Cultivation
K562	Human chronic myelogenous leukemia cell line	IMDM + 10 % (v/v) FBS + 1 % (v/v) P/S
OVCAR-4	Human ovarian cancer cell line	RPMI with GLUTAMAX-I + 10 % (v/v) FBS + 1 % (v/v) P/S
Schneider 2 (S2) cells	Drosophila cell line derived from late-stage embryo	Schneider's Drosophila medium + 10 % (v/v) FBS + 1 % (v/v) P/S
XL-1 blue	*E.coli*	LB medium

2.1.9 Software

For the analysis of flow cytometry data, FlowJo V10 was used.

GraphPad Prism 7 was used to create the graphs and to calculate the *p*-values using paired or unpaired Student's *t*-tests. Unpaired *t*-tests were performed without Welch's corrections. ns, not significant ($p \geq 0.05$), *p < 0.05, **p < 0.01, ***p < 0.001; ****p ≤ 0.0001

Finally, ImageJ and Microsoft Office 2013 were used.

2.2 Methods

2.2.1 Cell biological methods

2.2.1.1 Cultivation of cells

K562 cells were maintained in IMDM supplemented with 10 % (v/v) FBS and 1 % (v/v) penicillin/streptomycin (P/S) solution, while OVCAR-4 cells were cultured in RPMI 1640 with GLUTAMAX-I + 10 % (v/v) FBS and 1 % (v/v) P/S. Depending on their growth rate, all cells were passaged two to three times per week. To detach OVCAR-4 trypsin was used. Drosophila Schneider 2 (S2) cells were maintained in Schneider's Drosophila medium + 10 % (v/v) FBS and 1 % (v/v) P/S and incubated at 27 °C without CO_2. All cells were regularly tested for mycoplasma contamination by PCR and only mycoplasma-negative cells were used for the assays. Primary NK cells were cultured in IMDM supplemented with 10 % (v/v) FBS and 1 % (v/v) P/S at a cell density of $1*10^6$/ml, while monocytes where differentiated into macrophages in RPMI 1640 with GLUTAMAX-I + 5 % (v/v) human AB serum + 1 % (v/v) sodium pyruvate without any addition of cytokines. Additionally, primary cells were cultivated in cell-free ascites from ovarian cancer patients as indicated. Besides S2 cells, all cells were maintained at 37 °C and 5 % CO_2.

2.2.1.2 Transfection and generation of S2 ULBP2 cells

S2 cells were co-transfected with the expression vector pAc5.1/V5-His_ULBP2 and the selection vector pCoBlast in a ratio of 19:1 using the calcium phosphate

transfection kit (Thermo Fisher Scientific) according to the manufacturer's protocol. The cells were selected with 25 µg/ml Blasticidin for 2-3 weeks until the expression of ULBP2 reached almost 100 %.

2.2.1.3 Isolation of PBMCs from buffy coats and LRS chambers

In order to isolate the PBMCs from buffy coats and LRS chambers, ficoll density gradient centrifugation was performed. Monocytes were further purified from remaining cells by adherent cell positive selection. They were cultivated at least six days to generate monocyte-derived macrophages (MDMs). NK cells were negatively selected using the human NK cell isolation kit (Miltenyi Biotec). For resting NK cells, the cells were incubated with 10 U/ml IL-2 and for activated NK cells, they were stimulated with 200 U/ml IL-2 and 10 ng/ml IL-15 overnight.

2.2.1.4 Processing of ascites and isolation of PBMCs from ascites

Ascites samples of high grade serous ovarian carcinoma patients were provided by the University Hospital of Marburg. Included in the study are only patients, who did not receive treatment yet and who undergo first-line surgery. The study was approved by the institutional ethics committee (reference number AZ 205_10). Mononuclear cells were purified from the ascites using density gradient centrifugation. Cell-free ascites was generated by serial centrifugation.

2.2.1.5 Treatment of macrophages

Monocytes were differentiated at least six days into MDMs without the addition of cytokines. Then, MDMs were treated with 100 ng/ml LPS for the indicated time points.

2.2.1.6 Antibody crosslinking

For crosslinking, 10 µg/ml CD16 antibody or IgG control were added to 1x coating buffer. 100 µl of the mix were pipetted per well into a MaxiSorp^{TM} 96-well-plate and incubated overnight at 4 °C. On the next day, the plate was washed twice with complete IMDM medium, followed by 30 minutes incubation with complete medium at room temperature for blocking of the plate. NK cells were seeded into the plate at a concentration of $1*10^6$/ml for the indicated time points. For inhibitor

treatment, NK cells were pretreated with 40 nM P17 inhibitor for 30 minutes at room temperature, before the cells were seeded into the antibody-coated plate. The inhibitor was present throughout the whole duration of the assay.

2.2.1.7 Flow cytometry

MDMs were detached using accutase. Here, MDMs were incubated for at least 30 minutes at 37 °C and then rinsed from the tissue culture plate. Suspension cells were washed with PBS and then stained. In general, cells were stained with fluorochrome-labeled antibodies for 30 minutes at 4 °C, before they were washed with FACS buffer and analyzed on a FACS Canto II cytometer (BD Bioscience). For staining with the NKG2D-FC recombinant receptor, cells were incubated for 30 minutes at 4 °C with the recombinant receptor, washed with FACS buffer and then stained with an anti-human FC-AF647 antibody for another 30 minutes at 4 °C, before the cells were analyzed. For the depicted MFI, the background geometric mean of the isotype was subtracted from the geometric mean of the specific staining of each sample. A list of antibodies used for flow cytometry is found in the materials section (see section 2.1.5).

2.2.1.8 Killing assay

NK cells were treated with 10 U/ml IL-2 to generate resting NK cells or stimulated with 200 U/ml IL-2 and 10 ng/ml IL-15 overnight to induce activation of NK cells. On the next day, for blocking experiments, NK cells were pretreated with 10 µg/ml blocking antibody or IgG control for 30 minutes at room temperature. Target cells were stained with 5 µM CellTracker™ Violet BMQC (Invitrogen) fluorescent dye in serum-free medium for 45 minutes at 37 °C. Then, cells were washed twice with complete medium. NK cells and target cells were seeded into a 96-well-plate with round bottom at the indicated effector to target (E:T) ratios. The plate was centrifuged at 100 g for one minute to bring cells into proximity and then incubated for three hours at 37 °C. Next, samples were washed with FACS buffer and stained with 50 ng 7-AAD solution, before they were analyzed on the FACS Canto II cytometer (BD Bioscience).

2.2.1.9 Degranulation assay

NK cells were pre-treated like in the killing assay. NK cells and target cells were seeded into 96-well-plate with a round bottom at the indicated E:T ratios. The plate was centrifuged at 100 g for one minute to bring cells into proximity and then incubated for two hours at 37 °C. Then, 400 ng CD107a-PE and 2 µM Monensin (Biolegend) per well were added to the samples, followed by four hours of co-cultivation at 37 °C. Next, cells were washed with FACS buffer and stained with 60 ng CD56-BV421 or 25 ng NKp46-AF674 for 30 minutes at 4 °C. The cells were washed with FACS buffer and analyzed on the FACS Canto II cytometer (BD Bioscience).

2.2.2 Molecular biological methods

2.2.2.1 Cloning

The pAc5.1/V5-His expression vector was used as a backbone, which contains an ampicillin resistance. The ULBP2 cDNA was ordered from IDT and was flanked by EcoRI and XhoI restriction sites. The vector and cDNA were digested with fast digest EcoRI and XhoI enzymes (Thermo Fisher Scientific) according to the manufacture's protocol. Next, the digested vector and insert were ligated at a 1:3 vector:insert ratio using T4 Ligase (Thermo Fisher Scientific) overnight at 16 °C. 5 µl of the ligation mix was used for the transformation of XL1 blue competent bacteria. In brief, they were incubated at 42 °C for 90 seconds, followed by two minutes on ice, before they were recovered for 20 minutes in LB medium. Finally, they were spread on an agar plate containing ampicillin.

2.2.2.2 RNA isolation and cDNA synthesis

The cells were lysed in 1 ml TriFast and stored at -20 °C. In order to isolate the RNA, samples were thawed and 200 µl chloroform was added. The samples were mixed for 15 seconds by hand shaking and then incubated for two to three minutes at room temperature before they were centrifuged for 15 minutes at 12,000 g and 4 °C. Next, the aqueous phase was transferred to a fresh tube, mixed with 500 µl isopropanol by vortexing and incubated for 10 minutes at room temperature. Afterward, the samples were centrifuged for 10 minutes at 12,000 g

and 4 °C. The supernatant was discarded and the RNA was washed with 1 ml 70 % ethanol and centrifuged for 5 minutes at 7500 g and 4 °C. Finally, the supernatant was removed and the RNA pellet was air-dried for 5 minutes before it was resuspended in nuclease-free H_2O.

The cDNA synthesis was performed using the RevertAid RT Reverse Transcription Kit from Thermo Fisher Scientific according to the manufacturer's protocol. Here, 1 µl Oligo (dT) 18 primers (Thermo Fisher Scientific) and 1 µl random hexamer primers were used. Between 100 and 500 ng RNA was transcribed and cDNA was diluted 1:5, 1:10 or 1:20 with nuclease-free H_2O.

2.2.2.3 RNA-seq and bioinformatics analysis

RNA of the samples was isolated using the phenol-chloroform-extraction method described in the RNA isolation section (section 2.2.2.2). Possible DNA contamination was removed with the DNA-free™ DNA Removal Kit (Invitrogen) according to the manufacturer's instructions. The quality of the RNA was verified using the Experion RNA StdSens Analysis Kit or using the Qubit fluorometer (Thermo Fisher Scientific). Next, RNA-libraries were generated from total RNA by using the TruSeq Stranded mRNA Library kit according to the manufacturer's instructions. The sequencing was conducted on the Illumina HiSeq 1500 or HiSeq 4000. A Run with 50 base single reads was performed.

For the identification of NKG2D-Ls, sequencing was performed on an Illumina HiSeq 4000. Raw reads were aligned to the human and Drosophila genomes (retrieved from Ensembl 97) using STAR 2.6.1d. Reads aligning to the Drosophila genome were subtracted from the human alignment. Read counts were quantified in exonic regions of protein-coding transcripts and normalized to transcripts per million reads (TPM). Differential gene expression was assessed via edgeR (version 3.24.3) at a threshold of FDR ≤ 0.05 and |log2FC| ≥ 1. The samples were analyzed by the IKMB (University Kiel), and bioinformatics analysis was performed by Dr. Florian Finkernagel.

For the comparison of differentially expressed genes of healthy donor NK cells vs. ascites-derived NK cells, raw reads were aligned to the human genome

(retrieved from Ensembl 92) using STAR 2.4.1a. RNA-seq data from healthy blood donors were obtained from the deposited data of Linsley *et al.* (E-GEOD-60424) [129]. Read counts were quantified in exonic regions of protein-coding transcripts and normalized to TPM. Fold change of each gene was calculated by division of the patient TPM value by the healthy donor TPM value. Genes were considered to be upregulated in patients, if the TPM value of the patient gene was at least 10 and the fold change was at least 2-fold. If the fold change was 0.35 or lower, and the TPM value of the healthy donor gene was at least 10, the gene was considered to be downregulated in patients. Enrichment analysis was performed using DAVID functional annotation clustering software (v6.8; https://david.ncifcrf.gov/). The samples were analyzed by the genomics core facility (University Marburg), and bioinformatic analysis was performed by Dr. Florian Finkernagel.

Table 9: Enrichment analysis results.

Term	Genes	P-Value	Benjamini
Natural killer cell-mediated cytotoxicity (hsa04650)	23	$9*10^{-7}$	$7,3*10^{-5}$
Complement and coagulation cascades (hsa04610)	20	$1,1*10^{-4}$	$2,1*10^{-3}$
Hippo signaling pathway (hsa04390)	24	$6,5*10^{-2}$	$2,7*10^{-1}$

2.2.2.4 Quantitative real-time PCR

For the qRT-PCR, the Absolute qPCR SYBR Green Mix (Thermo Fisher Scientific) was used, according to the manufacturer's protocol. The samples were measured in triplicates and analyzed on the Thermo Cycler Mx3005P from Stratagene.

The following program was run:

Initial activation step:	95 °C	15 min	
Denaturation:	95 °C	15s	40 cycles
Annealing:	60 °C	20s	
Elongation:	72 °C	15s	
Denaturation:	95 °C	60s	
Melting curve:	72 °C-95 °C	30s	

Raw data were analyzed with the MxPro 4.01 software from Stratagene for the calculation of Ct values or with the Cy0 method. Genes that showed a Ct/Cy0 value of 35 or higher were considered to be not expressed. In figures, this is indicated by a square. For the analysis, the Ct/Cy0 value of *hRPL27* or *hGAPDH* of each sample was subtracted from the Ct/Cy0 value of the gene of interest. Afterward, the mean *hRPL27* of all Ct/Cy0 values of the measurement was added to the calculated difference of the samples.

The standard deviation was calculated as follows:

Standard deviation $SD_{Total} = \sqrt{(SD^2_{(hRPL27)} + SD^2_{(gene\ of\ interest)})}$

2.2.3 Protein biochemical methods

2.2.3.1 Western Blot

Whole-cell lysates were made with RIPA lysis buffer together with protease inhibitors (1:1000) and phosphatase inhibitors (1:10). Protein concentration was determined by using the BCA protein assay kit (Thermo Fisher Scientific) according to the manufacture's protocol. 5 µg protein was loaded onto an 8 % or 12.5 % SDS polyacrylamide gel and separated with 1x SDS running buffer. Next, the samples were blotted on 0.2 µm nitrocellulose membranes (GE Healthcare) using 1x blotting buffer. The membrane was blocked with 5 % BSA in TBS-T for one hour at room temperature before it was incubated with primary antibody in 5 % BSA in TBS-T overnight at 4 °C. After washing with TBS-T, the membrane was incubated with HRP-labeled secondary antibody in TBS-T. Following several rounds of TBS-T washing steps, the proteins were detected with Immobilon Forte Western HRP substrate solution (Millipore) using the chemiluminescence imager ChemiDoc (Bio-Rad).

2.2.3.2 ELISA

The IFNγ ELISA (ELISA MAX^{TM} Standard Set Human IFN-γ) was obtained from Biolegend and conducted according to the manufacturer's protocol. Supernatants were centrifuged at 300 g for 5 minutes and used either undiluted or diluted up to 1:20 with assay diluent.

3 Results

NK cells are a crucial part of the innate immune system and play a major role in tumor immune surveillance. However, healthy cells should not be attacked by NK cells. Since the NK cell response is very powerful, it needs to be tightly controlled by the balance between activating and inhibitory receptor signaling [219].

3.1 Human macrophages do not express NKG2D and macrophage killing by NK cells occurs NKG2D-independent

One of the best-characterized activating receptors of NK cells is NKG2D, which binds to MICA/B and ULBP1-6 in humans. Those ligands are expressed on malignant or virus-infected cells but are absent on healthy cells [179].

Of note, reflecting its importance NK cell function of many tumor patients is restricted, which is often due to tumor-associated immune escape mechanisms. One described mechanism is the shedding of membrane-bound NKG2D-Ls via metalloproteases, which leads to a downregulation of NKG2D and thus impairs NK cell and T cell function [80] [202] [222].

High amounts of soluble MICA (sMICA) and soluble ULBP2 (sULBP2) were detectable in the ascites of ovarian cancer patients and negatively correlated with the RFS of the patients. Moreover, high amounts of sNKG2D-Ls also positively correlate with the amount of pro-tumorigenic $CD163^{+}CD206^{+}$ TAMs [221]. Surprisingly, NKG2D expression on patient-derived NK cells is not reduced [221] suggesting that the role of soluble NKG2D ligands within the ovarian cancer microenvironment is more complex than anticipated and does not exclusively function via NKG2D downregulation.

It has been described that NKG2D is expressed on activated murine macrophages [59] indicating that NKG2D-NKG2D-L axis may also interfere with macrophage activity or polarization. Nevertheless, the expression of NKG2D on human macrophages is still under debate. Therefore, NKG2D expression was analyzed in freshly isolated ascites samples of ovarian cancer patients. In these samples, NKG2D was not detectable on the surface of TAMs (Fig. 1A). Moreover, NKG2D was undetectable on the surface of human healthy donor monocyte-

derived macrophages (MDMs) (Fig. 1B), but it could be detected on NK cells and its expression was upregulated by stimulation with IL-2 and IL-15 (Fig. 1C). Furthermore, NKG2D was also not expressed in MDMs on mRNA level, while it was expressed in NK cells and T cells. Stimulation with LPS did not induce the expression of *KLRK1* (NKG2D receptor) (Fig. 1D).

In mice, Deng *et al.* nicely showed that NKG2D-L-expressing macrophages engage NKG2D on NK cells, and thereby induce NKG2D internalization and desensitization of NK cells. Of note, soluble NKG2D-Ls blocked these interactions, and restored NKG2D expression, thereby stimulating anti-tumor activity of NK cells and inducing tumor rejection [58]. The scenario in the ovarian cancer TME is obviously different since soluble NKG2D ligands in the ovarian TME are associated with a short survival time [221]. To test whether a NKG2D-ligand and NKG2D-mediated crosstalk between macrophages and NK cells is at least possible, I investigated whether NKG2D-Ls are expressed and inducible with LPS on macrophages from healthy donors and TAMs. Therefore, monocytes of healthy donors were differentiated into macrophages for at least six days without the polarization through cytokines, before they were treated with LPS for the indicated time points. On mRNA level, *MICA* and *MICB* were detectable and the expression was further increased by LPS stimulation (Fig. 1E and F; see Table S1 and S2 for Ct values). Since the expression of *ULBP2* was close to the detection limit, the variation between the donors was higher and no significant differences were seen after 48 hours and 72 hours of stimulation. However, the same tendency as for *MICA* and *MICB* could be seen (Fig. 1G; see Table S3 for Ct values). The expression of *ULBP1* and *ULBP3* could not be detected. However, MICA and MICB were not detected on the surface of healthy donor macrophages, while ULBP2 was weakly expressed (data not shown). In addition, MICA and MICB were also not expressed on the surface of TAMs (data not shown). Conversely, ULBP2 was clearly expressed on TAMs of two patients, while it was almost absent on TAMs of one patient (Fig. 1H). Thus, this data suggests that the NKG2D pathway might play a role in macrophage-NK cell crosstalk in the ovarian TME.

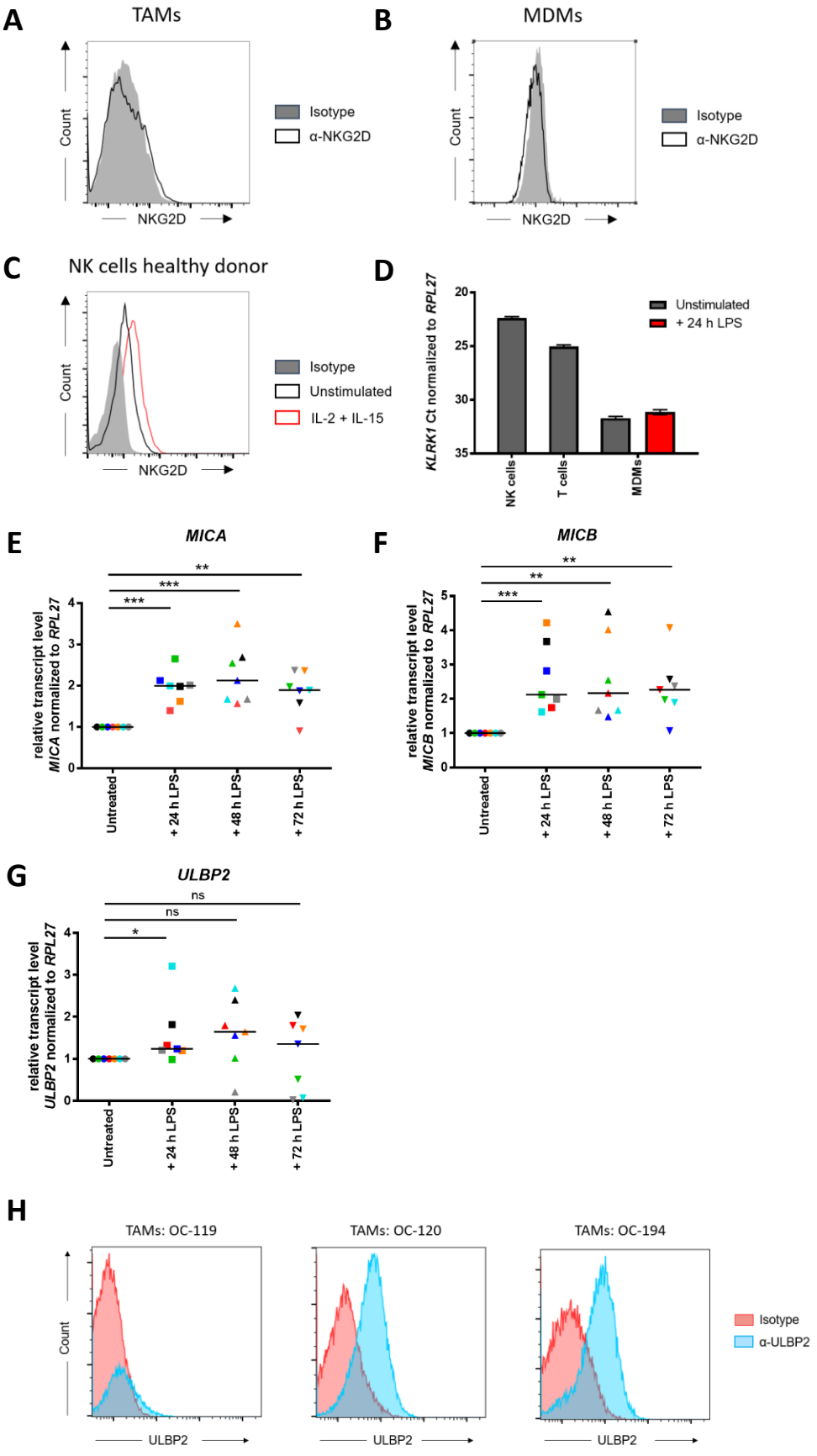
A
TAMs
Count
NKG2D
Isotype
α-NKG2D
B
MDMs
Count
NKG2D
Isotype
α-NKG2D
C
NK cells healthy donor
Count
NKG2D
Isotype
Unstimulated
IL-2 + IL-15
D
KLRK1 Ct normalized to RPL27
Unstimulated
+ 24 h LPS
NK cells
T cells
MDMs
E
MICA
relative transcript level MICA normalized to RPL27
Untreated
+ 24 h LPS
+ 48 h LPS
+ 72 h LPS
F
MICB
relative transcript level MICB normalized to RPL27
Untreated
+ 24 h LPS
+ 48 h LPS
+ 72 h LPS
G
ULBP2
relative transcript level ULBP2 normalized to RPL27
ns
ns
*
Untreated
+ 24 h LPS
+ 48 h LPS
+ 72 h LPS
H
TAMs: OC-119
TAMs: OC-120
TAMs: OC-194
Count
ULBP2
Isotype
α-ULBP2

Fig. 1: NKG2D receptor and ligand expression on immune cells.

Flow cytometry analysis of NKG2D receptor expression on TAMs **(A)**, healthy donor MDMs **(B)** and healthy donor NK cells (positive control) **(C)**. NK cells were stimulated with 200 U/ml IL-2 and 10 ng/ml IL-15 overnight to induce enhanced NKG2D expression (red histogram). Representative data of three independent biological replicates are displayed. qRT-PCR analysis of NKG2D receptor expression was performed for NK cells, T cells and MDMs **(D)**. MDMs were differentiated for 6 days and then stimulated with 100 ng/ml LPS for 24 hours before harvesting. Representative data of two independent biological replicates are displayed. Bar graphs represent means of triplicates ± technical SD. MDMs were stimulated with 100 ng/ml LPS for 24, 48 or 72 hours. qRT-PCR analysis of *MICA* **(E)**, *MICB* **(F)** and *ULBP2* **(G)** of MDMs was performed. Each color denotes a biological replicate (n = 7) and the median values are indicated by horizontal bars. For *ULBP1* and *ULBP3,* no Ct values were measured for any condition. Statistical significances were calculated using paired *t*-tests. **(H)** Flow cytometry analysis of ULBP2 expression on the surface of TAMs was performed. Data shown in Figure 1A and 1C was previously published in Vyas *et al.*, 2017 [221].

ns, not significant ($p \geq 0.05$), *p < 0.05, **p < 0.01, ***p < 0.001; MDMs, monocyte-derived macrophages; TAMs, tumor-associated macrophages; SD, standard deviation; LPS, lipopolysaccharide

Next, I investigated, whether the ascites of ovarian cancer patients influences the expression of NKG2D-Ls on healthy donor macrophages on mRNA level and whether the amount of sNKG2D-Ls present in the ascites has an impact on the expression. Monocytes were differentiated into macrophages in the presence of ascites with high or low amounts of sNKG2D-Ls. In fact, the presence of ascites led to a reduced expression of *MICA* and *MICB* seen as a tendency. However, no differences were observed between ascites with high or low amounts of sNKG2D-Ls (Fig. 2).

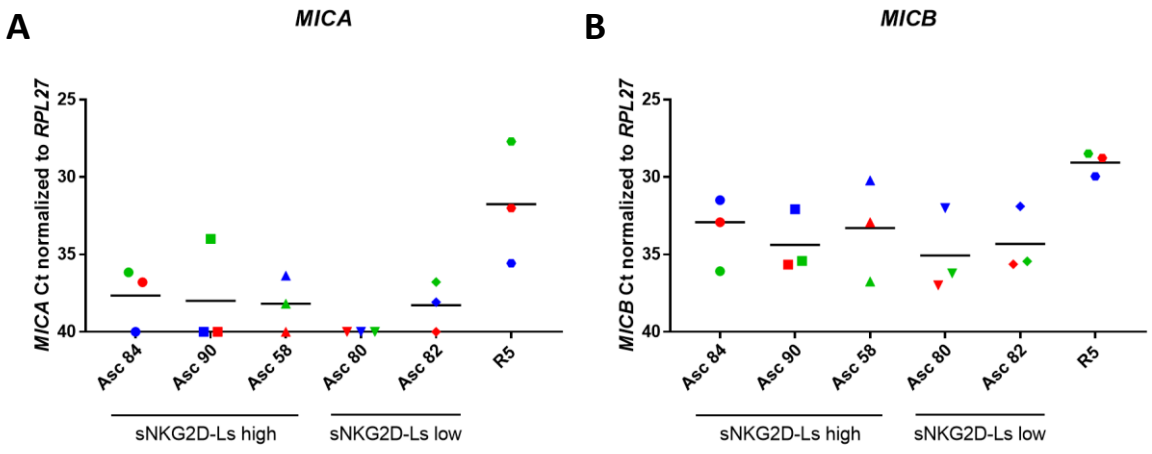

Fig. 2: Influence of ascites on the NKG2D-L expression of MDMs.

qRT-PCR analysis of *MICA* **(A)** and *MICB* **(B)** of MDMs. MDMs were differentiated for 6 days either in R5 medium or in 100 % ascites. The ascites samples were divided into two groups - one that contained high amounts of sNKG2D-Ls (asc 84, asc 90 and asc 58) and one that contained low amounts of sNKG2D-Ls (asc 80 and asc 82). Each color denotes a biological replicate (n = 3) and the median values are indicated by horizontal bars.

MDMs, monocyte-derived macrophages; asc, ascites; sNKG2D-Ls, soluble NKG2D ligands

Having seen that LPS induced upregulation of *MICA* and *MICB* on the transcriptional level (Fig. 1E and F), I analyzed, if LPS-treated macrophages are lysed more efficiently by NK cells in comparison to untreated macrophages owing to NKG2D signaling. Due to the LPS treatment, the macrophages showed higher basal viability, but they were not lysed more efficiently by NK cells. Furthermore, blocking of the NKG2D signaling did not result in reduced killing (Fig. 3), demonstrating that NK cell-mediated killing of macrophages is NKG2D-independent.

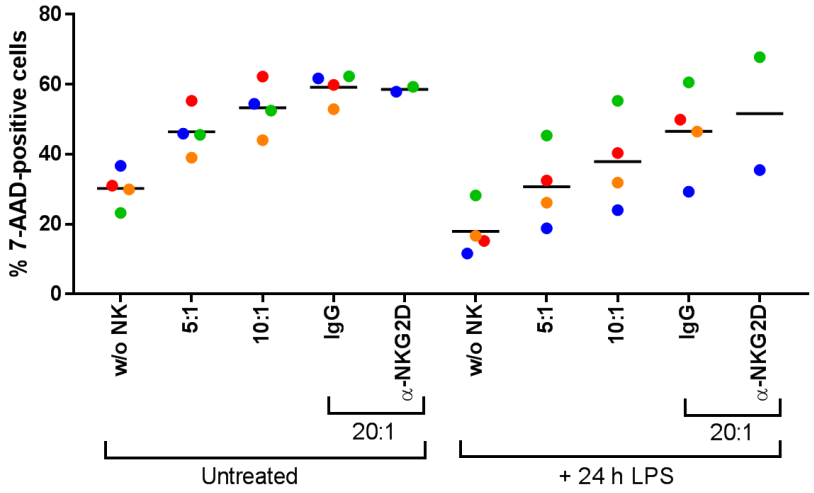

Fig. 3: Killing of MDMs by NK cells.

Cytotoxic potential of activated NK cells against LPS-stimulated MDMs was determined in a FACS-based killing assay. MDMs were differentiated for 6 days, before half of the cells were further stimulated with 100 ng/ml LPS for 24 hours. NK cells were activated overnight with 200 U/ml IL-2 and 10 ng/ml IL-15 and then incubated with untreated or LPS-treated MDMs as target cells at the effector to target cell (E:T) ratios 5:1, 10:1 and 20:1. Additionally, at the E:T ratio 20:1, NK cells were pre-incubated with 10 µg/ml α-NKG2D blocking antibody or matching isotype control before the co-incubation. Each color denotes a biological replicate (n = 2-4) and the median values are indicated by horizontal bars.

MDMs, monocyte-derived macrophages; LPS, lipopolysaccharide; E:T, effector to target cell ratio; w/o, without; NK, NK cell; 7-AAD, 7-aminoactinomycin D

Taken together, the NKG2D receptor is not expressed on human healthy donor and ovarian cancer-associated macrophages, but the NKG2D-Ls *MICA, MICB* and *ULBP2* are detectable on mRNA level and can be further induced by treatment with LPS. Expression of ULBP2 but not MICA/B was detectable on the protein level by flow cytometry. However, LPS-treated macrophages are not killed more efficiently by NK cells than untreated macrophages and the killing is NKG2D-independent. The expression of NKG2D-ligands of macrophages which are differentiated from monocytes in the presence of ascites was not affected or slightly reduced.

3.2 Membrane-bound NKG2D-Ls (mNKG2D-Ls) and soluble NKG2D-Ls (sNKG2D-Ls) induce different target genes

As described in section 3.1, the ascites of ovarian cancer patients contains high amounts of sMICA and sULBP2, but NKG2D is not downregulated on the surface of ovarian cancer patient-derived NK cells [221]. Therefore, the question arose, whether sNKG2D-Ls only passively block the receptor activation or whether the sNKG2D-Ls are able to induce signaling and gene expression via NKG2D receptor.

To address this question, a system in which solely the NKG2D signal could be monitored without any signal from other receptors was needed. Hence, the Drosophila cell line Schneider S2 was used, which does not express any known ligands binding to NK cell receptors, due to their evolutionary distinction [29]. An S2 cell line was generated, which stably expressed ULBP2 on its surface (Fig. 4A) and which bound to the recombinant NKG2D receptor (Fig. 4B), confirming proper folding and functionality of the ligand.

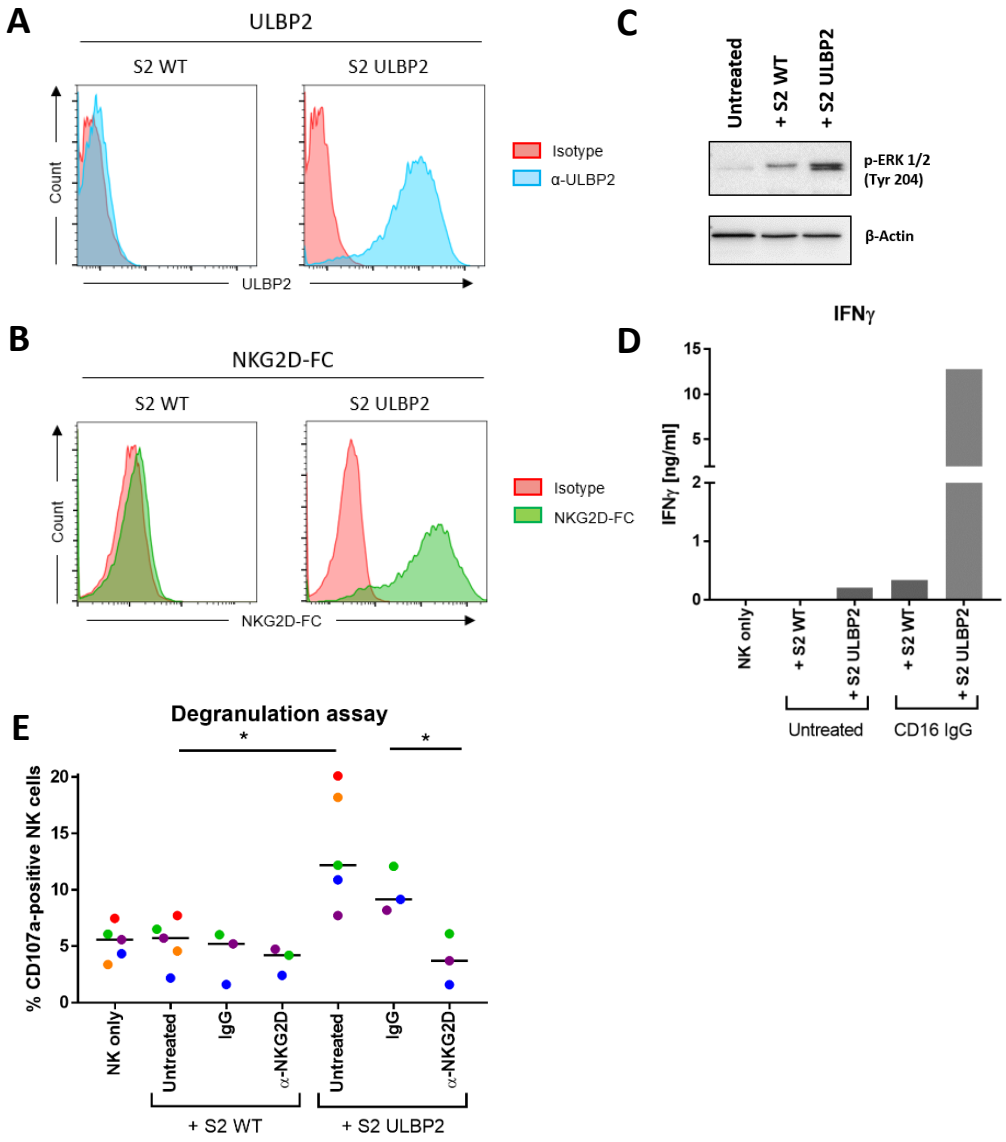

Fig. 4: Generation of ULBP2-positive S2 cells.

(A) Flow cytometry analysis of ULBP2 expression on S2 WT cells and stably transfected S2 ULBP2 cells. Representative data of seven independent replicates are shown. **(B)** Flow cytometry analysis of bound recombinant NKG2D receptor on S2 WT cells and stably transfected S2 ULBP2 cells was performed. Representative data of two independent replicates are shown. **(C)** Immunoblot analysis of pERK 1/2 was performed. IL-2 and IL-15-primed NK cells were incubated with S2 WT and S2 ULBP2 cells at the E:T ratio of 1:1 for 15 min at 37 °C before they were lysed. Representative data of four independent biological replicates are shown. Note, phosphorylation of ERK 1/2 after co-incubation with S2 ULBP2 cells was only visible in four out of eight donors. **(D)** IL-2 and IL-15-primed NK cells were incubated with S2 WT and S2 ULBP2 cells at the E:T ratio of 1:1 for 48 hours at 37 °C before the supernatant was collected, and the IFNγ level was measured by ELISA. In addition, S2 cells were incubated with a polyclonal α-S2 antibody for 30 min, before they were co-incubated for 48 hours with NK cells in order to stimulate the NK cells

via CD16 as a positive control. Representative data of three to five independent biological replicates. **(E)** Cytotoxic potential of activated NK cells against S2 WT and S2 ULBP2 cells was determined in a FACS-based degranulation assay. NK cells were activated overnight with 200 U/ml IL-2 and 10 ng/ml IL-15 and then incubated with S2 cells as target cells at the E:T ratio 1:1. In parallel, NK cells were pre-incubated with 10 µg/ml α-NKG2D blocking antibody or matching isotype control before the co-incubation. Each color denotes a biological replicate (n = 3-5) and the median values are indicated by horizontal bars. Statistical significances were calculated using paired *t*-tests (pairing based on replicate groups).

*p < 0.05; WT, wild type; E:T, effector to target cell; min, minutes; crossl., crosslinking

Next, it was tested if ULBP2-expressing S2 cells can activate primary human NK cells. Indeed, the cultivation of NK cells with S2-ULBP2 cells led to phosphorylation of extracellular signal-regulated kinase 1/2 (ERK1/2) (Fig. 4C). However, it must be noted, that this was highly donor-dependent and could not be seen in all donors tested. Furthermore, the cultivation of NK cells with S2-ULBP2 cells, but not with S2 WT cells, led to the secretion of IFNγ. The level was even higher when the NK cells were stimulated in parallel via the CD16 receptor, showing a synergistic effect (Fig. 4D). This is in line with the function of NKG2D as a co-stimulating receptor [30]. Finally, the cultivation of NK cells with S2-ULBP2 cells led to the degranulation of NK cells, shown by the increased presence of CD107a on the surface of NK cells. The degranulation was not observed, when the NKG2D receptor was blocked shortly before the assay was conducted, showing, that the degranulation of NK cells was NKG2D-dependent (Fig. 4E).

Since S2-ULBP2 cells can activate NK cells in a NKG2D-dependent manner, these cells were used as a model for NKG2D-engagement via membrane-bound NKG2D-L (mULBP2). To analyze the activity of soluble NKG2D-Ls, a recombinant protein was used. This protein (immunoligand) is a fusion protein of ULBP2 and an antibody fragment (BB4). It was previously shown that coating of target cells with an immunoligand enhanced the activation of NK cells by NKG2D signaling [172]. However, if the ligand is used without target cells, it should mimic the engagement of a sNKG2D-L. In order to prime NK cells and upregulate NKG2D, the cells were stimulated with IL-2 and IL-15 before the cells were incubated with S2 WT, S2 ULBP2 cells (mULBP2) or sULBP2-BB4 (sULBP2). To

identify target genes of NKG2D-stimulation through membrane-bound versus soluble ULBP2, RNA-seq was performed. NK cells stimulated with IL-2 and IL-15 alone were used as a control. Due to a short co-cultivation time of NK cells and S2 cells, the cells could not be separated before the RNA isolation. However, since S2 cells originated from a different species, the Drosophila specific reads within the RNA-seq could be subtracted from the human alignment. Through the RNA-seq, ten mULBP2-specific target genes and twelve sULBP2-specific target genes could be identified (Table 10; see Table S4 and S6 for TPM values, and S5 and S7 for fold change values). Looking at the mNKG2D-L-specific target genes, *CCR6* was the only one being downregulated, while all other genes were induced, amongst them classical activation genes of NKG2D signaling, like *CD69* and *TNF*. As expected, human *ULBP2* could be detected due to the presence of S2 ULBP2 cells, serving as an internal control (Table 10; see Table S4 for TPM values, and S5 for fold change values). Genes that were induced after sNKG2D-L engagement were, for example, *ACOD1, CEMIP, CLEC4E,* and *PLA2G7* (Table 10; see Table S6 for TPM values, and S7 for fold change values).

Table 10: Identification of membrane-bound ULBP2 (mULBP2) and soluble ULBP2 (sULBP2) target genes via RNA-seq and expression status in comparison to the corresponding control.

NK cells were primed with IL-2 and IL-15 for 16 hours and then incubated with S2 WT (negative control) or S2 ULBP2 cells (membrane-bound ULBP2) at the E:T ratio of 1:1 for 2 hours at 37 °C before they were lysed. In parallel, NK cells were stimulated with IL-2, IL-15 and 20 µg/ml sULBP2-BB4 (sULBP2) for 18 hours at 37 °C before the cells were lysed, RNA was isolated, and cDNA libraries were sequenced on an Illumina HiSeq 1500. As a control for the sULBP2, NK cells were only stimulated with IL-2 and IL-15 for 18 hours at 37 °C. In this experiment, a total of three independent biological replicates was used. Raw reads were aligned to the human and Drosophila genomes (retrieved from Ensembl 97) using STAR 2.6.1d. Reads aligning to the Drosophila genome were subtracted from the human alignment. Read counts were quantified in exonic regions of protein-coding transcripts and normalized to TPM. Differential gene expression was assessed via edgeR (version 3.24.3) at a threshold of FDR ≤ 0.05 and |log2FC| ≥ 1. Arrows and equation signs show whether the genes were upregulated, downregulated or whether the expression status was unaltered in at least two out of three donors, after stimulation with mULBP2 or sULBP2.

The RNA-seq was conducted by the IKMB (University Kiel), and the data were analyzed by Dr. Florian Finkernagel.

mULBP2 target genes

	mULBP2	sULBP2
CCR6	↓	=
CD69	↑	=
EGR1	↑	=
FOS	↑	=
NR4A2	↑	=
RAET1L	↑	=
TNF	↑	=
TNFRSF9	↑	=
TNFSF9	↑	=
ULBP2	↑	=

sULBP2 target genes

	mULBP2	sULBP2
ACOD1	=	↑
AQP9	=	↑
CEMIP	=	↑
CLEC4E	=	↑
CXCL8	=	↑
DSC1	=	↑
FRMD4A	=	↑
HHIPL1	↑	↑
IL1B	↑	↑
INHBA	↑	↑
NXPH4	=	↑
PLA2G7	↓	↑

Next, the identified target genes were validated via qRT-PCR. *ACOD1* (Fig. 5A), *CLEC4E* (Fig. 5B) and *PLA2G7* (Fig. 5C) were not expressed in freshly isolated NK cells. Priming with IL-2 and IL-15 led to weak basal expression of the genes, but stimulation with sULBP2-BB4 led to increased gene expression. To exclude any contribution of the BB4 part of the ULBP2 fusion protein, soluble BB4 was used as a control. sBB4 did not induce expression of the identified target genes. Furthermore, commercially available, recombinant sULBP2-His also induced the expression of *ACOD1*, *CLEC4E,* and *PLA2G7*, even though the upregulation was not as strong as after engagement of sULBP2-BB4 (Fig. 5).

Summing up, I could provide first evidence that sNKG2D-Ls induce target gene expression. Novel target genes of NKG2D by engagement of mNKG2D-Ls (see above) and by engagement of sNKG2D-Ls (*ACOD1*, *CLEC4E,* and *PLA2G7*) were identified.

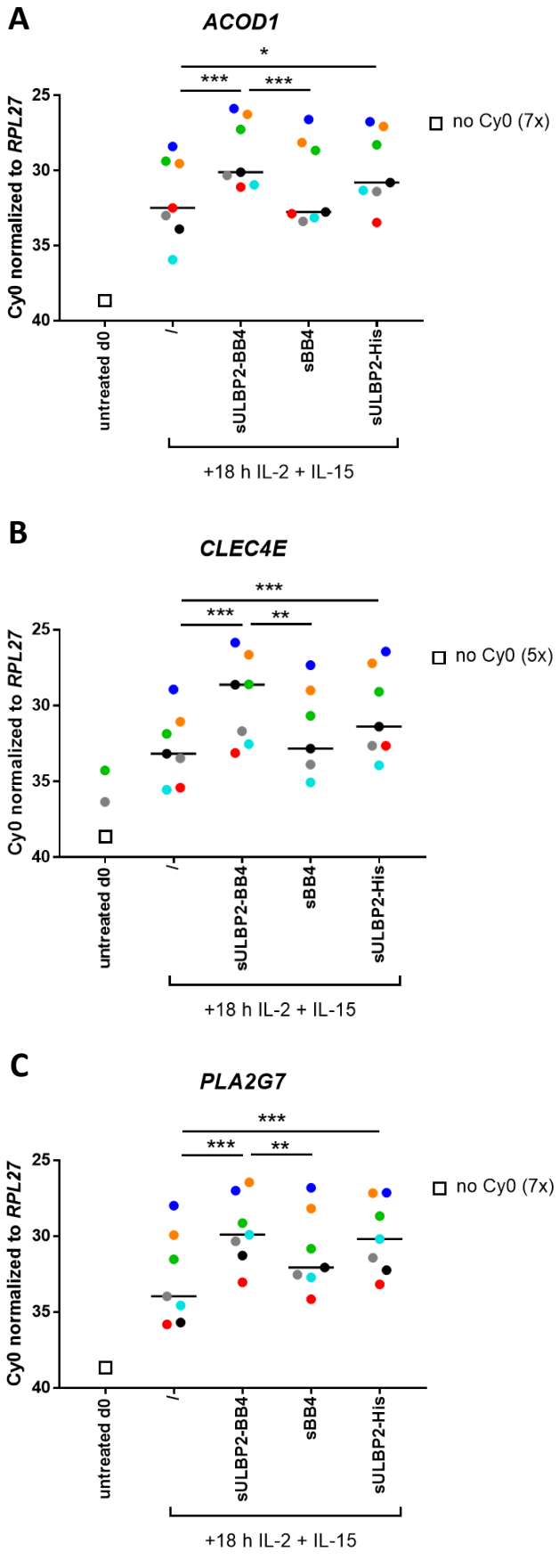
A
ACOD1
*
***
***
Cy0 normalized to RPL27
25
30
35
40
no Cy0 (7x)
untreated d0
/
sULBP2-BB4
sBB4
sULBP2-His
+18 h IL-2 + IL-15
B
CLEC4E
***
***
**
Cy0 normalized to RPL27
25
30
35
40
no Cy0 (5x)
untreated d0
/
sULBP2-BB4
sBB4
sULBP2-His
+18 h IL-2 + IL-15
C
PLA2G7
***
***
**
Cy0 normalized to RPL27
25
30
35
40
no Cy0 (7x)
untreated d0
/
sULBP2-BB4
sBB4
sULBP2-His
+18 h IL-2 + IL-15

Fig. 5: qRT-PCR validation of soluble ULBP2-induced target genes.

Validation of RNA-seq hits, which were significantly upregulated by sULBP2-BB4, via qRT-PCR analysis of **(A)** *ACOD1*, **(B)** *CLEC4E* and **(C)** *PLA2G7* was conducted. The graphs show the Cy0 values of the indicated genes that were normalized to *RPL27*. Each color denotes an independent biological replicate (n = 7) and the median values are indicated by horizontal bars. Squares indicate no measured Cy0 value. Statistical significances were calculated using paired *t*-tests for samples by which a Cy0 value was measured.

*p < 0.05, **p < 0.01, ***p < 0.001; s, soluble; d0, day 0

3.3 Ovarian cancer patient-derived NK cells show a tumor-associated phenotype

NK cells play an important role in the recognition and elimination of malignant cells [115]. Therefore, tumor cells try to avoid NK cell recognition by various escape mechanisms, such as shedding of activating ligands via metalloproteases [80] [222]. However, in ovarian cancer, NK cell impairment does not follow conventional inhibition strategies. Therefore, a global characterization of tumor-associated NK cells is needed to understand their role in ovarian cancer and thus, to identify novel potential target sites.

At first, surface expression of various NK cell activating receptors and inhibitory receptors, as well as the expression of exhaustion markers was investigated in one of the largest cohorts so far. Therefore, peripheral blood mononuclear cells (PBMCs) and ascites-derived peritoneal cells (PCs) of ovarian cancer patients were analyzed using flow cytometry. PBMCs from healthy blood donors were used as a control.

The number of NK cells within the ascites was slightly increased, even though this did not reach statistical significance (Fig. 6A). However, the MFI of CD56 was increased, hinting at an increased number of $CD56_{bright}$ $CD16_{low}$ NK cells, which produce higher amounts of cytokines but are less cytotoxic than $CD56_{dim}$ $CD16_{high}$ NK cells [51] (Fig. 6B). This was in line with a reduced expression of CD16 (Fig. 6C and D).

Since the NKG2 family consists of activating and inhibitory receptors, it was important to determine the status of those in ovarian cancer, because the balance

between those receptors determines whether the NK cells are activated or not [115]. While NKG2A (an inhibitory receptor) and NKG2D (an activating receptor), were upregulated, NKG2C, which is also an activating receptor, was downregulated on ascites-derived NK cells (Fig. 7) [22].

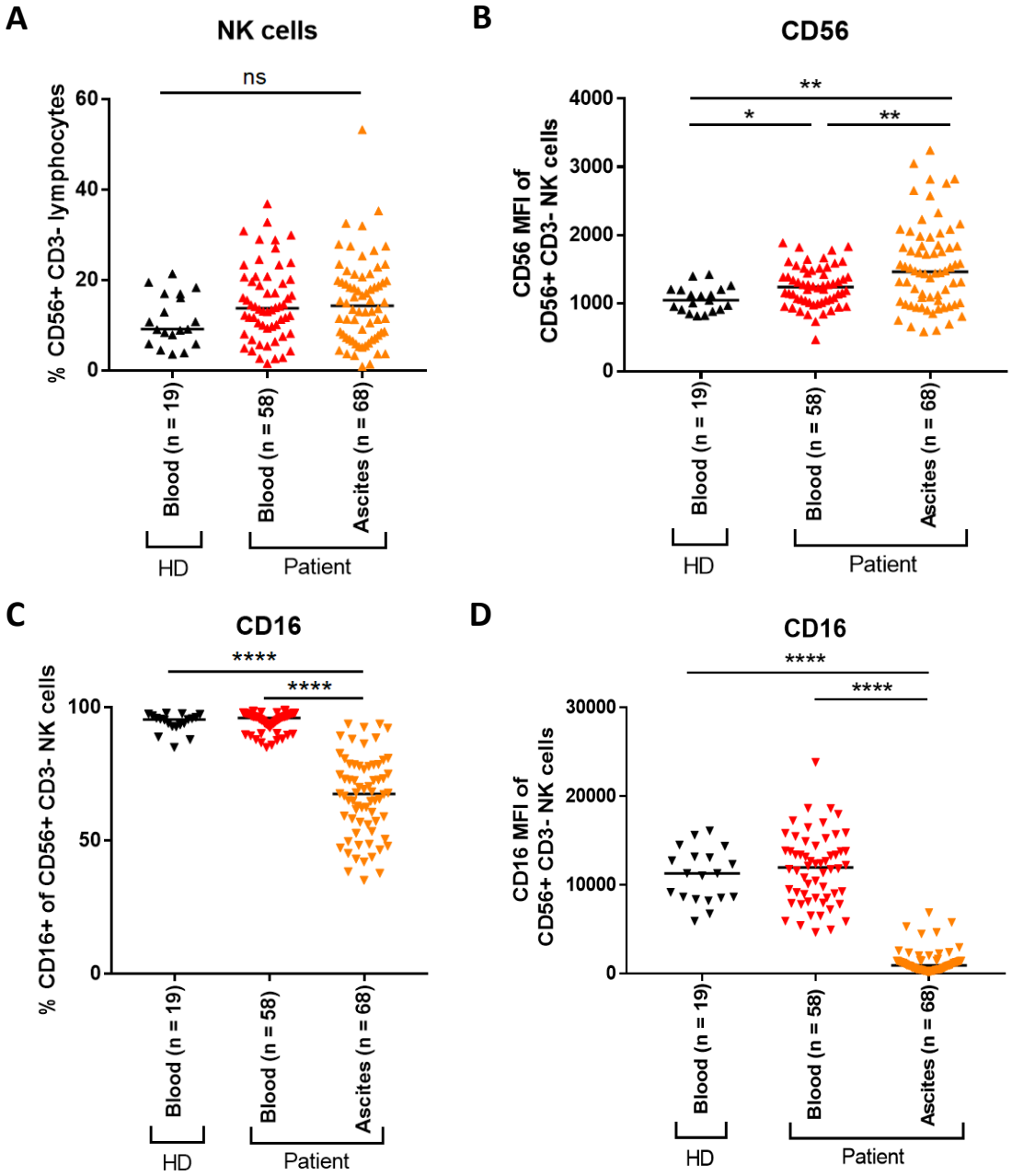

Fig. 6: Characterization of NK cells of ovarian cancer patients.

PBLs of healthy donors, PBMCs of the blood and ascites-derived PCs of ovarian cancer patients were analyzed using flow cytometry. Scatter plots show the percent NK cells of lymphocytes **(A)**, MFI of CD56 **(B)**, percent CD16-positive NK cells **(C)** and MFI of CD16 **(D)**. Each symbol denotes

a biological replicate (n = 19-68) and the median values are indicated by horizontal bars. Statistical significances were calculated using unpaired *t*-tests without Welch's corrections.

ns, not significant ($p \geq 0.05$), *p < 0.05, **p < 0.01, ****p ≤ 0.0001; PBL, peripheral blood lymphocytes; PBMCs, peripheral blood mononuclear cells; PCs, peritoneal cells; HD, healthy donor; MFI, mean fluorescence intensity

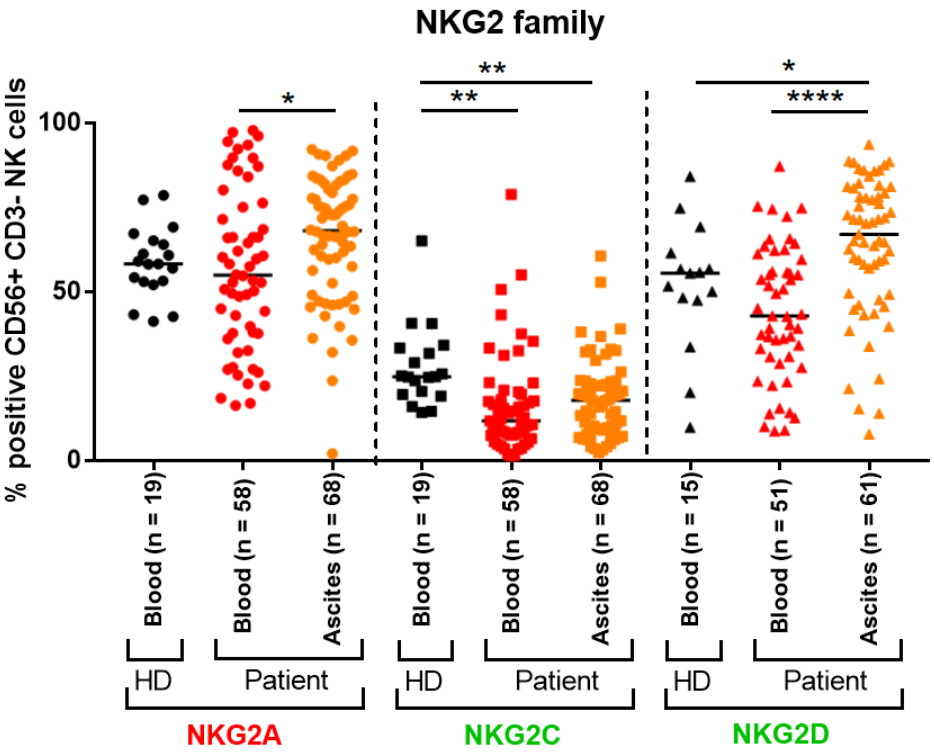

Fig. 7: Analysis of NKG2 family member expression on ovarian cancer patient-derived NK cells.

PBLs of healthy donors, PBMCs of the blood and ascites-derived PCs of ovarian cancer patients were analyzed using flow cytometry. Scatter plots show the percentage of NKG2A, NKG2C, NKG2D, and CD94 positive NK cells. Each symbol denotes a biological replicate (n = 15-68) and the median values are indicated by horizontal bars. Statistical significances were calculated using unpaired *t*-tests without Welch's corrections.

*p < 0.05, **p < 0.01, ****p ≤ 0.0001; PBL, peripheral blood lymphocytes; PBMCs, peripheral blood mononuclear cells; PCs, peritoneal cells; HD, healthy donor

Another prominent family providing activating receptors are the NCRs. To this family belong the receptors NKp30, NKp44 and NKp46 [166] [199] [218], which are all downregulated on patient-derived NK cells (Fig. 8). Furthermore, yet another prominent activating receptor, DNAM-1, was strongly downregulated on patient-derived NK cells (Fig. 8).

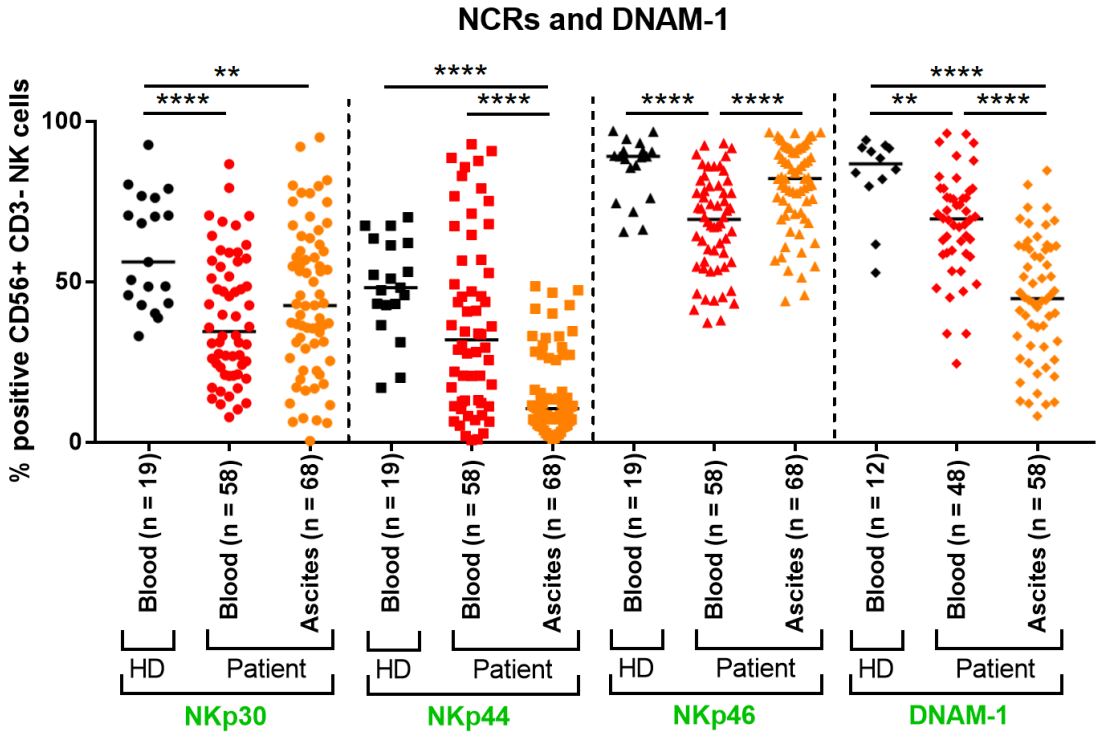

Fig. 8: Analysis of NCR family member and DNAM-1 expression on ovarian cancer patient-derived NK cells.

PBLs of healthy donors, PBMCs of the blood and ascites-derived PCs of ovarian cancer patients were analyzed using flow cytometry. Scatter plots show the percentage of NKp30, NKp44, NKp46, and DNAM-1 positive NK cells. Each symbol denotes a biological replicate (n = 12-68) and the median values are indicated by horizontal bars. Statistical significances were calculated using unpaired *t*-tests without Welch's corrections.

*p < 0.05, **p < 0.01, ***p < 0.001, ****p ≤ 0.0001; PBL, peripheral blood lymphocytes; PBMCs, peripheral blood mononuclear cells; PCs, peritoneal cells; HD, healthy donor; NCR, natural cytotoxicity receptors

KIRs consist of inhibitory receptors and a few activating receptors. CD158a (KIR2DL1), CD158b (KIR2DL3) and CD158e (KIR3DL1) all belong to the inhibitory receptors [74]. The CD158a expression was not altered in comparison to healthy donor NK cells, but CD158b and especially CD158e were downregulated on ascites-derived NK cells (Fig. 9).

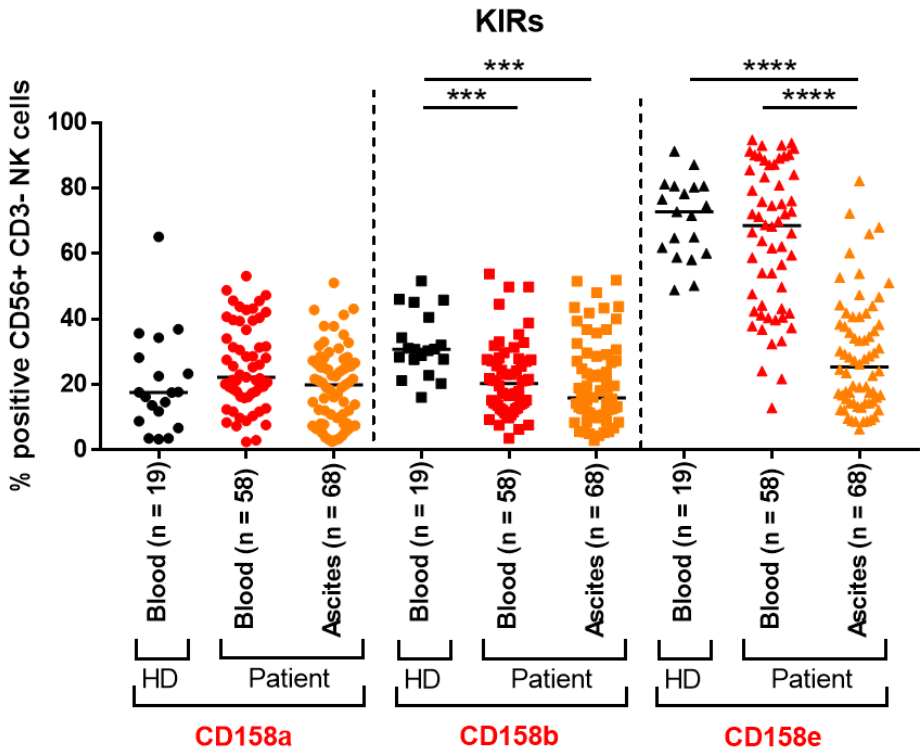

Fig. 9: Analysis of KIR family member expression on ovarian cancer patient-derived NK cells.

PBLs of healthy donors, PBMCs of the blood and ascites-derived PCs of ovarian cancer patients were analyzed using flow cytometry. Scatter plots show the percentage of CD158a, CD158b, and CD158e positive NK cells**.** Each symbol denotes a biological replicate (n = 19-68) and the median values are indicated by horizontal bars. Statistical significances were calculated using unpaired *t*-tests without Welch's corrections.

***p < 0.001, ****p ≤ 0.0001; PBL, peripheral blood lymphocytes; PBMCs, peripheral blood mononuclear cells; PCs, peritoneal cells; HD, healthy donor; KIR, killer-cell immunoglobulin-like receptors

Finally, the activation and exhaustion status of the NK cells was analyzed. CD69, an early activation marker, was strongly expressed on ascites-derived NK cells. Moreover, expression of the co-inhibitory receptors PD-1 and TIM-3, also known as immune checkpoint targets, was detected on NK cells of some patients. Surprisingly, the expression of another co-inhibitory receptor, TIGIT, was downregulated on the ascites-derived NK cells (Fig. 10).

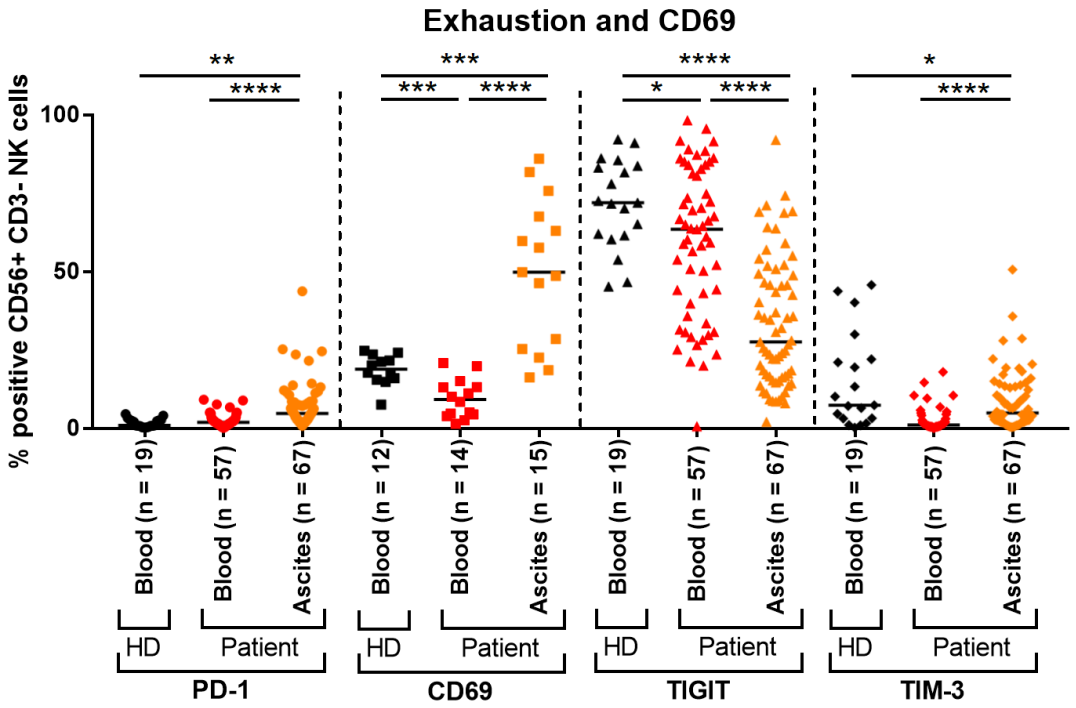

Fig. 10: Analysis of exhaustion marker and the early activation marker CD69 expression on ovarian cancer patient-derived NK cells.

PBLs of healthy donors, PBMCs of the blood and ascites-derived PCs of ovarian cancer patients were analyzed using flow cytometry. Scatter plots show the percentage of PD-1, CD69, TIGIT, and TIM-3 positive NK cells. Each symbol denotes a biological replicate (n = 12-67) and the median values are indicated by horizontal bars. Statistical significances were calculated using unpaired *t*-tests without Welch's corrections.

ns, not significant ($p \geq 0.05$), *p < 0.05, **p < 0.01, ***p < 0.001, ****p ≤ 0.0001; PBL, peripheral blood lymphocytes; PBMCs, peripheral blood mononuclear cells; PCs, peritoneal cells; HD, healthy donor

In conclusion, patient-derived NK cells show a mixed tumor-associated phenotype, in which most of the activating receptors are downregulated and the expression status of the inhibitory receptors was mixed (Table 11). Furthermore, they showed a high expression of the early activation marker CD69 and NKG2D, which are known as cytotoxicity receptors. Besides, the expression of exhaustion markers (PD-1 and TIM-3) was detectable (see Table 11 as a summary).

Table 11: Summary surface marker expression on patient-derived NK cells in comparison to healthy donor NK cells.

Activating receptors	Inhibitory receptors	Exhaustion
NKG2C ↓	NKG2A ↑	PD-1 ↑
NKG2D ↑	CD158a =	TIM-3 ↑
NKp30 ↓	CD158b ↓	TIGIT ↓
NKp44 ↓	CD158e ↓	
NKp46 =		
DNAM-1 ↓		
CD69 ↑		

3.4 Reduced cytotoxic potential of ovarian cancer patient-derived NK cells can be partially restored by IL-2 and IL-15

Since the expression of various activating receptors was downregulated whereas expression of CD69 and NKG2D was enhanced, I investigated the cytotoxic potential of patient-derived NK cells. Therefore, freshly isolated ascites-derived NK cells were cultivated with K562 target cells either in standard medium or medium supplemented with 25 % ascites. Both showed a strongly reduced degranulation against target cells in comparison to healthy donor NK cells (18.5 % vs. 39 %). However, this reduced cytotoxic potential is restored, when the NK cells were stimulated with IL-2 and IL-15. The killing activity could be further increased, when NK cells were cultivated without any addition of ascites fluid (Fig. 11). Of note, basal degranulation of freshly isolated NK cells and resting NK cells without target cells was around 5 %, while basal degranulation of activated NK cells without target cells was slightly increased up to around 11 % (data not shown).

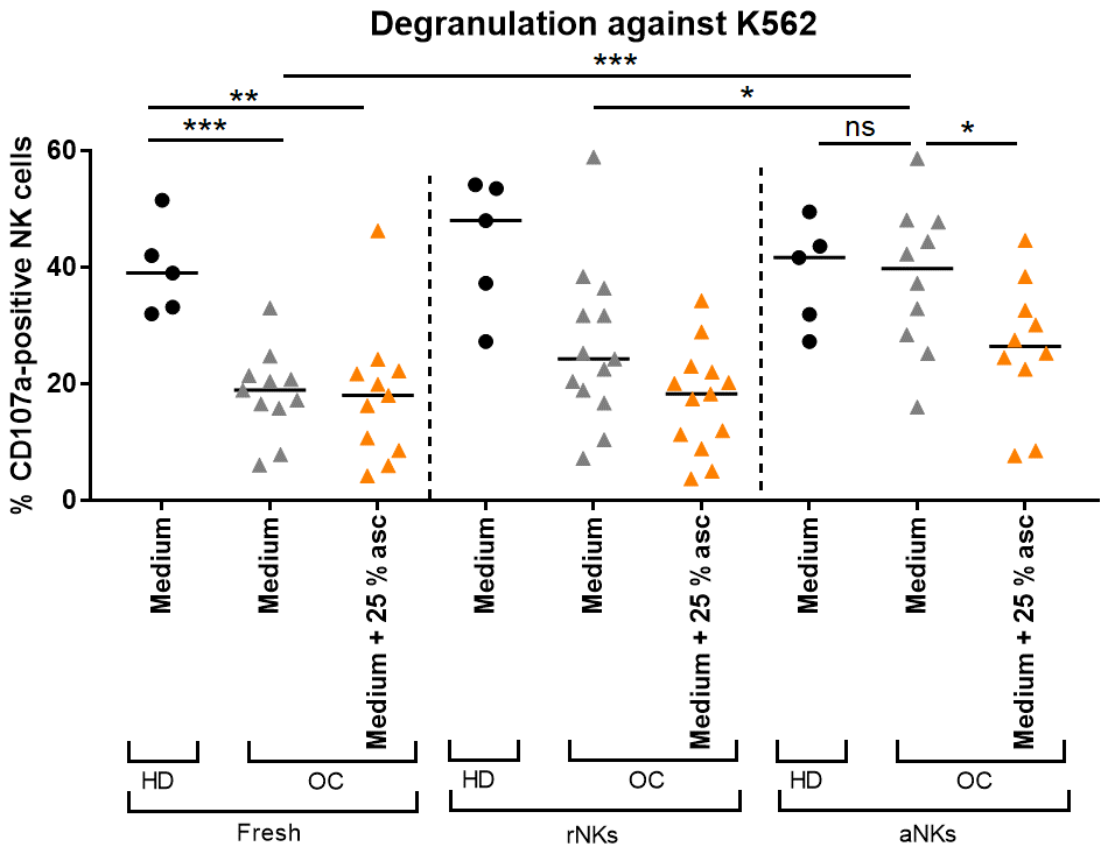

Fig. 11: Cytotoxic activity of healthy donor NK cells and ovarian cancer patient ascites-derived NK cells against K562.

Cytotoxic potential of freshly isolated NK cells, resting NK cells (rNKs; 10 U/ml IL-2 overnight) and activated NK cells (aNKs; 200 U/ml IL-2 and 10 ng/ml IL-15 overnight) against K562 as target a target cell line was determined in a FACS-based degranulation assay. NK cells and K562 were co-cultivated at an E:T ratio of 5:1 for six hours, before degranulation was analyzed using flow cytometry. Healthy donor NK cells (HD) were cultivated in medium. Ascites-derived NK cells (OC) were cultivated with normal medium and normal medium supplemented with 25 % ascites. For freshly isolated NK cells, the assay itself was conducted in medium or medium supplemented with 25 % ascites. Each symbol denotes a biological replicate (HD: n = 5, OC: n = 10-13) and the median values are indicated by horizontal bars. Statistical significances were calculated using unpaired *t*-tests.

ns, not significant ($p \geq 0.05$), *p < 0.05, **p < 0.01, ***p < 0.001; HD, healthy donor; OC, ovarian cancer patient; rNK, resting NK cells; aNKs, activated NK cells; asc, ascites; E:T, effector : target

Next, I analyzed which activating receptors play a major role in the recognition and elimination of ovarian cancer cells. Therefore, the ovarian cancer cell line OVCAR-4 was used as target cells and different activating receptors were blocked. Resting peripheral blood lymphocytes (rPBLs) showed significantly lower degranulation and less killing of OVCAR-4, when the activating receptors DNAM-1 and NKG2D were blocked (Fig. 12A and B). The degranulation of the PBLs and killing of the target cells was higher when they were primed with IL-2 and IL-15 overnight (aPBLs), as expected. Again this was dependent on DNAM-1 and NKG2D, too (Fig. 12C and D). Furthermore, blocking of CD16 led to a reduced killing of the target cells, but interestingly to a higher degranulation (Fig. 12C and D). However, the killing of the target cells and the degranulation of the NK cells was not completely abolished by blocking a single activating receptor, hinting to a dependency on multiple activating receptors. Nonetheless, when the healthy PBLs were cultivated in ascites, they were no longer able to degranulate and kill the target cells (Fig. 12E and F).

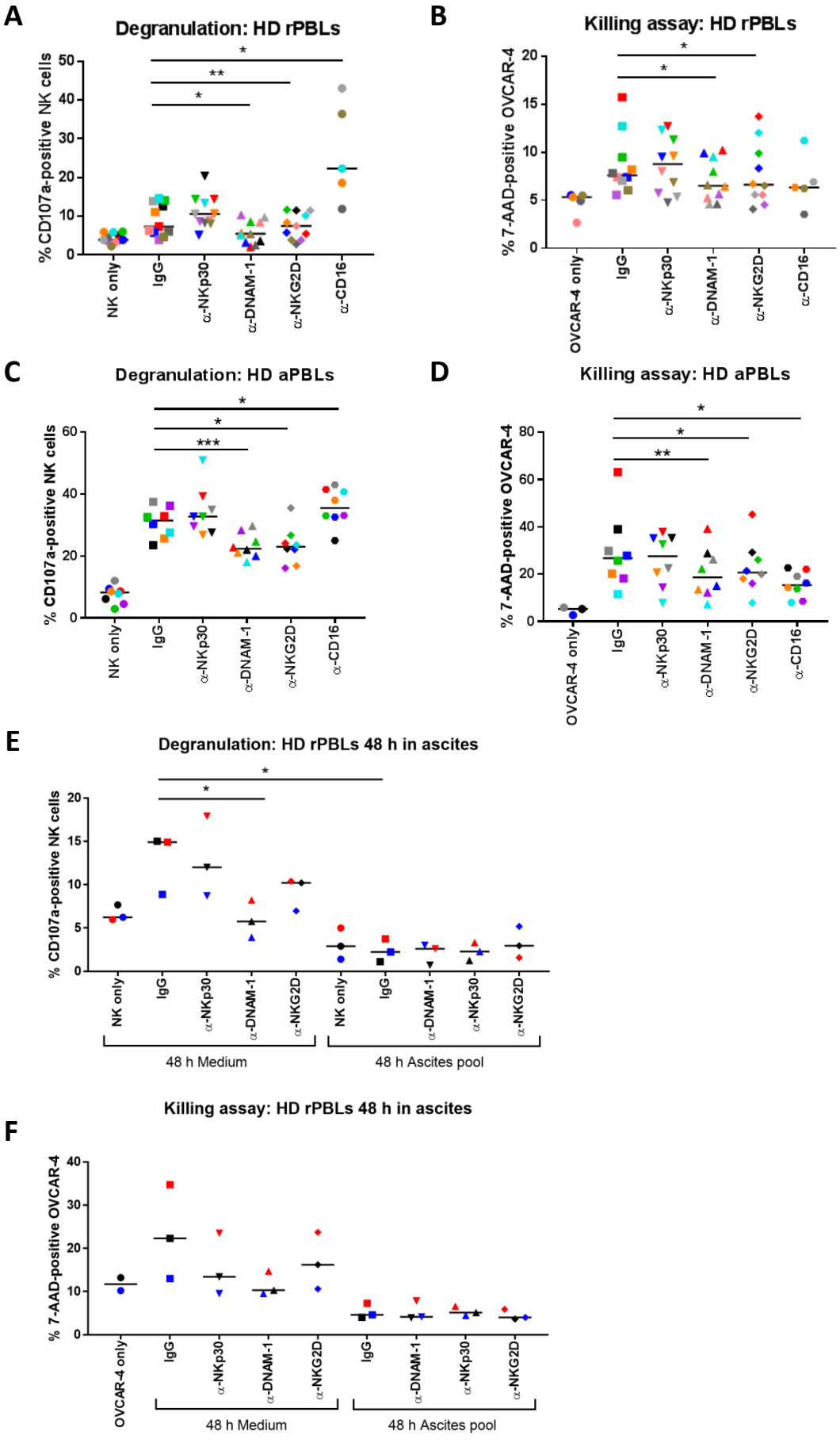
A
Degranulation: HD rPBLs
% CD107a-positive NK cells
NK only
IgG
α-NKp30
α-DNAM-1
α-NKG2D
α-CD16
B
Killing assay: HD rPBLs
% 7-AAD-positive OVCAR-4
OVCAR-4 only
C
Degranulation: HD aPBLs
D
Killing assay: HD aPBLs
E
Degranulation: HD rPBLs 48 h in ascites
48 h Medium
48 h Ascites pool
F
Killing assay: HD rPBLs 48 h in ascites

Fig. 12: The impact of ascites on healthy donor NK cells and the role of different NK cell activation receptors for the recognition and lysis of OVCAR-4.

Cytotoxic potential of resting (untreated) or activated healthy donor PBLs (200 U/ml IL-2 and 10 ng/ml IL-15 overnight) against OVCAR-4 was determined in a FACS-based assay. PBLs were pre-treated with 10 µg/ml blocking antibodies against NKp30, DNAM-1, NKG2D, and CD16, respectively or matching isotype control for 30 minutes before the assay was performed. **(A)** rPBLs and OVCAR-4 were co-cultivated at an E:T ratio of 100:1 for 6 hours, before degranulation was analyzed using flow cytometry. For the analysis, NKp46-positive NK cells were gated. Each color denotes a biological replicate (n = 11), and the median values are indicated by horizontal bars. **(B)** Depicted is a FACS-based killing assay of healthy donor rPBLs against OVCAR-4 at an E:T ratio of 100:1. Each color denotes a biological replicate (n = 10) and the median values are indicated by horizontal bars. **(C)** aPBLs and OVCAR-4 were co-cultivated at an E:T ratio of 100:1 for 6 hours, before degranulation was analyzed using flow cytometry. For the analysis, it was gated on NKp46-positive NK cells. Each color denotes a biological replicate (n = 8) and the median values are indicated by horizontal bars. **(D)** FACS-based killing assay of healthy donor aPBLs against OVCAR-4 at an E:T ratio of 100:1 were performed. Each color denotes a biological replicate (n = 8) and the median values are indicated by horizontal bars. Statistical significances were calculated using paired *t*-tests. **(E)** PBLs were incubated for 48 hours in medium or 100 % ascites of an ascites pool of 5 patients, together with 10 U/ml IL-2. Then, a FACS-based degranulation assay was performed at an E:T ratio of 100:1. For the analysis, it was gated on NKp46-positive NK cells. Each color denotes a biological replicate (n = 3) and the median values are indicated by horizontal bars. **(F)** PBLs were incubated for 48 hours in medium or 100 % ascites of an ascites pool of 5 patients, together with 10 U/ml IL-2. Then, a FACS-based killing assay was performed at an E:T ratio of 100:1. Each color denotes a biological replicate (n = 3) and the median values are indicated by horizontal bars.

ns, not significant ($p \geq 0.05$), *p < 0.05, **p < 0.01, ***p < 0.001; HD, healthy donor; rPBL, resting peripheral blood lymphocytes; aPBL, activated peripheral blood lymphocytes; E:T, effector : target

Taken together, ascites-derived NK cells show a diminished cytotoxic potential, which can be restored when the cells are activated by IL-2 and IL-15 and are no longer influenced by the ascites. Hence, the effect of ascites is reversible. Conversely, healthy donors NK cells are immediately influenced by the presence of ascites and are no longer able to kill target cells. Furthermore, the killing of ovarian cancer cells is predominantly dependent on DNAM-1 and NKG2D signaling.

3.5 TGFβ in ovarian cancer ascites mediates DNAM-1 downregulation and impairs NK cell cytotoxicity

In section 3.4 it was observed that the killing of ovarian cancer cells depends on the signaling of NKG2D and DNAM-1. Nevertheless, it was also observed that NKG2D was not downregulated on ascites-derived NK cells, but the DNAM-1 expression was strongly decreased (Fig. 7 and 8). Therefore, I wanted to investigate which factor present in the ascites is responsible for the downregulation of DNAM-1. It has already been described that TGFβ can reduce the expression of DNAM-1 [83] and that TGFβ is present in the ascites of ovarian cancer patients. In particular, TGFβ1 was associated with a reduced RFS [181].

Hence, the effect of ascites on the expression of DNAM-1 with or without TGFβ inhibition was analyzed. Cultivation of healthy donor NK cells in ascites led to a downregulation of DNAM-1 on mRNA and on protein level, which could be abrogated by both a TGFβ receptor kinase inhibitor or a TGFβ blocking antibody (Fig. 13). Moreover, recombinant TGFβ1 downregulates DNAM-1 on mRNA level and on protein level and this downregulation could be partially blocked by the presence of a TGFβ receptor kinase inhibitor (SB-431542) or a TGFβ blocking antibody (Fig. 13). However, no detectable differences were observed on the magnitude of *CD226* downregulation, when ascites of patients with high or low amounts of TGFβ1 were used (data not shown). Nevertheless, it must be noted that only a small sample size was analyzed. Moreover, it was observed that the effect of TGFβ1 and ascites had a greater impact on the expression of the *CD226* mRNA than on the expression of DNAM-1 on the surface. Of note, the cultivation of primary NK cells itself led to diminished expression of *CD226* on mRNA level, but this was not as strong as in the presence of TGFβ and not affected by TGFβ inhibition (data not shown).

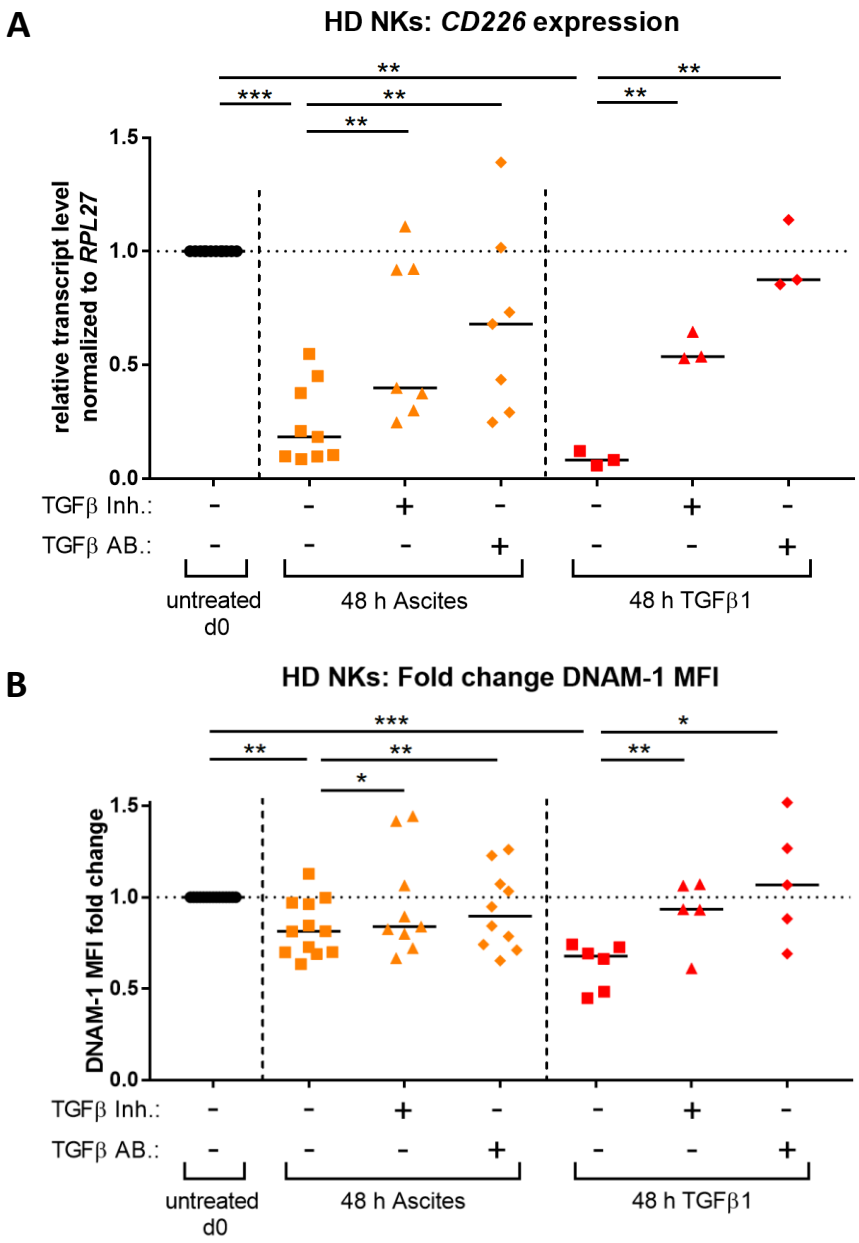

Fig. 13: DNAM-1 expression of healthy donor NK cells is decreased by TGFβ that is found in ovarian cancer ascites.

(A) The Scatter plot displays the *CD226* expression in healthy donor NK cells that were cultivated in medium + 1 ng/ml TGFβ1 or 100 % ascites. Furthermore, the effect of TGFβ was blocked by using a TGFβ blocking antibody (5 µg/ml) or a TGFβ receptor kinase inhibitor (SB-431542; 10 µM). Each symbol denotes a biological replicate (n = 3-12) and the median values are indicated by horizontal bars. Statistical significances were calculated using paired *t*-tests. **(B)** DNAM-1 expression on the surface of healthy donor NK cells was analyzed using flow cytometry. NK cells were cultivated and treated as in **(A)**. Each symbol denotes a biological replicate (n = 5-15) and the median values are indicated by horizontal bars. Statistical significances were calculated using paired *t*-tests. Of note, viability of NK cells was monitored and cultivation of

primary human NK cells led to decreased viability. However, the lower viability had only a minor impact on the expression of DNAM-1. Plasma was not used as a control for the ascites since pure plasma is much higher concentrated than within the blood and viability of the cells cultured in pure plasma is strongly decreased. Therefore, it does not mimic the physiological situation.

*p < 0.05, **p < 0.01, ***p < 0.001, ****p ≤ 0.0001; HD, healthy donor; asc, ascites; AB, antibody; Inh., inhibitor; MFI, mean fluorescence intensity; d0, day 0

Next, it was investigated, whether abrogation of the TGFβ signaling could restore the degranulation capacity of patient-derived NK cells. Therefore, the target cell line K562 was used, as their killing is also dependent on DNAM-1 (Fig. 14A). Indeed, blockage of the TGFβ signaling led to a higher degranulation of resting ascites-derived NK cells (Fig. 14B). Here, the degranulation of resting NK cells after blockage of the TGFβ signaling was as high as the degranulation of cytokine-primed, activated NK cells after blockage of the TGFβ signaling (data not shown). This showed that the TGFβ present in the ascites of the patients is responsible for the lower cytotoxic potential of the NK cells. The blockage of the TGFβ signaling fully restored the cytotoxic potential of the NK cells with no requirement for activation by cytokines. Freshly isolated NK cells did not respond to the blocking of the TGFβ signaling probably due to the short assay duration. Moreover, the TGFβ signaling blockage also led to enhanced expression of DNAM-1 on the surface of the patient-derived NK cells (Fig. 14C).

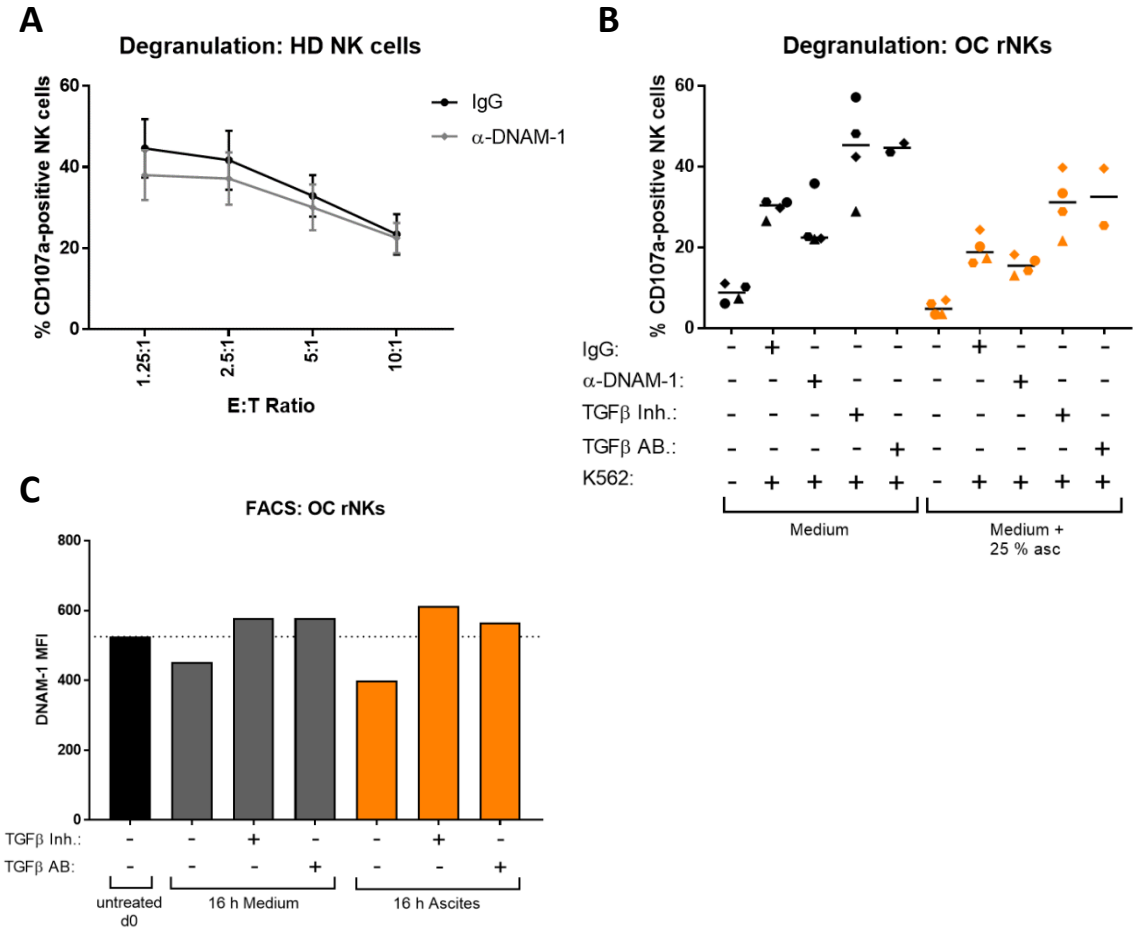

Fig. 14: Impact of DNAM-1 and TGFβ blockage on the cytotoxicity of NK cells against K562 cells.

(A) FACS-based degranulation assay of healthy donor NK cells using K562 as a target cell line at different E:T ratios with or without DNAM-1 blockage was performed. Dots represent the means of four independent biological replicates ± SD. **(B)** Depicted is a degranulation assay of ovarian cancer patient NK cells. The ascites-derived NK cells were cultivated with normal medium or normal medium supplemented with 25 % ascites and stimulated with 10 U/ml IL-2 overnight (rNKs), before the killing of K562 was determined in a FACS-based degranulation assay. In parallel, TGFβ signaling was blocked before the cells were seeded by using a TGFβ blocking antibody (5 µg/ml) or a TGFβ receptor kinase inhibitor (SB-431542; 10 µM). The antibody and the inhibitor were present during the whole cultivation time. NK cells and K562 were co-cultivated at an E:T ratio of 5:1 for 6 h, before degranulation was analyzed using flow cytometry. In addition, NK cells were pre-treated with 10 µg/ml DNAM-1 blocking antibody or matching isotype control for 30 minutes before the degranulation assay was performed. Each symbol denotes a biological replicate (n = 1-4) and the median values are indicated by horizontal bars. **(C)** Shown is the DNAM-1 expression of ascites-derived NK cells after cultivation overnight with 10 U/ml IL-2 and TGFβ blocking antibody (5 µg/ml) or a TGFβ receptor kinase inhibitor (SB-431542; 10 µM).

Representative data of two biological independent replicates (for the blocking antibody just one patient) is shown.

HD, healthy donor; OC, ovarian cancer patient; rNK, resting NK cells; asc, ascites; E:T, effector : target; AB, antibody; Inh., inhibitor; MFI, mean fluorescence intensity; d0, day 0

Summing up, TGFβ present in the ascites of ovarian cancer patients is responsible for the downregulation of DNAM-1 on mRNA and protein level. Hence, a blockage of the TGFβ signaling leads to an increased expression of DNAM-1 on patient-derived NK cells and restored cytotoxic potential of the NK cells.

3.6 Tumor-associated NK cells show dysregulation of the kegg pathways natural killer cell-mediated cytotoxicity, the Hippo pathway, and several complement factors

I have shown that the balance between activating and inhibitory receptors of patient-derived NK cells is altered and that the NK cells show a reduced cytotoxic potential. However, the molecular changes were not analyzed yet. Thus, RNA-seq of NK cells derived from six patients was performed and the results were compared to RNA-seq results of healthy donor NK cells. Here, 1811 genes were upregulated in patient-derived NK cells, while 1224 genes were downregulated in comparison to healthy donor NK cells. Enrichment analysis using DAVID functional annotation clustering software identified several pathways being dysregulated in patient-derived NK cells. Among these was the kegg pathway natural killer cell-mediated cytotoxicity (hsa04650) from which 23 genes showed an altered gene expression (Fig. 15A). To those genes belonged *ZAP70, FCGR3A, VAV1,* and *VAV3,* which were all downregulated in patient-derived NK cells (Fig. 15B and C). Next, the RNA-seq results were validated using qRT-PCR and it could be confirmed that the expression of *FCGR3A, VAV1, CD226,* and *HLA-E* was diminished in the ascites-derived NK cells (Fig. 15D).

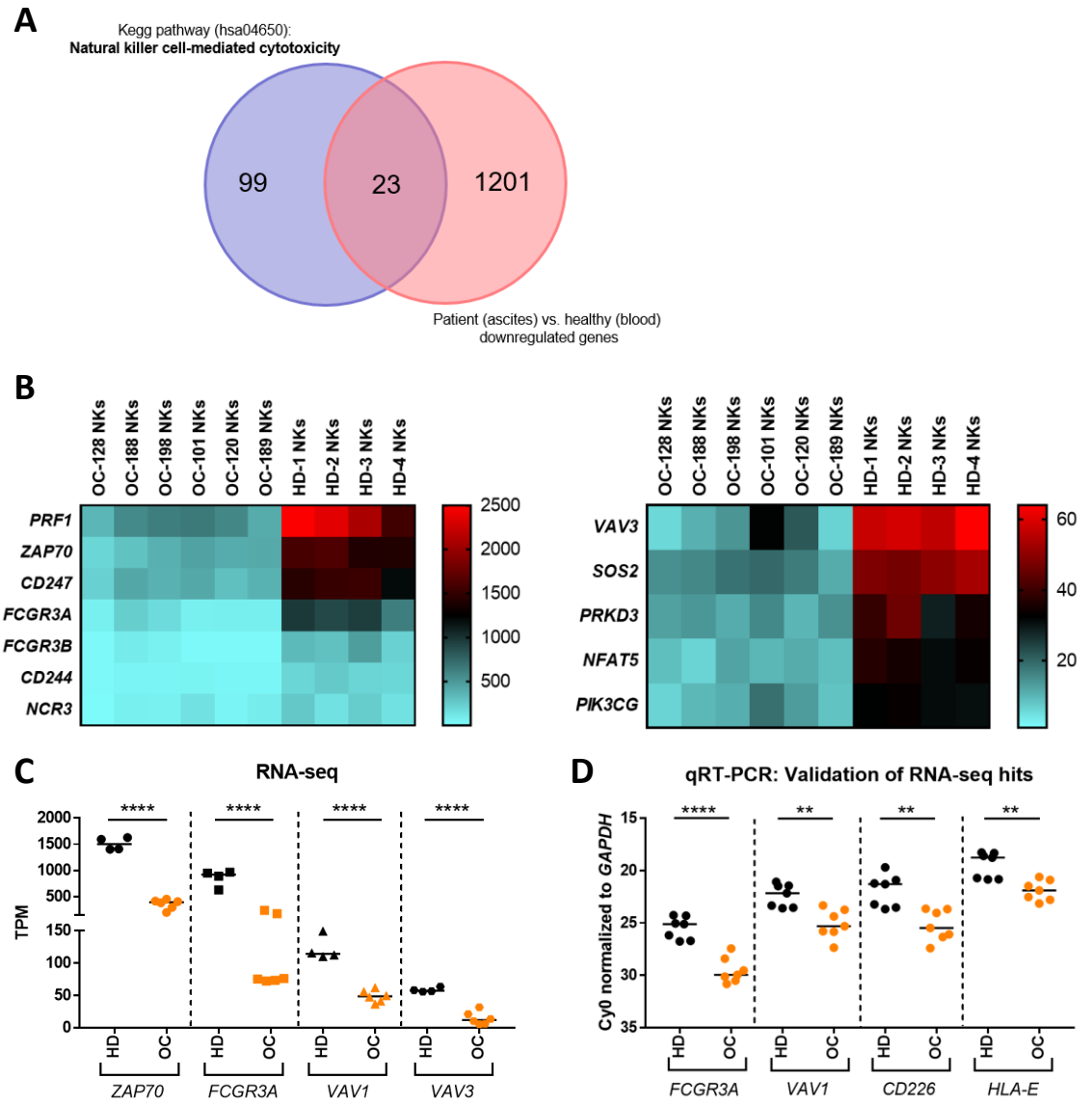

Fig. 15: Comparison of healthy donor NK cells and ascites -derived ovarian cancer patient NK cells by RNA-seq defines a dysregulation of natural killer cell-mediated cytotoxicity genes.

Identification of differentially expressed genes in healthy donor NK cells (HD) versus ascites-derived patient NK cells (OC) based on RNA-seq data. Raw reads were aligned to the human genome (retrieved from Ensembl 92) using STAR 2.4.1a. Read counts were quantified in exonic regions of protein-coding transcripts and normalized to TPM. **(A)** The Venn diagram shows the overlap of genes that were downregulated in patient-derived NK cells in comparison to healthy donor NK cells, and genes belonging to the kegg pathway natural killer cell-mediated cytotoxicity. **(B)** The heatmap shows the expression of cytotoxicity genes (depicted is the TPM value) that were significantly differentially expressed between healthy donor NK cells and ovarian cancer patient NK cells. **(C)** Scatter plot showing TPM values of *ZAP70, FCGR3A, VAV1,* and *VAV3* based on RNA-seq results. Each symbol denotes a replicate (n = 4-6) and the median values are

indicated by horizontal bars. **(D)** The validation of RNA-seq hits via qRT-PCR analysis of significantly differentially expressed genes is depicted. The graph shows the Cy0 values of the indicated genes that were normalized to *GAPDH*. Each symbol denotes an independent biological replicate (n = 7) and the median values are indicated by horizontal bars. Statistical significances were calculated using unpaired *t*-tests without Welch's corrections.

**p < 0.01, ****p ≤ 0.0001; HD, healthy donor; OC, ovarian cancer patient; TPM, transcripts per million reads

The RNA-seq was conducted by the genomics core facility (University Marburg), and the data was analyzed by Dr. Florian Finkernagel.

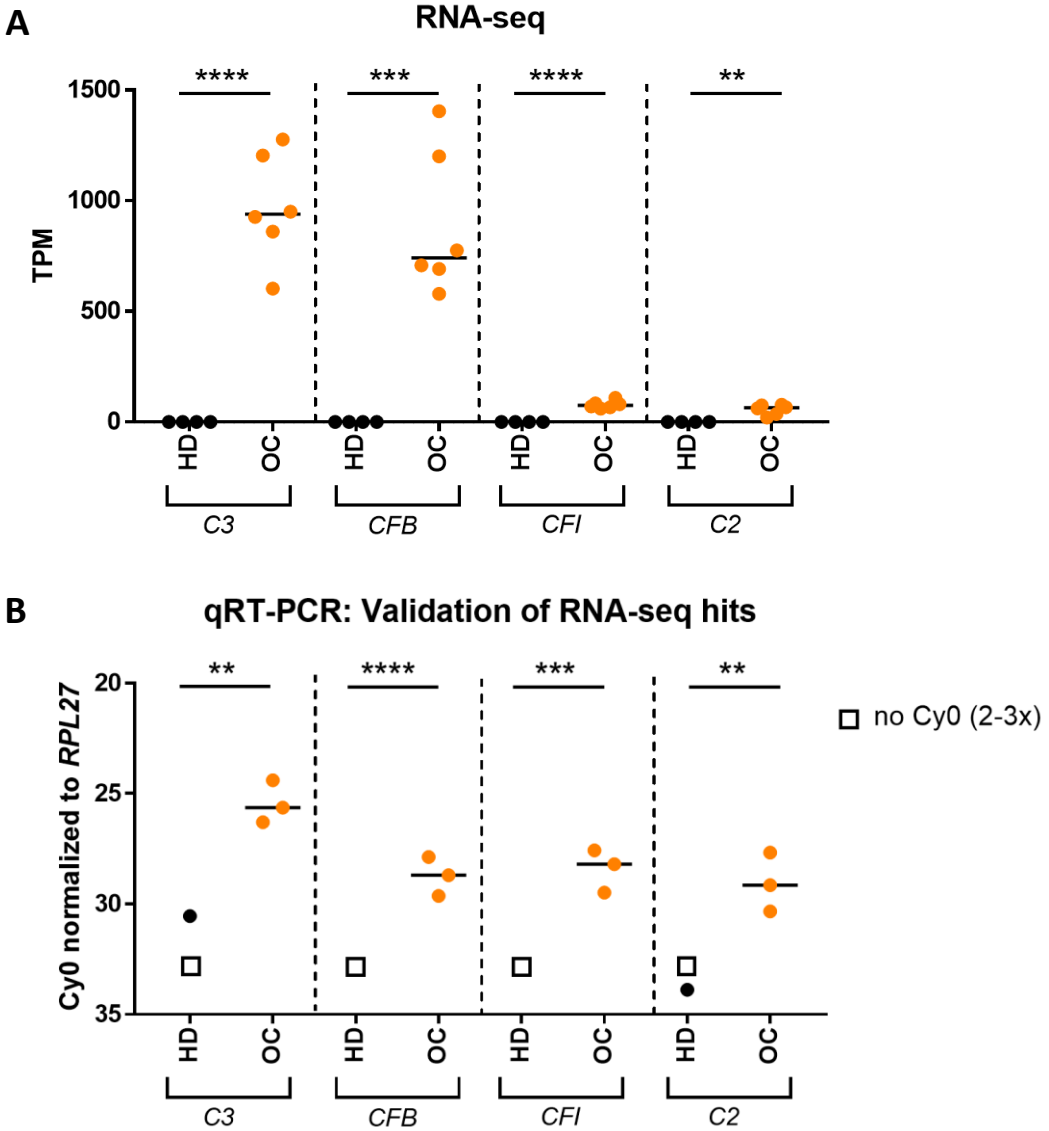

Fig. 16: Comparison of healthy donor NK cells and ascites-derived ovarian cancer patient NK cells by RNA-seq identifies upregulation of complement factors.

Identification of differentially expressed genes of the complement system in healthy donor NK cells (HD) versus ascites-derived patient NK cells (OC) based on RNA-seq data. Raw reads were aligned to the human genome (retrieved from Ensembl 92) using STAR 2.4.1a. Read counts were

quantified in exonic regions of protein-coding transcripts and normalized to TPM. Scatter plot showing TPM values of *C3, CFB, CFI,* and *C2* based on RNA-seq results **(A)**. Each symbol denotes a replicate (n = 4-6) and the median values are indicated by horizontal bars. **(B)** Depicted is the validation of RNA-seq hits via qRT-PCR analysis of significantly differentially expressed genes of the complement system. The graphs show the Cy0 values of the indicated genes that were normalized to *RPL27*. Each symbol denotes an independent biological replicate (n = 3) and the median values are indicated by horizontal bars. Squares indicate no measured Cy0 value. Statistical significances were calculated using unpaired *t*-tests without Welch's corrections for samples by which a Cy0 value was measured.

**p < 0.01, ***p < 0.001, ****p ≤ 0.0001; HD, healthy donor; OC, ovarian cancer patient; TPM, transcripts per million reads

The RNA-seq was conducted by the genomics core facility (University Marburg), and the data was analyzed by Dr. Florian Finkernagel.

Another important group showing aberrant regulation is the group of the complement factors. *C3, CFB, CFI,* and *C2* were not expressed in healthy donor NK cells, but expressed in patient-derived NK cells (Fig. 16A). This could be confirmed using qRT-PCR (Fig. 16B). *C1S* and *C1R* were also upregulated in patient-derived NK cells, but this could not be confirmed by qRT-PCR since reliable primers could not be obtained.

The second pathway that was dysregulated in patient-derived NK cells is the Hippo pathway (hsa04390) of which 24 genes showed an altered gene expression (Fig. 17A). Genes, that are usually active within the Hippo pathway, such as *LATS1, LATS2, MOB1A,* and *MOB1B* showed a decreased expression in patient-derived NK cells, while genes, which are usually silenced, like *YAP1* or *TEAD4,* showed an increased expression (Fig. 17B and C). Furthermore, target genes of the Hippo pathway, such as *CTGF* and *AMOTL2*, were also expressed in ascites-derived NK cells, while they were not expressed in healthy donor NK cells (Fig. 17D). However, this did not apply to all potential target genes. *AREG* was higher expressed in the healthy donor NK cells in comparison to the patient-derived NK cells (Fig. 17D). The results from the RNA-seq could be confirmed using qRT-PCR for the target genes analyzed, besides *AREG,* which did not show significant differences (Fig. 17E and F).

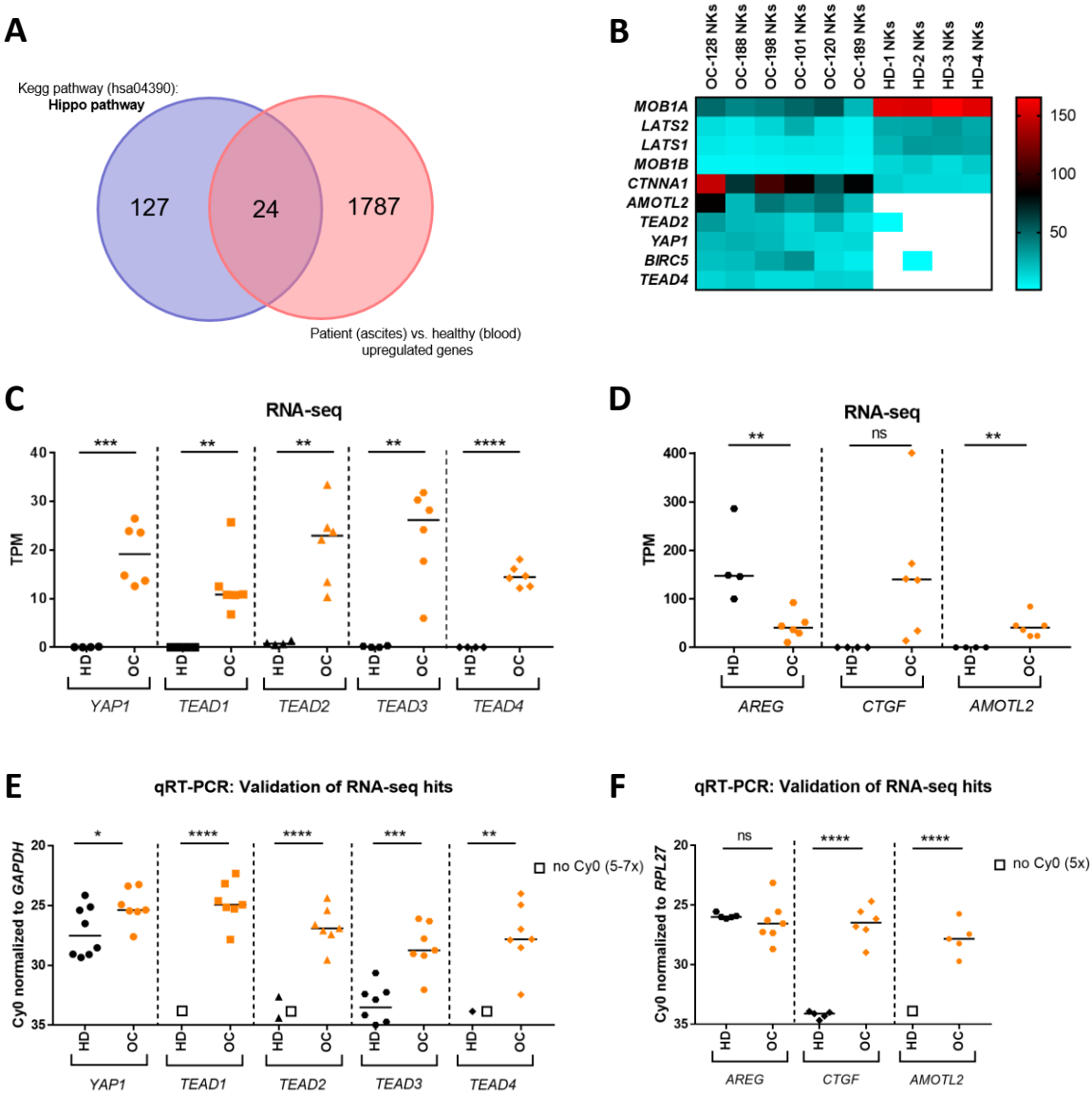

Fig. 17: Comparison of healthy donor NK cells and ascites-derived ovarian cancer patient NK cells by RNA-seq defines dysregulation of the Hippo pathway.

Identification of differentially expressed genes in healthy donor NK cells (HD) versus ascites-derived patient NK cells (OC) based on RNA-seq data. Raw reads were aligned to the human genome (retrieved from Ensembl 92) using STAR 2.4.1a. Read counts were quantified in exonic regions of protein-coding transcripts and normalized to TPM. **(A)** Depicted is the Venn diagram showing the overlap of genes that were upregulated in patient-derived NK cells in comparison to healthy donor NK cells, and genes belonging to the Hippo pathway. **(B)** The Heatmap shows the expression of Hippo pathway genes (depicted is the TPM value) that were significantly differentially expressed between healthy donor NK cells and ovarian cancer patient NK cells. **(C)** The Scatter plot shows TPM values of *YAP1, TEAD1, TEAD2, TEAD3* and *TEAD4* and of the Hippo target genes *AREG, CTGF,* and *AMOTL2* based on RNA-seq results **(D)**. Each symbol denotes a biological replicate (n = 4-6) and the median values are indicated by horizontal bars.

(E and F) Validation of RNA-seq hits via qRT-PCR analysis of significantly differentially expressed genes of the Hippo pathway **(E)** and the Hippo target genes **(F)** was performed. The graphs show the Cy0 values of the indicated genes that were normalized to *GAPDH* or *RPL27*. Each symbol denotes an independent biological replicate (n = 3-7) and the median values are indicated by horizontal bars. Squares indicate no measured Cy0 value. Statistical significances were calculated using unpaired *t*-tests without Welch's corrections for samples by which a Cy0 value was measured.

ns, not significant ($p \geq 0.05$), *p < 0.05, **p < 0.01, ***p < 0.001, ****p ≤ 0.0001; HD, healthy donor; OC, ovarian cancer patient; TPM, transcripts per million reads

The RNA-seq was conducted by the genomics core facility (Marburg) and the data was analyzed by Dr. Florian Finkernagel.

Since *TEAD4* and the other TEAD family members were exclusively expressed in patient-derived NK cells, I focused on the transcription factor TEAD4 and its potential coactivators. It has been described that it mainly binds to YAP1, but it can also interact with p160 proteins (*e.g.* NCOA1) and VGLL proteins [128] (Fig. 18A). Therefore, the expression of the coactivators was measured. The expression of *NCOA1* was strongly reduced, while the expression of *VGLL1* was induced and not expressed in healthy donor NK cells (Fig. 18B and C). Furthermore, TEAD4 protein expression was enhanced, as well as a decreased NCOA1 expression in patient-derived NK cells (Fig. 18D). Interestingly, YAP1 was strongly phosphorylated in ascites-derived NK cells, while it was not phosphorylated in healthy donor NK cells (Fig. 18D). If YAP1 is phosphorylated, it cannot enter the nucleus and induce the expression of target genes. Furthermore, it is marked for ubiquitination and can be degraded [253].

Next, it was investigated, if the ascites is responsible for the downregulation of *NCOA1* and if it also influences the expression of the transcription factor yin yang 1 (*YY1*), which has been described to act as a repressor on the transcription of IFNγ [240]. Indeed, *NCOA1* was downregulated in healthy donor NK cells after treatment with ascites (Fig. 19A). This was also true for *YY1*, but it must be noted that donor-dependent differences were observed (Fig. 19B).

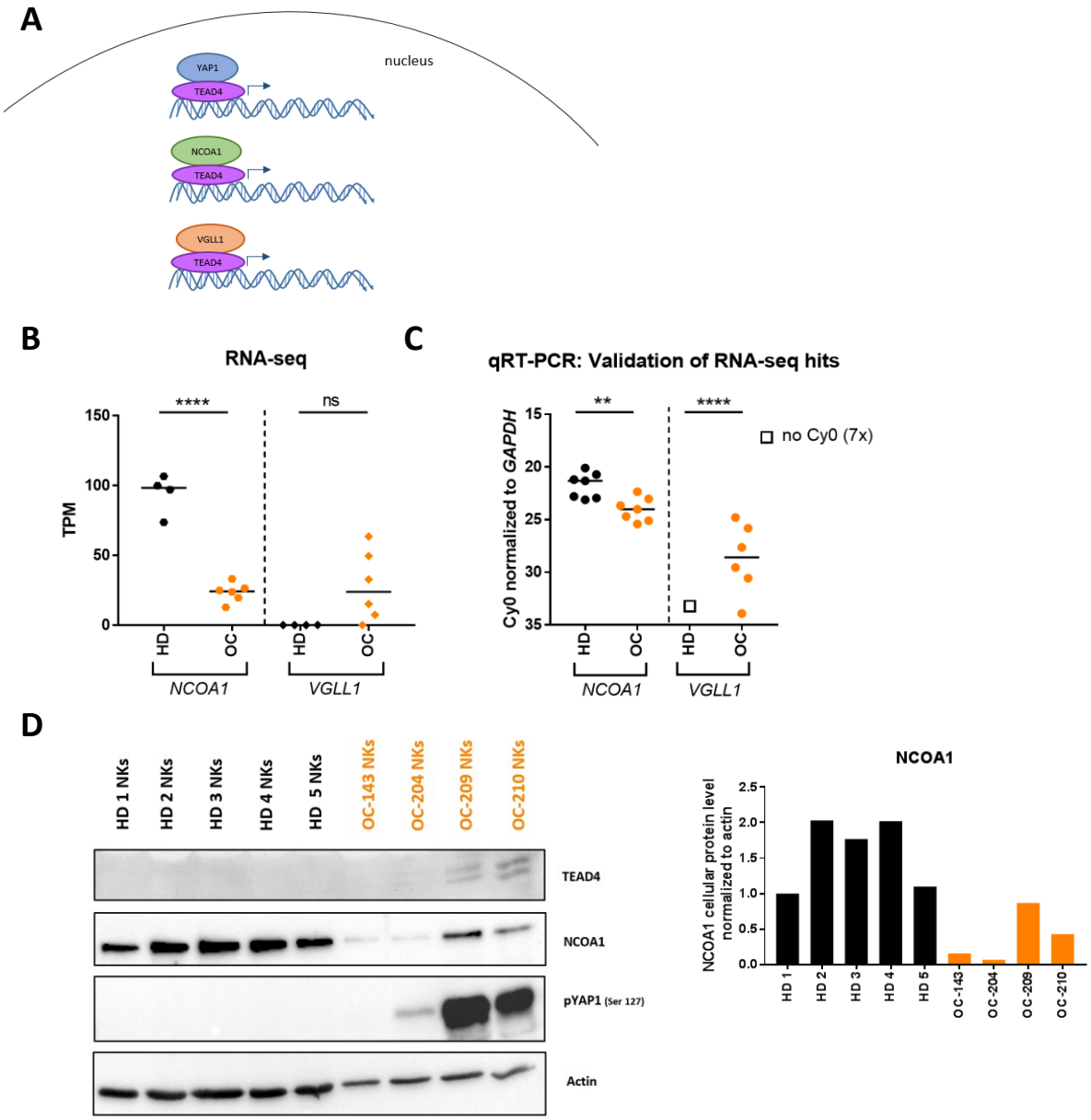

Fig. 18: Expression of TEAD4 binding partners in healthy donor NK cells and ovarian cancer patient-derived NK cells.

(A) Depicted is a schematic representation of TEAD4 binding partners within the nucleus that can induce transcription. **(B)** The Scatter plot shows TPM values of the TEAD4 binding partners *NCOA1* and *VGLL1* based on RNA-seq results. Each symbol denotes a replicate (n = 4-6) and the median values are indicated by horizontal bars. Raw reads were aligned to the human genome (retrieved from Ensembl 92) using STAR 2.4.1a. Read counts were quantified in exonic regions of protein-coding transcripts and normalized to TPM. **(C)** Validation of RNA-seq results via qRT-PCR analysis was performed. Each symbol denotes an independent biological replicate (n = 7), and the median values are indicated by horizontal bars. The square indicates no measured Cy0 value. Statistical significances were calculated using unpaired *t*-tests without

Welch's corrections for samples by which a Cy0 value was measured. **(D)** Depicted is the immunoblot analysis of TEAD4, NCOA1 and phosphorylation of YAP1 in healthy donor NK cells (HD) and patient-derived NK cells (OC). The right graph shows the quantification of cellular NCOA1 level normalized to actin.

ns, not significant ($p \geq 0.05$), **p < 0.01, ****p ≤ 0.0001; HD, healthy donor; OC, ovarian cancer patient; TPM, transcripts per million reads

The RNA-seq was conducted by the genomics core facility (Marburg) and the data was analyzed by Dr. Florian Finkernagel.

In conclusion, using RNA-seq, several pathways dysregulated in tumor-associated NK cells – including the kegg pathway natural killer cell-mediated cytotoxicity and the Hippo pathway – were identified. Furthermore, an induction of complement factors was observed. The expression of the components of the killer cell-mediated cytotoxicity pathway was mostly reduced and the Hippo pathway was turned off, leading to a decreased expression of *LATS1* and *LATS2*, and an enhanced expression of *YAP1* and *TEAD4*. While one of the potential coactivators of TEAD4, *NCOA1*, is downregulated and the other one, *VGLL1,* is upregulated.

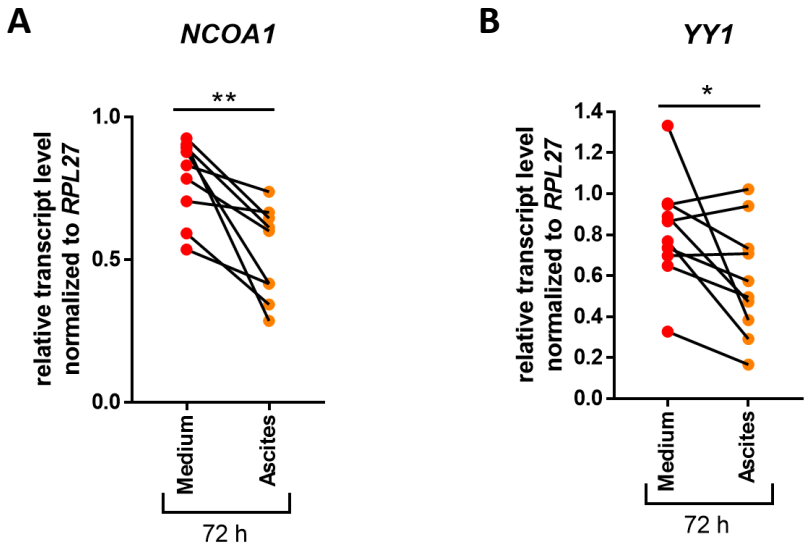

Fig. 19: Influence of ascites on the expression of *NCOA1* and *YY1* in healthy donor NK cells.

Healthy donor NK cells were cultivated for 72 hours in medium or ascites before they were analyzed. Depicted is the qRT-PCR analysis of *NCOA1* **(A)** and *YY1* **(B)**. Cy0 values of *NCOA1* and *YY1* were normalized to *RPL27,* and relative expression of transcripts from medium-cultivated or ascites-cultivated NK cells was calculated relative to the freshly isolated untreated

NK cells at d0. Each symbol denotes an independent biological replicate (n = 9-10). Statistical significances were calculated using paired *t*-tests.

*p < 0.05, **p < 0.01; d0, day 0

3.7 Crosslinking of TGFβ, IL-2 and CD16 induces TEAD4 and reduces T-bet expression in healthy donor NK cells

I have uncovered that TEAD4 is exclusively expressed in patient-derived NK cells, but not in healthy donor-derived NK cells. Therefore, the factors inducing the expression of TEAD4 in healthy donor NK cells should be identified. Culturing of healthy donor NK cells in ascites did not lead to an induction of *TEAD4*, which is probably due to the fact, that the NK cells cannot be cultured for a sufficient period of time without dying. Furthermore, culturing NK cells with TAMs or monocytes with or without ascites also did not induce *TEAD4* expression or change any other Hippo target gene expression (*e.g. CTGF* and *AMOTL2*).

So far, little is known about the role of the Hippo pathway in immune cells. However, it has been described that YAP1 is expressed in T_{regs} and that it plays an important role in the regulatory function of T_{regs}. Furthermore, YAP1 expression in T_{regs} can be induced by stimulation of naïve T cells with IL-2, TGFβ and stimulation of the T cell receptor (TCR) by CD3/CD28 Dynabeads after 4 days [160]. Therefore, healthy donor NK cells were stimulated with IL-2 and TGFβ and together with a strong NK cell activation stimulus for 4 days. As a strong activation stimulus, the activation of CD16 by CD16 crosslinking was chosen. Indeed, it was observed, that *TEAD4* expression was induced upon stimulation with all three factors, but not if one of them was missing (Fig. 20A). Furthermore, downregulation of NKp30 (Fig. 20B), NKG2D (Fig. 20D) and DNAM-1 were observed, but which was mainly induced by the presence of TGFβ. However, NKp44 was upregulated upon cultivation with all three stimuli (Fig. 20C). CD16 was not influenced by the presence of TGFβ but was downregulated after CD16 crosslinking (data not shown).

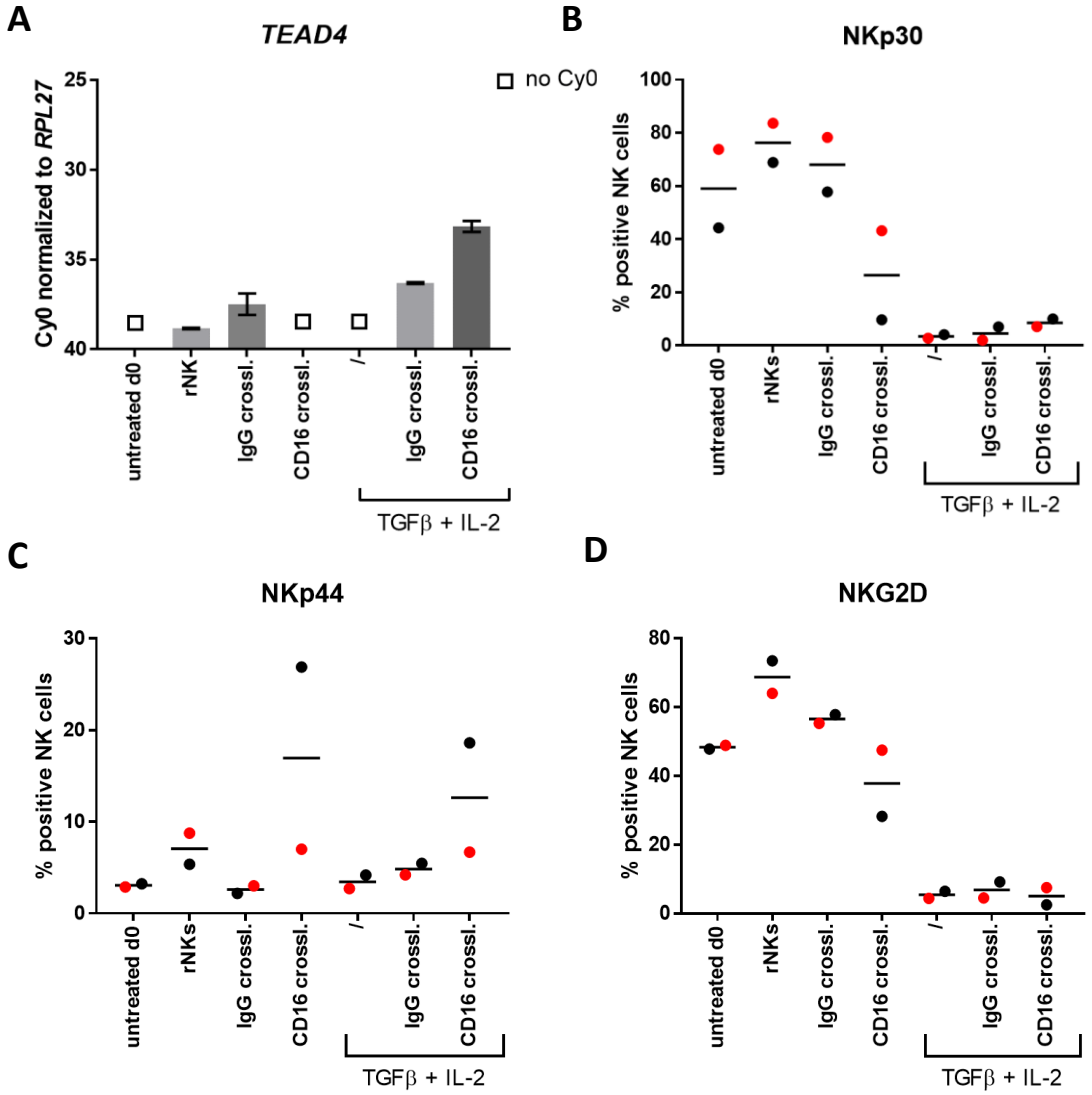

Fig. 20: Induction of *TEAD4* in healthy donor NK cells.

Healthy donor NK cells were stimulated and cultivated for 96 hours before they were analyzed. The cells were stimulated as follows: rNKs (10 U/ml IL-2), IgG and CD16 crosslinking (10 µg/ml plate-bound antibody), TGFβ (5 ng/ml), IL-2 (100 U/ml). Freshly isolated NK cells (untreated d0) were used as a control. **(A)** qRT-PCR analysis of *TEAD4*. Shown are the Cy0 values of *TEAD4* that were normalized to *RPL27*. Representative data of three independent biological replicates were shown. Bar graphs represent means of triplicates ± technical SD. **(B-E)** Flow cytometry analysis of activating receptor expressions on stimulated healthy donor NK cells. Scatter plots show the expression of NKp30 **(B)**, NKp44 **(C)** and NKG2D **(D)**. Each color denotes an independent biological replicate (n = 2) and the median values are indicated by horizontal bars.

rNKs, resting NK cells; crossl., crosslinking; d0, day 0

Since the NK cell viability decreases with each day of cultivation, a time-course experiment to monitor the expression of *TEAD4* and cellular viability was performed. Here, *TEAD4* was already expressed after 24 hours, but the expression was further increased after 48 hours and stayed at this level until 96 hours of stimulation. After 48 hours of stimulation, NK cells still showed acceptable viability (data not shown). Hence, for further assays, NK cells were stimulated for 48 hours. After 48 hours, ten out of eleven donors showed induction of *TEAD4* upon stimulation with all three stimuli in comparison to the IgG control (Fig. 21A). The median viability of the cells was 93 % for the IgG crosslinked cells and 81 % for the CD16 crosslinked cells (Fig. 21B). However, the expression level of *TEAD4* and the viability of the cells was strongly donor-dependent (Fig. 21). Moreover, the expression of other dysregulated genes after treatment with IL-2, TGFβ and CD16 crosslinking was analyzed, but no significant changes were seen in this setting. Those genes were: *YAP1, TEAD1, TEAD2, TEAD3, TRIP6, C3, CFB, CFI*, and *C2*.

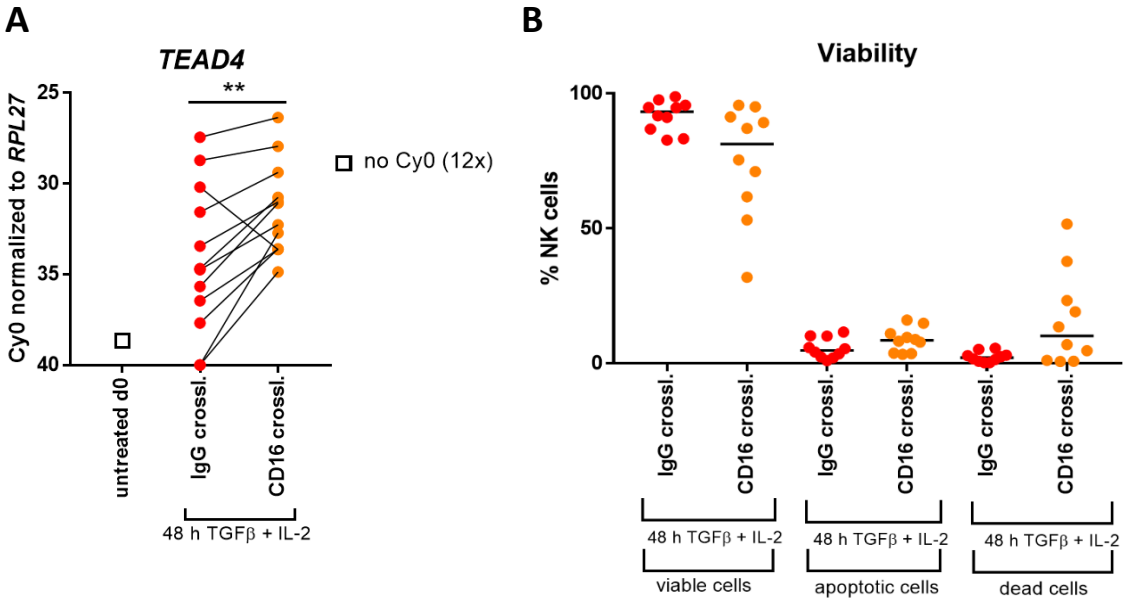

Fig. 21: Impact of CD16 crosslinking on the expression of activating receptors.

Healthy donor NK cells were stimulated and cultivated for 48 hours before they were analyzed. The cells were stimulated as follows: IgG and CD16 crosslinking (10 µg/ml plate-bound antibody), TGFβ (5 ng/ml), IL-2 (100 U/ml). Freshly isolated NK cells (untreated d0) were used as a control. **(A)** qRT-PCR analysis of *TEAD4* was performed. Shown are the Cy0 values of *TEAD4* that were normalized to *RPL27*. **(B)** Depicted is the flow cytometry analysis of the viability of stimulated healthy donor NK cells after 48 hours. The scatter plot shows the percentage of viable cells

(Annexin V^-/ 7-AAD^-), the percentage of apoptotic cells (Annexin V^+/ 7-AAD^-) and the percentage of dead cells (Annexin V^+/ 7-AAD). Each symbol denotes an independent biological replicate (n = 11-12) and the median values are indicated by horizontal bars. Statistical significances were calculated using paired *t*-tests for samples by which a Cy0 value was measured.

**p < 0.01; crossl., crosslinking; d0, day 0

Moreover, it was observed that T-bet (*TBX21*) expression was reduced in patient-derived NK cells in comparison to healthy donor NK cells (Fig. 22A and B). T-bet is a transcription factor known to drive the differentiation and function of NK cells [79] [138]. Therefore, it was studied, if *TBX21* is also downregulated in TEAD4-expressing NK cells. Indeed, it could be confirmed that *TBX21* is downregulated after TGFβ, IL-2 and CD16 stimulation (Fig. 22C).

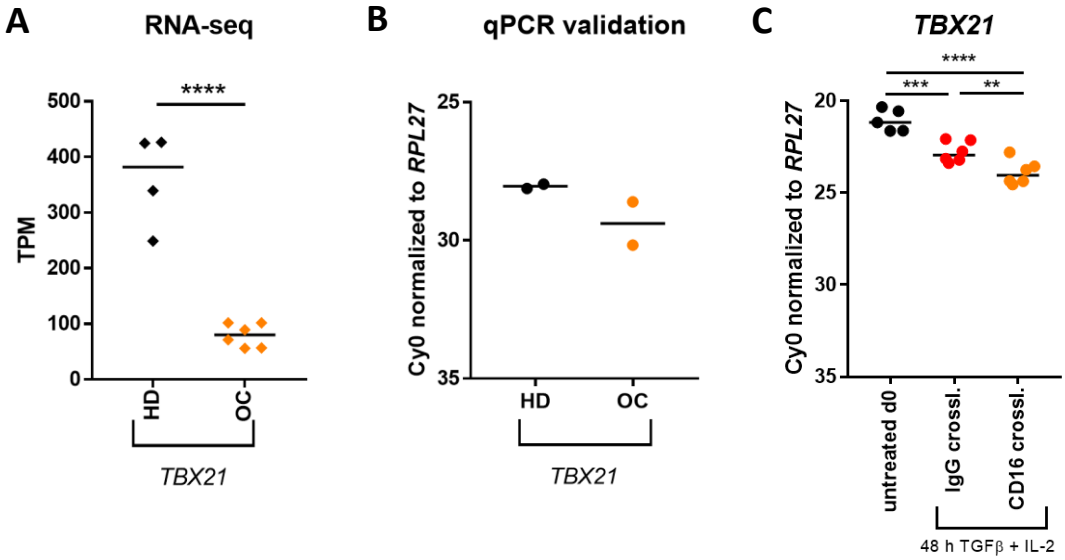

Fig. 22: *TBX21* expression in patient-derived NK cells and healthy donor NK cells.

(A) *TBX21* expression in healthy donor NK cells (HD) versus ascites-derived patient NK cells (OC) based on RNA-seq data was analyzed. The scatter plot shows TPM values of *TBX21*. Each symbol denotes a replicate (n = 4-6) and the median values are indicated by horizontal bars. **(B)** Validation of RNA-seq results via qRT-PCR analysis of *TBX21* was performed. The graphs show the Cy0 values of *TBX21* that were normalized to *RPL27*. Each symbol denotes an independent biological replicate (n = 2) and the median values are indicated by horizontal bars. **(C)** Healthy donor NK cells were stimulated and cultivated for 48 hours before they were analyzed. The cells were stimulated as follows: IgG and CD16 crosslinking (10 µg/ml plate-bound antibody), TGFβ (5 ng/ml), IL-2 (100 U/ml). Freshly isolated NK cells (untreated d0) were used as a control. Each symbol denotes an independent biological replicate (n = 5-6) and the median values are indicated

by horizontal bars. Statistical significances were calculated using unpaired *t*-tests without Welch's corrections.

**p < 0.01, ***p < 0.001, ****p ≤ 0.0001; HD, healthy donor; OC, ovarian cancer patient; TPM, transcripts per million reads; d0, day 0

The RNA-seq was conducted by the genomics core facility (Marburg) and the data was analyzed by Dr. Florian Finkernagel.

3.8 Crosslinking of TGFβ, IL-2, and CD16 induces TEAD4-dependent TIM-3 expression in healthy donor NK cells

Then, I asked how the expression of TEAD4 influences the expression of inhibitory receptors and exhaustion markers. After stimulation with IL-2, TGFβ and CD16 crosslinking, the KIR CD158a was upregulated, while CD158e was strongly downregulated (Fig. 23A). PD-1 was not expressed on stimulated NK cells, whereas TIM-3 was strongly induced and TIGIT was higher expressed on stimulated NK cells. Nevertheless, this was still lower than the untreated status on d0 (Fig. 23B). To investigate, whether the observed changes are indeed TEAD4-dependent, the cells were incubated with a TEAD4 inhibitor called peptide 17 (P17). This inhibitor disrupts the YAP-TEAD interaction. The co-incubation with the inhibitor showed a lower expression of TIM-3 than with the solvent (Fig. 23C). CD158a did not show any differential expression after treatment with the inhibitor. In summary, DNAM-1, NKG2D and NKp30 were downregulated by TGFβ alone, while upregulation of TEAD4 and TIM-3 required additional CD16 crosslinking. CD158a, CD158e, and TIGIT expression levels were changed after TGFβ treatment in combination with CD16 crosslinking. Here, CD158e and TIGIT mainly depended on the CD16 crosslinking and CD158a did not show differences between TGFβ alone and additional crosslinking in an initial experiment (Table 12).

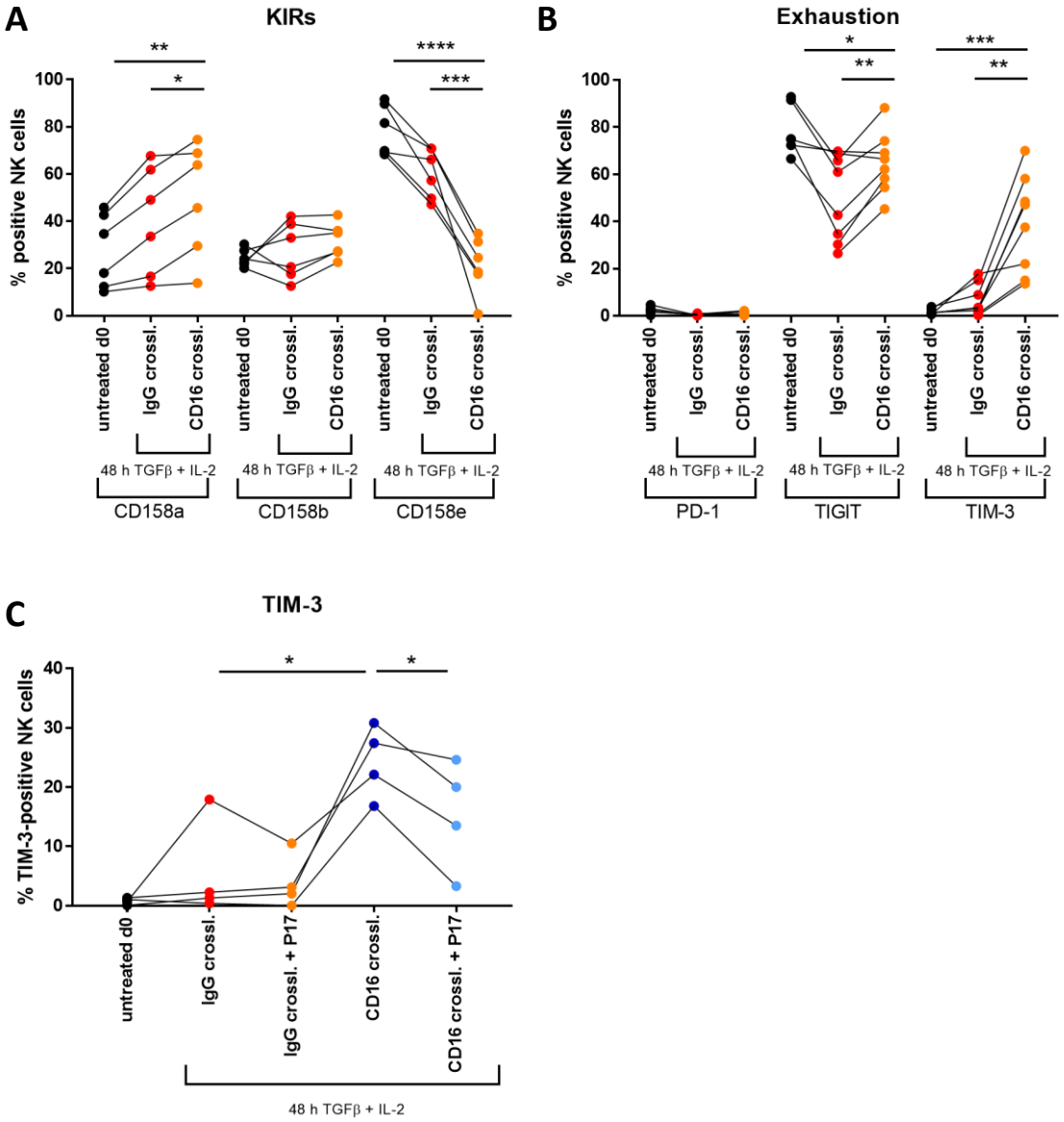

Fig. 23: Impact of CD16 crosslinking and TEAD4 expression on the expression of KIRs and exhaustion markers.

Healthy donor NK cells were stimulated and cultivated for 48 hours before they were analyzed. The cells were stimulated as follows: IgG and CD16 crosslinking (10 µg/ml plate-bound antibody), TGFβ (5 ng/ml), IL-2 (100 U/ml). Freshly isolated NK cells (untreated d0) were used as a control. **(A-C)** Depicted is the flow cytometry analysis of surface marker expression of stimulated healthy donor NK cells after 48 hours. Scatter plots show the expression of KIRs **(A)**, markers for exhaustion **(B)** and TIM-3 **(C)**. Additionally, for **(C)**, NK cells were incubated with 40 nM Peptide 17 (TEAD4 inhibitor) for 30 min at room temperature prior to the stimulation. The inhibitor was present for the whole 48 hours of stimulation. Each symbol denotes an independent biological replicate (n = 4-8) and the median values are indicated by horizontal bars. Statistical significances were calculated using paired *t*-tests.

*p < 0.05, **p < 0.01, ***p < 0.001, ****p ≤ 0.0001; KIRs, killer-cell immunoglobulin-like receptors; crossl., crosslinking; P17, Peptide 17; min, minutes; d0, day 0

Table 12: Genes influenced by TGFβ or TGFβ and CD16 crosslinking.

Summary of genes that are affected by either TGFβ treatment alone or in combination with CD16 crosslinking.

crossl., crosslinking

	TGFβ	TGFβ and CD16 crossl.
CD226 (DNAM-1)	Yes	Yes
HAVCR2 (TIM-3)	weak	Yes
KIR2DL1 (CD158a)	?	Yes
KIR3DL1 (CD158e)	No	Yes
KLRK1 (NKG2D)	Yes	Yes
NCR3 (NKp30)	Yes	Yes
TEAD4	No	Yes
TIGIT	No	Yes

3.9 Crosslinking of TGFβ, IL-2, and CD16 converts healthy donor NK cells to an immunosuppressive-like state

I hypothesized that the TEAD4-expressing NK cells adopt some kind of regulatory function and therefore aimed to analyze their functional impact on T cells. In order to investigate this hypothesis, NK cells were stimulated to express TEAD4 and co-cultured with CFSE-stained T cells for 7 days. The T cells were stimulated to induce proliferation. At first, CD3/CD28 Dynabeads at a bead-to-cell ratio of 1:1 were used to induce the proliferation of CD3 T cells. However, the stimulus was too strong to permit an inhibitory effect of the NK cells. Next, $CD8^+$ T cells were stimulated with IL-2, IL-7, and IL-15 – a weaker proliferation stimulus. Nonetheless, the stimulus was too weak to observe changes. Finally, $CD8^+$ $CD45RA^-$ $CCR7^-$ T cells were sorted, stained with CFSE and co-cultivated with the TEAD4-expressing NK cells. They were stimulated with a low CD3/CD28 bead-to-cell ratio (0.1:1) to induce proliferation. Here it was revealed, that co-cultivation with TEAD4-expressing NK cells led to diminished T cell proliferation

in comparison to co-cultivation with non-TEAD4-expressing NK cells. The inhibitor P17 partially reversed this effect (Fig. 24). Nevertheless, it should be noted that this effect is highly donor-dependent and requires further investigation.

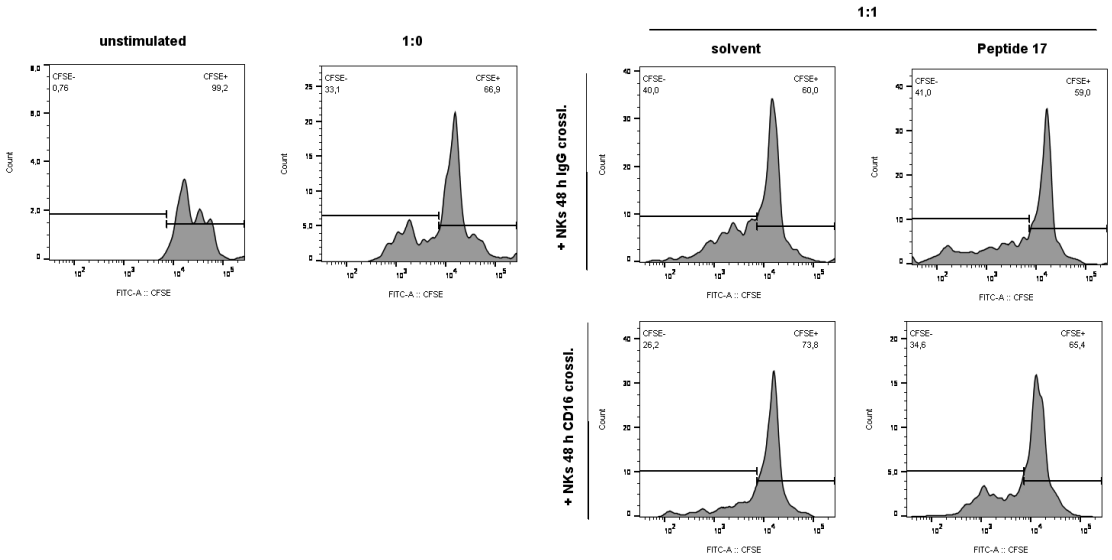

Fig. 24: Functional impact of CD16 crosslinking and TEAD4 expression in NK cells.

Healthy donor NK cells were stimulated and cultivated for 48 hours prior to analysis. The cells were stimulated as follows: IgG and CD16 crosslinking (10 µg/ml plate-bound antibody), TGFβ (5 ng/ml), IL-2 (100 U/ml). Additionally, NK cells were incubated with 40 nM Peptide 17 (TEAD4 inhibitor) for 30 min at room temperature prior to the stimulation. The inhibitor was present for the whole 48 hours of stimulation. $CD8^+$ $CD45RA^-$ $CCR7^-$ sorted T cells were co-cultivated with stimulated NK cells at the ratio of 1:1 for seven days at 37 °C before the proliferation of the T cells was measured using flow cytometry analysis. To induce proliferation, T cells were stimulated with CD3/CD28 Dynabeads at a bead to cell ratio of 0.1:1. T cells were stained with CFSE right before the stimulation, in order to monitor the proliferation. Displayed are representative data of four independent biological replicates.

3.10 Identification of potential TEAD4 target genes

Finally, the gene list of altered genes of patient-derived NK cells vs. healthy donor NK cells obtained from the RNA-seq was compared to a gene list containing genes with TEAD4 binding sites [132] (Table 13). The TEAD4 binding sites were obtained from TEAD4 ChIP-seq analysis, which was performed in the cell lines A549, HCT116, SK-N-SH, and ECC1 [132]. For my analysis, genes with TEAD4 binding sites close to the transcription start site (TSS) were chosen.

Table 13: Dysregulated genes and potential TEAD4 target genes.

Comparison of genes, that are altered between patient-derived NK cells and healthy donor NK cells identified through RNA-seq and genes, which have TEAD4 binding sites [132]. The distance of the TEAD4 binding sites to the TSS is shown in brackets.

Genes	Status in OC NKs	TEAD4 binding sites
CREB3L2	downregulated	Yes (-152; -198; -234)
PMEPA1	upregulated	Yes (-27)
TBX21 (T-Bet)	downregulated	No
TGM2	upregulated	Yes (-2934; -2850; -2912)
TRIP6	upregulated	Yes (+15; -20; -25)
WWTR1	upregulated	Yes (-338)
YAP1	upregulated	Yes (-186)
YY1	downregulated	Yes (+1589)

Summing up, I could show that stimulation of healthy donor NK cells with IL-2, TGFβ and CD16 crosslinking induces the expression of *TEAD4*. Moreover, TEAD4-expressing NK cells show a TEAD4-dependent upregulation of TIM3 and have the capacity to inhibit the proliferation of $CD8^+$ $CD45RA^-$ $CCR7^-$ T cells.

3.11 Summary of main findings

In brief, in this study, it was demonstrated that NK cells of ovarian cancer patients show a mixed tumor-associated phenotype, in which the expression of activating receptors, such as DNAM-1, is mostly downregulated and signs of exhaustion, such as PD-1 and TIM-3 expression, could be detected. NK cells show an impaired effector function, which could be restored by activation with IL-2 and IL-15, in combination with blockage of TGFβ signaling. TGFβ in ovarian cancer ascites reduces DNAM-1 expression, and a blockage of the TGFβ signaling abrogates ascites-mediated downregulation of DNAM-1. Besides, the natural killer cell-mediated cytotoxicity pathway and the Hippo pathway were dysregulated. Expression of the Hippo pathway protein TEAD4 was exclusively detected in patient-derived NK cells and was inducible in healthy NK cells with TGFβ, IL-2 and CD16 engagement. TEAD4-expressing NK cells express high levels of TIM-3 and inhibited the proliferation of T cells.

4 Discussion

The immune system is essential for the elimination and the control of malignant cells. However, in many cancers, the immune system is dysregulated through multiple ways leading to impaired immune surveillance [71]. This also applies for ovarian cancer [232]. Therefore, it is essential to understand the molecular and phenotypical changes of the immune system in the TME of ovarian cancer to finally improve immunotherapy options and the outcome of the patients.

4.1 Novel mechanism of NKG2D-L-mediated immune escape: sNKG2D-Ls induce gene expression in NK cells?

NK cells - as a crucial part of the innate immune system - play a major role in the immune surveillance of tumors. One of the best-characterized activating receptors of NK cells is the NKG2D receptor, which enables the downstream signaling when membrane-associated NKG2D-Ls are engaged. Those ligands (*e.g.* MICA/B, ULBP2) are expressed on malignant or virus-infected cells but are absent on healthy cells (Fig. 25A; depicted as a scheme) [179].

NK cell function of many tumor patients is restricted and the overall results of NK cell-based immunotherapy are disappointing. This is often due to tumor-associated immune escape mechanisms. One described mechanism is the shedding of membrane-bound NKG2D-Ls via metalloproteases rendering tumor cells invisible for NKG2D-dependent target cell recognition. Moreover, sNKG2D-Ls lead to a downregulation of NKG2D and thus impairs NK cell function in many epithelial tumors, *e.g.* lung, breast and colon carcinoma (Fig. 25B; depicted as a scheme) [80] [222]. Furthermore, our group showed that in CLL and Hodgkin Lymphoma patients the ligands for NKG2D were elevated in the serum and are associated with a diminished NKG2D expression and cytotoxicity of patient NK cells [183] [184].

Interestingly, data of this thesis suggest that the current paradigm of the role of the NKG2D-NKG2D-Ls in tumors does not apply to ovarian cancer. In the ascites of ovarian cancer patients, high amounts of sMICA and sULBP2 were measured and the NKG2D expression on NK cells and T cells was not reduced, but

unaltered or even increased. Interestingly, the amount of sNKG2D-Ls positively correlated with the accumulation of pro-tumorigenic $CD163^{+}CD206^{+}$ TAMs and reduced memory effector CD4/CD8 T cells [221], which is a novel observation and has not been described for other cancers. In mice, Xiao *et al.* showed that sMICB promotes the expansion of MDSCs and that it polarizes macrophages into the alternative, immunosuppressive phenotype, via signal transducer and activator of transcription 3 (STAT3) activation [234]. Furthermore, it is known that NKG2D is expressed on activated murine macrophages [59], while the expression of NKG2D on human macrophages is still under debate. Therefore, I tested whether human macrophages from healthy donors or ovarian cancer patients expressed the NKG2D receptor and could clearly demonstrate that the NKG2D receptor expression on human macrophages could not be detected on protein or mRNA level (Fig. 1A, B and D). This shows that sNKG2D-Ls from ovarian cancer ascites do not directly interact with human macrophages via binding to the NKG2D receptor and that the positive correlation of the sNKG2D-L levels with the amount of TAMs is based on a different mechanism.

In mice, Deng *et al.* observed that NKG2D-Ls on myeloid cells consistently stimulate NK cells and thereby induce NKG2D internalization and NK cell desensitization (Fig. 25C; depicted as a scheme) [58]. However, the soluble NKG2D-L MULT-1 can block this interaction and promote tumor rejection [58]. Hence, the NK cells will not be desensitized and can recognize tumor cells via other activating receptors (Fig. 25D; depicted as a scheme). In my study, I could show that NKG2D-Ls were expressed in human macrophages on mRNA level and the expression was enhanced when they were stimulated with LPS (Fig. 1E-G). This was in accordance with data from murine macrophages, where the NKG2D-L RAE-1 was upregulated after TLR stimulation [86]. Surprisingly, MICA and MICB were not detected on the surface of human healthy donor macrophages and ovarian cancer TAMs (data not shown). Moreover, ULBP2 was weakly expressed on the surface of human healthy donor macrophages (data not shown), while some ovarian cancer patients (2/3) revealed a robust expression of ULBP2 on TAMs (Fig. 1H). In our setting, the fold induction of NKG2D-Ls was between two- to four-fold (Fig. 1E-G), which is much lower in comparison to work

from Hamerman *et al.* in which murine macrophages displayed a 30-50-fold RAE-1 induction after LPS treatment [86]. Furthermore, the highest measured normalized Ct value of the NKG2D-Ls was 27 and many Ct values were close to the detection limit (Table S1-S3). The low mRNA expression levels of NKG2D-Ls and the low surface expression of NKG2D-Ls suggest that NKG2D-L expression of macrophages might not have a major functional impact.

In line, the killing of macrophages was not NKG2D-dependent (Fig. 3). Zhou *et al.* showed, that murine polyriboinosinic-polyribocytidilic acid (poly I:C)-treated macrophages activated NK cells via NKG2D, but protected themselves from killing via expression of Qa-1, the ligand for the inhibitory receptor NKG2A [255]. A possible upregulation of inhibitory or protecting receptors on macrophages was not addressed in this thesis.

Taken together, human healthy donor macrophages and ovarian cancer TAMs do not express the NKG2D receptor, but on mRNA level, they express the NKG2D-Ls *MICA*, *MICB* and *ULBP2*. Nonetheless, only ULBP2 was detected on their surface. However, the killing of macrophages is not NKG2D-dependent. High amounts of sNKG2D-Ls in ovarian cancer ascites correlate with a short relapse free survival of patients, an increased amount of TAMs and a reduced accumulation of memory effector T cells. However, the NKG2D expression on NK cells and T cells is not reduced. This demonstrates that the function of sNKG2D-Ls in ovarian cancer is more complex than initially thought. Here, they do not carry out their known function, but rather display additional, yet unknown functions that need to be investigated further.

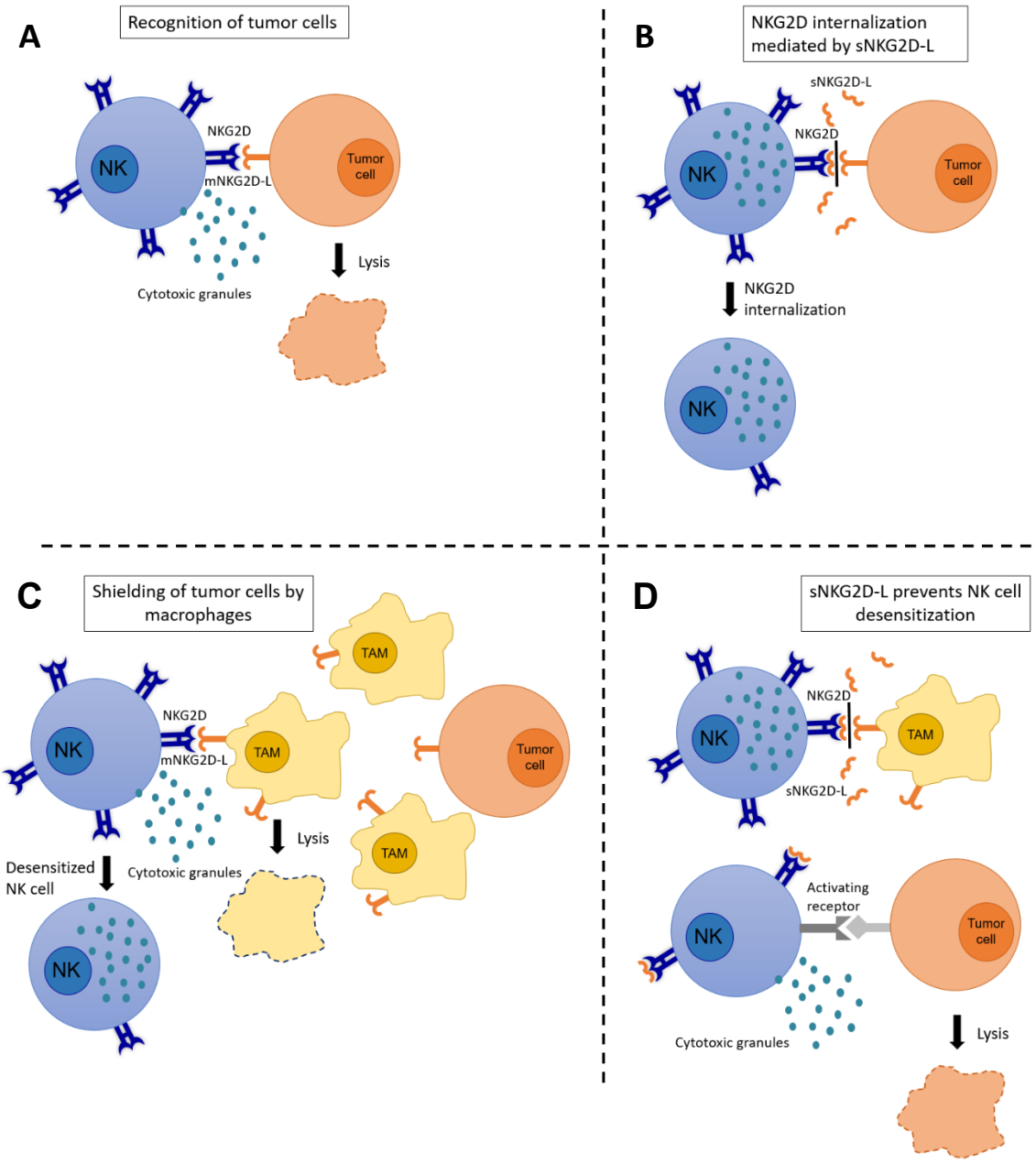

Fig. 25: NKG2D-NKG2D-L – mediated NK cells activation.

(A) NKG2D-NKG2D-L – mediated NK cell activation, leads to the release of perforin and granzyme and therefore, to the elimination of the tumor cells. **(B)** sNKG2D-Ls compete with mNKG2D-L for the binding to the NKG2D receptor. Hence, sNKG2D-Ls prevent mNKG2D-L binding to the receptor, NKG2D receptors are internalized and tumor cells are not eliminated. **(C)** NK cells are activated via NKG2D-NKG2D-L interaction, leading to the release of perforin and granzyme and therefore, to the lysis of the TAM. Furthermore, this leads to the desensitization of the NK cells, in which NKG2D receptors are being internalized. Thereby, TAMs are shielding tumor cells against the recognition and elimination by NK cells. **(D)** sNKG2D-Ls compete with mNKG2D-L for the binding to the NKG2D receptor. Hence, sNKG2D-Ls prevent mNKG2D-L

binding to the receptor and desensitization of the NK cells. NK cells are then able to kill tumor cells via signaling of other activation receptors.

TME, tumor microenvironment; TAMs, tumor-associated macrophages; sNKG2D-Ls, soluble NKG2D ligands; mNKG2D-L, membrane-bound NKG2D ligands

4.2 Soluble ULBP2 alters gene expression of tumor-related genes

Since sNKG2D-Ls from the ovarian cancer ascites did not induce NKG2D internalization in NK cells [221] and did not influence the killing of macrophages (Fig. 2 and 3), I hypothesized that, the function of the ligands depends on different mechanisms.

To test whether sNKG2D-Ls act via NKG2D-dependent signaling, RNA-seq was used to identify different target genes of NKG2D induced by the engagement of mNKG2D-Ls and sNKG2D-Ls. Here, ten mULBP2-specific target genes and twelve sULBP2-specific target genes were identified, respectively (Table 10).

Among the mULBP2-specific target genes were known target genes for mNKG2D-Ls, like *CD69* or *TNF,* showing that the method itself is valid. CD69 is an unspecific, early activation marker that is induced by various stimuli, such as IL-2, phorbol 12-myristate 13-acetate (PMA) or IFN-α [21]. More importantly, it is also induced upon engagement of NKG2D-Ls expressed by macrophages and DCs with NKG2D on NK cells [207]. It triggers NK cell-mediated cytotoxicity, proliferation and induces the expression of CD25 and TNF-α secretion, which can be abolished by CD94 stimulation [21]. Moreover, *ULBP2* was detected, which was overexpressed on S2 cells present in the culture. This serves as an internal control. *RAET1L* (*ULBP6*) was also found, sharing a 97% sequence identity with ULBP2 [61]. Furthermore, transcription factors like c-fos (*FOS*), which are known to play a role in NK cell activation, were induced [175]. Interestingly, the nuclear orphan receptor *NR4A2* was one of the hits, which is poorly investigated in NK cells. Sekiya *et al.* demonstrated that ectopic expression of NR4A2 in naïve $CD4^+$ T cells conveyed T_{reg} functions by inducing the expression of Foxp3 and by inhibition of IL-2 and IFNγ production [191]. In NK cells, NR4A2 expression was increased after CD16-stimulation [164].

All of the genes identified as targets for sNKG2D-Ls play a described role in cancer and are used or discussed as therapeutic targets. Moreover, RNA-seq data revealed that two out of ten of the sNKG2D-L-induced target genes in NK cells were also significantly higher expressed in ovarian cancer TANKs and these are *CEMIP* and *NXPH4* (data not shown). However, only four out of the twelve sNKG2D-specific target genes have been described in NK cells so far. Those genes are *CXCL8, IL1B, INHBA* and *CLEC4E*. While CXCL8 and IL-1β play a role in NK cell homeostasis and differentiation [94] [151], INHBA and CLEC4E have been exclusively described in uterine NK cells [69] [73].

CEMIP encodes a protein that induces cell migration and is associated with carcinogenesis. Shen *et al.* showed that CEMIP expression in ovarian cancer tissue is increased and that silencing of CEMIP resulted in reduced cell proliferation and cell migration of ovarian cancer cell lines [192]. However, a role of CEMIP in NK cells has not been described so far.

ACOD1 (also known as IRG1, which encodes the aconitate decarboxylase 1), *CLEC4E* (also referred as Mincle) and *PLA2G7* were identified as novel target genes after sNKG2D-L engagement (Table 10; Fig. 5). The expression of ACOD1 was shown to play a role in murine macrophages. Here, ACOD1 was upregulated after the stimulation with various cytokines, such as IFNγ, or TLR agonists, such as LPS or CpG. Furthermore, it is associated with mitochondria [56]. It was demonstrated, that the enzyme encoded by *ACOD1* decarboxylates *cis*-aconita and thereby catalyzes the production of itaconic acid. Itaconic acid inhibits isocitrate lyase of bacteria and thereby prevents its growth [149]. Moreover, itaconic acid promotes tumor growth in various cancer types [163] [229]. About *ACOD1* expression in NK cells nothing is known so far, but it would be interesting to study the role of ACOD1 in the context of NKG2D signaling and ovarian cancer.

CLEC4E is a type II transmembrane c-type lectin receptor that is upregulated in macrophages after stimulation with LPS, IL-6, TNF-α or IFN-γ [144]. Decidual NK (dNK) cells of women with multiple pregnancies show a specific phenotype, in which NKG2C is highly expressed. Those pregnancy-trained decidual NK cells show enhanced expression of *CLEC4E* [73]. In fact, tumor infiltrating NK cells

show a similar phenotype than dNK cells, *e.g.* they express VEGF and promote angiogenesis [85] [123], suggesting a possible role of *CLEC4E* in TANKs as well. However, the function of CLEC4E in human NK cells is still elusive.

Finally, Low *et al.* showed that *PLA2G7* expression in human macrophages was induced after co-cultivation with different tumor cell lines and that secreted PLA2G7 induced the migration of the tumor cells [135]. Moreover, PLA2G7 is associated with early relapse in HGSOC [181]. Again, *PLA2G7* expression in NK cells has not been described so far.

Taken together, I demonstrated for the first time that engagement of NKG2D receptor by soluble ligands induces changes in gene expression. All of them with reported overexpression or function in tumor pathogenesis. Besides *CXCL*8 and *IL1B*, little is known about the role of those genes including *ACOD1*, *CLEC4E*, and *PLA2G7* in NK cells.

4.3 Ovarian cancer NK cells display a mixed tumor-associated phenotype

NK cells play a crucial role in the recognition and elimination of tumor cells. It is published that the expression of activating and inhibitory receptors of NK cells is altered in ovarian cancer, but in general not much is known about the phenotype of tumor-associated NK cells in ovarian cancer [14] [36] [66] [111] [221]. Furthermore, those studies analyzed only small cohorts with mostly less than ten patients included. Therefore, the aim of this thesis was to characterize NK cells of ovarian cancer patients on a molecular and functional level in a larger cohort, in order to discover novel potential target sites.

Patient-derived NK cells exhibited a phenotype, in which the expression of CD56 was high and the expression of CD16 was low (Fig. 6). This is in line with previous findings by Belisle *et al.* in which 40 % of the peritoneal fluid NK cells displayed the $CD56^{bright}$ $CD16^{-}$ phenotype [14]. Furthermore, this was also confirmed by Carlsten *et al.* [36].

Besides NKG2D, NKp46, and CD69, all activating receptors were downregulated on ascites-derived NK cells, from which NKp44 and DNAM-1 were the strongest

affected (Fig. 7 and 8). The expression of NKG2D was even upregulated, which is contrary to previously described data, in which the expression of NKG2D was not altered or even decreased (Fig. 7) [14] [111] [221]. Conversely, Carlsten *et al.* observed an increased NKG2D expression on ascites-derived NK cells [36]. Overall, the NKG2D expression among the patients strongly varied and some patients also displayed a decrease in NKG2D expression (Fig. 7). However, it must be taken into account that average blood donors are younger than ovarian cancer patients [97] [256]. In order to rule out the effect of age and gender on the expression of the surface molecules, donors were gender- and age-matched. Moreover, these data represent one of the biggest cohorts so far (up to 68 ascites samples measured). The observed differences can be probably attributed to the smaller sample size (mostly less than 10 samples) analyzed without gender- and age-match.

Regarding inhibitory receptors, the results were mixed. NKG2A was upregulated (Fig. 7), while CD158e was strongly downregulated (Fig. 9). In breast cancer, it was already demonstrated that NKG2A was upregulated on NK cells and that this correlated with an impaired NK cell function [139]. Currently, treatment with monalizumab, an antibody against NKG2A, in combination with an anti-PD-L1 treatment, shows promising results to restore NK cell function [6]. Reduced CD158e expression corroborates with previously described data [14] [66]. Moreover, the NK cells exhibited an exhausted phenotype, as PD-1 and TIM-3 expression was increased (Fig.10). In multiple myeloma patients, NK cells expressed PD-1 and inhibition of the PD1/PD-L1 signaling axis led to a restored NK cell function [17]. In addition, in ovarian cancer patients, Matsuzaki *et al.* showed that PD-1 is expressed on $CD8^+$ T cells of the patients leading to an impaired effector function [145]. Hence, targeting the PD1/PD-L1 signaling axis in ovarian cancer may revive the NK cell and CTL effector functions.

In addition, ascites-derived NK cells showed a reduced cytotoxic capacity against K562 target cells. However, this effect was reversible, when the NK cells were stimulated with IL-2 and IL-15 and they were no longer influenced by the ascites (Fig. 11). Lutgendorf *et al.* published that ascites-derived NK cells display a diminished cytotoxic potential and that this is further reduced by psychological

distress [137]. This was confirmed by findings of Carlsten *et al.*; here cytotoxicity of TANKs was reduced by half in comparison to peripheral blood NK cells of the patients [36].

Summing up, ovarian cancer patient-derived NK cells display a tumor-associated phenotype, in which most of the activating receptors are downregulated and the NK cells are exhausted (shown by the upregulation of PD-1, TIM-3, and NKG2A expression). Moreover, they show a reduced cytotoxic potential against target cells. Nevertheless, their function can be restored by treatment with IL-2 and IL-15 and by depletion of the ascites. It still needs to be investigated which factor (or factors) from ascites inhibits the NK cell functions. In this thesis, I showed that one of these factors is TGFβ (see section 4.4). For clinical applications, treatment with anti-PD-1 and/or anti-NKG2A may improve the clinical outcome of the patients, but further experiments in this direction are needed.

4.4 TGFβ from ascites contributes critically to the tumor-associated NK cell phenotype

Cultivation of healthy donor NK cells in ovarian cancer ascites inhibits NK cell cytotoxicity (Fig. 12E and F).

TGFβ is described to be a key player involved in immune evasion. It inhibits NK cells by downregulating various activating receptors, such as NKp30, NKG2D and DNAM-1 [83] [231]. Moreover, TGFβ1 is enriched in ovarian cancer ascites and was associated with a short RFS [181]. Hence, it was observed that TGFβ1 decreased DNAM-1 expression and that blocking of the TGFβ signaling enhanced the expression. Furthermore, the cultivation of healthy donor NK cells in ascites reduced the DNAM-1 expression, which could be partially restored by blocking TGFβ signaling. Interestingly, the anti-TGFβ antibody was more efficient than the TGFβ receptor kinase inhibitor under the conditions chosen here (Fig. 13). Moreover, the effect on mRNA level was stronger than on protein level, which could be due to a longer half-life of the protein.

Furthermore, if the TGFβ signaling pathway in ascites-derived NK cells is blocked and the cells are cultivated in medium, then the cytotoxic capacity of the NK cells

could be almost fully restored (Fig. 14B). This was associated with a higher DNAM-1 expression on the NK cells (Fig. 14C). However, the cytotoxic potential of the NK cells cultivated in the ascites could not be completely restored, hinting at a limitation of the blocking reagent and/or other important factors within the ascites influencing the cytotoxicity of NK cells. In hepatocellular carcinoma, it was shown, that fibroblasts produce prostaglandin E2 (PGE2) and indoleamine 2,3-dioxygenase (IDO), which are responsible for NK cell dysfunction by downregulating NKG2D and NKp30 expression [125]. Furthermore, Martinet *et al.* demonstrated that PGE2 binds to E-prostanoid 2 (EP2) and EP4 receptors on NK cells and thereby inhibits its NKG2D-, NCR- and CD16-mediated activation [142]. PGE2 plasma levels from ovarian cancer patients are enriched in comparison to healthy controls [212]. Hence, PGE2 could be one of the additional factors, which influence the cytotoxicity of NK cells in ovarian cancer. Future experiments to address this question could include neutralization of PGE2 in the ascites and the analysis of NK cell effector function. Moreover, NK cells could be activated via NKG2D and CD16 and treated with purified PGE2. Here, the activation of the NK cells should be blocked.

4.5 RNA-seq reveals dysregulation of various pathways in ovarian cancer NK cells

I have seen that the NK cells of ovarian cancer patients show a mixed tumor-associated phenotype, in which their function is impaired (Fig. 6-11). However, they are not suppressed by conventional inhibition strategies, such as downregulation of NKG2D by sNKG2D-Ls (Fig. 7) [221]. Therefore, global analysis of tumor-associated NK cells is required to understand their function in ovarian cancer and thus, to identify novel potential target sites.

Here, RNA-seq was performed and the gene expression profile of ascites-derived NK cells was compared to healthy donor-derived NK cells. I identified two important pathways being dysregulated in patient-derived NK cells – the kegg pathway natural killer cell-mediated cytotoxicity (Fig. 15) and the Hippo pathway (Fig. 17). Surprisingly, factors of the complement system were also expressed in patient-derived NK cells, while they were completely absent in healthy donor NK

cells (Fig. 16). Activation of the complement system has been shown to play a role in promoting tumor growth and metastasis [1]. However, they have not been described to be expressed by NK cells and therefore it would be interesting to further characterize the function of the complement factors in NK cells.

Components of the natural killer cell-mediated cytotoxicity pathway that were downregulated were for example, *FCGR3A* (CD16)*, VAV1* or *CD226* (DNAM-1) (Fig. 15). This was in agreement with previous experiments of this thesis in which CD16 expression of patient-derived NK cells was strongly reduced (Fig. 6C and D), as well as the DNAM-1 expression (Fig. 8). VAV1 was shown to be an effector molecule, that together with growth factor receptor bound protein 2 (Grb2) binds to DAP10, initiates tyrosine-phosphorylation and downstream signaling of NKG2D [214]. Hence, VAV1 is required for NKG2D-mediated cytotoxicity of NK cells and confirms the finding that patient-derived NK cells showed an impaired cytotoxic potential (Fig. 11).

Unexpectedly, the expression of Hippo pathway genes was altered. In ovarian cancer, it was demonstrated that YAP overexpression in cancer cells can transmit chemoresistance and that high amounts of nuclear YAP are associated with a poor prognosis [250]. So far, little is known about the role of the Hippo pathway in immune cells. Thaventhiran *et al.* revealed that activation of $CD8^+$ T cells by stimulation with IL-2 and with antigen-stimulation induced the expression of Hippo pathway components (such as SAV1, LATS1, MOB1, TEAD1, and TEAD3), which induced YAP degradation and Blimp-1 expression required for terminal differentiation of T cells [211]. In macrophages, YAP binds to IRF3 and thereby prevents its dimerization and translocation to the nucleus, leading to the blockage of the antiviral immune response of macrophages [225].

Here, I report the first evidence for a role of the Hippo pathway in NK cells. The expression of *LATS1* and *LATS2*, as well as *MOB1B,* which are important regulators of the Hippo pathway, were downregulated in patient-derived NK cells. Conversely, *YAP1* and the TEAD family members were upregulated (Fig. 17). Among the TEADs, *TEAD4* showed the highest significance and lowest variation within the RNA-seq. This shows, that the Hippo pathway in ascites-derived NK

cells is turned off, YAP can translocate to the nucleus and together with TEAD4 activate YAP/TEAD-dependent target gene transcription. In agreement with this, the classical Hippo target genes *CTGF* and *AMOTL2* were upregulated in patient-derived NK cells. Interestingly, the expression of *AREG* was downregulated (Fig. 17D and F). However, *AREG* was the only target gene that was already expressed in healthy donor-derived NK cells, hinting to an additional, Hippo-independent role of *AREG* in NK cells. It was described, that *AREG* is expressed in type 2 innate lymphoid cells (ILC2s) after stimulation with IL-25, IL-33 and thymic stromal lymphopoietin (TSLP) and that it plays an important role in tissue homeostasis following influenza infection [153] [203].

TEAD4 is mainly known to interact with YAP, but it can also bind to VGLLs and p160 proteins (Fig. 18A) [128] [12]. Surprisingly, YAP was phosphorylated in ascites-derived NK cells (Fig. 18D), implying for a YAP-independent role of TEAD4. Furthermore, the expression of *NCOA1* (belonging to the p160 proteins) was reduced in patient-derived NK cells, while the expression of *VGLL1* was induced (Fig. 18). Moreover, the expression of *NCOA1* in healthy donor NK cells could be diminished by cultivation in ascites (Fig. 19). Thus, VGLL1, instead of YAP and NCOA1, can be the potential coactivator of TEAD4 in NK cells of ovarian cancer patients.

Conclusively, these are the first data providing evidence for a role of the Hippo pathway, especially TEAD4 and possible target genes, such as CTGF and AMOTL2, in human NK cells (Fig. 26).

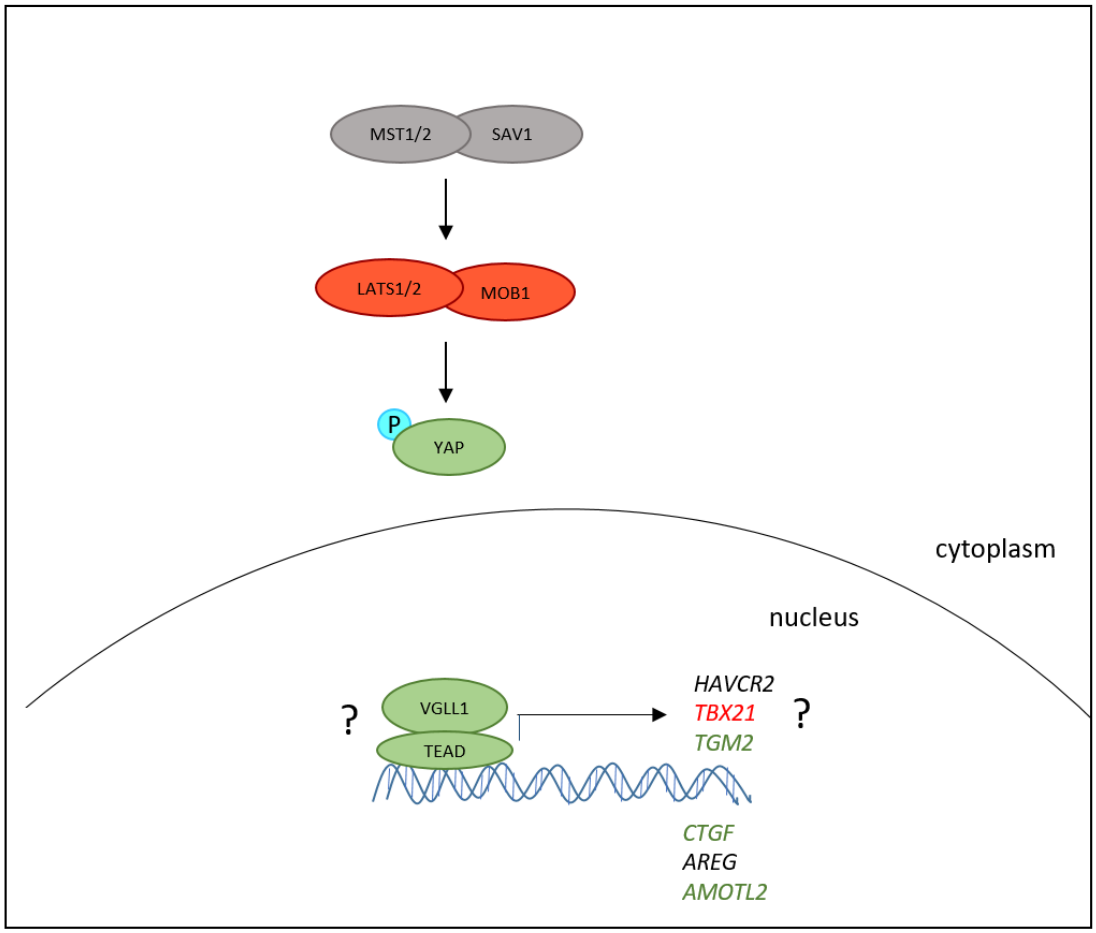

Fig. 26: Hippo pathway in ascites-derived NK cells.

LATS1/2 and MOB1 are downregulated in patient-derived NK cells. However, YAP is still phosphorylated and can probably not enter the nucleus. Conversely, VGLL1 is upregulated and can potentially bind to TEAD4 to induce target gene expression. The classical Hippo target genes *CTGF* and *AMOTL2* are upregulated. Further possible target genes of TEAD4 are *HAVCR2, TBX21,* and *TGM2*.

Red: downregulated in patients; green: upregulated in patients; grey: not altered

4.6 Cutting edge: TEAD4 expression is inducible in healthy donor NK cells

Based on the data, the next aim of this thesis was to identify factors that are responsible for the *TEAD4* expression in NK cells. However, incubation of healthy donor NK cells with ascites fluid was not sufficient to induce *TEAD4* expression. Similarly, cultivation of healthy donor NK cells with patient-derived peritoneal cells or TAMs with or without ascites did not induce *TEAD4* expression (data not shown). I hypothesized that the culture duration was too short to see a *TEAD4* induction, but the NK cells could not be maintained in ascites for longer than four days due to strongly diminished viability.

Furthermore, it was shown that S1P and LPA reduce the phosphorylation of YAP by turning off the Hippo pathway in ovarian cancer cells [33] [65]. LPA levels in ovarian cancer ascites are increased and correlate with short RFS [182]. Nevertheless, LPA did not induce expression of *TEAD4* in healthy donor NK cells.

In general, many signaling pathways influence the expression of TEAD4. However, I have already demonstrated that TGFβ from ovarian cancer plays an important role on NK cell function by influencing the expression of DNAM-1 and reducing NK cell cytotoxicity (Fig. 13 and 14). Furthermore, Ni *et al.* demonstrated that naïve T cells can be stimulated with IL-2, TGFβ and via TCR stimulation for four days to induce the expression of YAP. In turn, YAP facilitates FOXP3 expression and T_{reg} differentiation [160]. Since NK cells do not express the TCR, I stimulated them with IL-2, TGFβ and CD16, which was used as a target to mimic a strong activation. Moreover, like the TCR of T cells, CD16 associates with the CD3ζ chain and thereby induces activation [113]. Indeed, only the combination of all three stimuli increased the expression of *TEAD4* (Fig. 20A). Furthermore, NKG2D and NKp30 expression were reduced by TGFβ without the need for CD16 crosslinking. NKp44 did not show clear results (Fig. 20B, C and D) and further investigations are needed. This is in agreement with previous data, in which TGFβ downregulated the expression of activating receptors, such as NKG2D, NKp30 and DNAM-1 (this work, Fig. 20) [83] [231]. Indicating that TGFβ, IL-2 and

CD16 activation are the putative physiological stimuli within the ascites inducing a TEAD4-expressing phenotype.

Nevertheless, the longer the NK cells were maintained in culture, the lower their viability was. Therefore, a time-course experiment was performed to determine the optimal culture duration. The optimal culture time was set at 48 hours due to the highest expression of *TEAD4* and acceptable viability of the NK cells (over 80 %). Here, 11 out of 12 donors showed a *TEAD4* induction (Fig. 21A). However, it must be noted that the level of *TEAD4* expression was strongly donor-dependent and sometimes close to the detection limit. Hence, further stimuli and/or a longer stimulation time are required to further increase *TEAD4* expression, in order to reach the expression level of tumor-associated NK cells. Moreover, *YAP1* could not be induced using this system, again hinting to a YAP-independent role of TEAD4. Interestingly, I provide the first evidence that TEAD4 can be induced in healthy donor NK cells by the potential physiological stimuli TGFβ, IL-2 and through CD16 activation.

Furthermore, patient-derived NK cells downregulated *TBX21* (Fig. 22A and B). *TBX21* encodes the transcription factor T-bet, which is a master regulator of the effector functions of T cells [198]. Human NK cells constitutively express T-bet and it is necessary for the differentiation of peripheral blood NK cells. T-bet expression is reduced during exhaustion and low levels of T-bet are associated with a compromised anti-tumoral NK cell function [79] [138]. Stimulation of healthy donor NK cells with TGFβ, IL-2 and CD16 crosslinking diminished the *TBX21* expression (Fig. 22C), again hinting at an exhausted NK cell phenotype with an impaired effector function.

4.7 TEAD4 promotes TIM-3 expression and a regulatory NK cell phenotype

The last aim was to unravel the function of TEAD4 in NK cells. It was observed that the expression of CD158a and TIM-3 was induced on NK cells stimulated to express TEAD4, while the expression of CD158e was reduced (Fig. 23). This partially mimics the pattern observed in patient-derived NK cells, where TIM-3

expression was increased and CD158e was downregulated. CD158a, conversely, was not altered in patient-derived NK cells (Fig. 9 and 10). Next, I investigated whether the observed changes were indeed TEAD4-dependent. Thus, by using the YAP-TEAD inhibitor P17, which disrupts the YAP-TEAD interaction, I confirmed that the expression of TIM-3 was TEAD4-dependent (Fig. 23C). Moreover, the TIM-3 promotor contains TEAD4 binding sites hinting at a TEAD4-dependent *TIM-3* gene regulation [132]. The expression of CD158a and CD158e was not altered upon treatment with the inhibitor, pointing to a TEAD4-independent regulation. To support the findings and rule out the possibility that this is due to side effects of the inhibitor, additional experiments with a second inhibitor and a genetic knock-out of TEAD4 are required. Therefore, the well-established inhibitor verteporfin, which prohibits the association of YAP with TEAD, was tested, but it was inapplicable due to high autofluorescence of the compound. Thus, a genetic knock-out of TEAD4 is required to formally proof the causal link of TEAD4 induction and TIM-3 expression.

I hypothesized that tumor-associated NK cells in ovarian cancer may correspond to regulatory NK cells, *e.g.* reflected by their capability to suppress T cell activity, which are suppressed in ovarian cancer [232]. If TEAD4-expressing NK cells exhibit a regulatory phenotype, they should inhibit the proliferation of T cells. Therefore, TEAD4-expressing NK cells were co-cultivated with CFSE-labeled, stimulated T cells. Indeed, in 4 out of 6 donors, TEAD4-expressing NK cells inhibited the proliferation of the T cells (Fig. 24). Nevertheless, it must be noticed that the experiment is challenging. The assay worked best, if not all $CD3^+$ T cells were used, but a subtype of T cells, the $CD8^+$ T_{EM} cells, was employed. Moreover, the proliferation stimulus should not be too strong (high CD3/CD28 beads-to-cell ratio) or too weak (cytokine stimulation), since otherwise no inhibitory effects were detected. Finally, the magnitude of T cell inhibition was strongly donor-dependent. Hence, in order to validate the data, the assay should be conducted using genetic models, such as TEAD4 negative NK cells.

4.8 Future perspectives

Ovarian cancer ascites is a unique model for the analysis of immune cells in the TME. The functional and molecular characterization of tumor-associated NK cells in ovarian cancer revealed that target recognition and target cell killing was severely impaired. This correlated with an aberrant expression of molecules involved in the kegg pathways natural killer cell-mediated cytotoxicity and the Hippo pathway.

This thesis provides first evidence that TEAD4-expressing NK cells exert NK cell regulatory functions and are able to inhibit the proliferation of T cells. The effect on macrophages and NK cells themselves remains elusive. This could be investigated by measuring the ADCC of macrophages or NK cells with the presence or absence of TEAD4-expressing NK cells.

Moreover, the effects of TEAD4 on a molecular level have to be studied. In order to identify TEAD4 target genes, I already compared my RNA-seq list of differentially expressed genes from patient-derived NK cells vs. healthy donor NK cells, to a gene list containing TEAD4 binding sites [132]. Here, a list of seven potential candidates (Table 13) was identified. Currently, the promoter and enhancer regions of TIM-3 and TGM2 are cloned into luciferase reporter constructs to analyze TEAD4-dependent gene transcription. Next, TEAD4 binding sites will be mutated to validate their functional role.

In parallel, gain and loss of function experiments for TEAD4 in NK cells are planned. TEAD4 will be lentivirally transduced into primary NK cells to analyze whether this is sufficient to induce the TANK phenotype. Vice versa, TEAD4 will be silenced via CRISPR-Cas9 to investigate whether TEAD4 is necessary for the generation of the TGFβ/IL-2/CD16-induced TANK phenotype. To establish the system, the NK cell lines NK92 and NKL will be used.

These cell lines, *e.g.* TEAD4-overexpressing or TEAD4-deficient NK92 cells, can be used for *in vivo* mouse experiments. Their role in tumor progression will be analyzed upon transplantation in xenograft ovarian cancer mouse models.

4.9 Conclusions

NK cells of ovarian cancer patients show a mixed tumor-associated phenotype, in which most of the activating receptors are downregulated and signs of exhaustion can be detected. They show an impaired NK cell effector function, which can be restored by activation with IL-2 and IL-15, together with a blockage of TGFβ. Here, the first evidence for a role of the Hippo pathway in NK cells is provided, since RNA-seq identified a dysregulation of the Hippo pathway. TEAD4, a Hippo pathway protein, is highly expressed in ovarian cancer patient-derived NK cells, while the expression is completely absent in healthy NK cells. In addition to that, TGFβ, IL-2 and CD16 crosslinking induced the expression of TEAD4 in healthy NK cells and triggered TEAD4-dependent TIM-3 expression (see Fig. 27 as a model). NK cells gained a regulatory function, in which they were able to suppress T cell proliferation. These findings shed more light on the role of NK cells in the TME of ovarian cancer patients. Additional research will increase our knowledge of NK cell tumor surveillance, paving the way for strategies boosting anti-tumor NK cell functions.

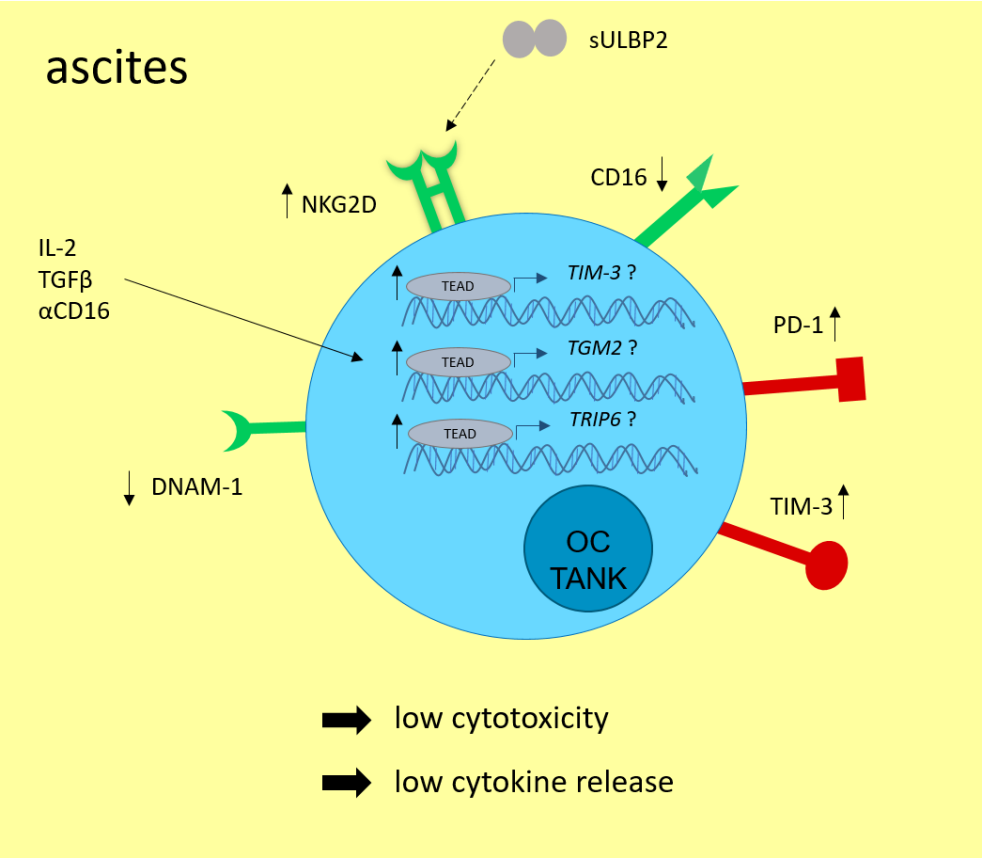

Fig. 27: Model of TANKs in ovarian cancer ascites.

TANKs showed a downregulation of the activating receptors DNAM-1 and CD16, while NKG2D was upregulated (depicted in green). Soluble ULBP2 engaged NKG2D and induced target gene transcription. Co-inhibitory receptors PD-1 and TIM-3 were upregulated (marked in red). IL-2, TGFβ and CD16 stimulation induced TEAD expression, which in turn potentially activates the transcription of *TIM-3, TGM2* and *TRIP6*. Subsequently, these alterations lead to a reduced cytotoxicity and a reduced cytokine release of the TANKs.

References

[1] Afshar-Kharghan, V. *The role of the complement system in cancer*. J Clin Invest, 2017. **127** (3): p. 780–789.

[2] Aktas, E., et al., *Relationship between CD107a expression and cytotoxic activity*. Cell Immunol, 2009. **254**: p. 149–54.

[3] Alimonti, J.B., et al., *Granzyme B induces BID-mediated cytochrome c release and mitochondrial permeability transition*. J Biol Chem, 2001. **276** (10): p. 6974-6982.

[4] Alter G., et al., *CD107a as a functional marker for the identification of natural killer cell activity*. J Immunol Methods, 2004. **294**: p. 15-22.

[5] Anderson, A.C., Joller, N. and Kuchroo, V.K., *Lag-3, Tim-3, and TIGIT: Co-inhibitory Receptors with Specialized Functions in Immune Regulation* Immunity, 2016. **44**: p. 989-1004.

[6] Andre, P., et al., *Anti-NKG2A mAb is a checkpoint inhibitor that promotes anti-tumor immunity by unleashing both T and NK cells.* Cell, 2018. **175**: p. 1731-1743.

[7] Ashiru, O., et al., *A GPI anchor explains the unique biological features of the common NKG2D-ligand allele MICA*008*. Biochem J, 2013. **454** (2): p. 295-302.

[8] Au Yeung. CL, et al., *Exosomal transfer of stroma-derived miR21 confers paclitaxel resistance in ovarian cancer cells through targeting APAF1.* Nat Commun, 2016. **7**: p. 11150.

[9] Bai, X., et al., *Mst1 positively regulates B-cell receptor signaling via CD19 transcriptional levels.* Blood Adv, 2016. **1** (3): p. 219–230.

[10] Bauer, S. et al., *Activation of NK Cells and T Cells by NKG2D, a Receptor for Stress-Inducible MICA.* Science, 1999. **285** (5428): p. 727-729.

[11] Baychelier, F., et al., *Identification of a cellular ligand for the natural cytotoxicity receptor NKp44.* Blood, 2013. **122** (17): p. 2935-2942.

[12] Belandia, B. and Parker, M.G., *Functional interaction between the p160 coactivator proteins and the transcriptional enhancer factor family of transcription factors.* J Biol Chem, 2000. **275**: p. 30801-30805.

[13] Beldi-Ferchiou A., et al. *PD-1 mediates functional exhaustion of activated NK cells in patients with Kaposi sarcoma*. Oncotarget, 2016. **7**: p. 72961–72977.

[14] Belisle, J. A., et al., *Peritoneal natural killer cells from epithelial ovarian cancer patients show an altered phenotype and bind to the tumourmarker MUC16 (CA125)*. Immunology, 2017. **122**: p. 418 – 429.

[15] Bell, D., et al., *Integrated genomic analyses of ovarian carcinoma*. Nature, 2011. **474: p.** 609–615.

[16] Bellon T., et al., *Triggering of effector functions on a CD8+ T cell clone upon the aggregation of an activatory CD94/kp39 heterodimer.* J Immunol, 1999. **162** (7): p. 3996–4002.

[17] Benson D.M. Jr, et al. *The PD-1/PD-L1 axis modulates the natural killer cell versus multiple myeloma effect: a therapeutic target for CT-011, a novel monoclonal anti-PD-1 antibody*. Blood, 2010. **116**: p. 2286–2294.

[18] Bevelacqua V., et al., *Nectin like-5 overexpression correlates with the malignant phenotype in cutaneous melanoma.* Oncotarget, 2012. **3**: p. 882–92.

[19] Bi, J. and Tian, Z., *NK Cell Exhaustion*. Front, Immunol, 2017. **8**: 760

[20] Borrego F., et al., *Recognition of human histocompatibility leukocyte antigen (HLA)-E complexed with HLA class I signal sequence-derived peptides by CD94/NKG2 confers protection from natural killer cell-mediated lysis.* J Exp Med, 1998. **187** (5): p. 813–818.

[21] Borrego, F., et al., *CD69 is a stimulatory receptor for natural killer cell and its cytotoxic effect is blocked by CD94 inhibitory receptor.* Immunology, 1999. **97**: p. 159-166.

[22] Borrego, F., et al., *The CD94/NKG2 family of receptors.* Immunol Res, 2006. **35**: p. 263–277.

[23] Bottino C., et al., *Identification of PVR (CD155) and Nectin-2 (CD112) as cell surface ligands for the human DNAM-1 (CD226) activating molecule.* J Exp Med, 2003. **198**: p. 557–67.

[24] Brandt, C.S., et al., *The B7 family member B7-H6 is a tumor cell ligand for the activating natural killer cell receptor NKp30 in humans*. J Exp Med, 2009. **206** (7): p. 1495-503.

[25] Braud V.M., et al., *HLA-E binds to natural killer cell receptors CD94/NKG2A, B and C*. Nature, 1998. **391** (6669): p. 795–799.

[26] Brooks A.G., et al., *NKG2A complexed with CD94 defines a novel inhibitory natural killer cell receptor*. J Exp Med, 1997. **185** (4): p. 795–800.

[27] Brown, M.H., et al., *2B4, the natural killer and T cell immunoglobulin superfamily surface protein, is a ligand for CD48*. J Exp Med, 1998. **188**: p. 2083–90

[28] Bruno, A., et al., *The proangiogenic phenotype of natural killer cells in patients with non-small cell lung cancer.* Neoplasia, 2013. **15**: p. 133–142.

[29] Bryceson Y. T., et al., *Cytolytic granule polarization and degranulation controlled by different receptors in resting NK cells.* J Exp Med, 2005. **202**: p. 1001-1012.

[30] Bryceson Y. T., et al., *Synergy among receptors on resting NK cells for the activation of natural cytotoxicity and cytokine secretion*. Blood, 2006. **107**: p. 159-66.

[31] Bubenik, J., *MHC class I down-regulation: tumour escape from immune surveillance? (Review)*. Int J Oncol, 2004. **25**: p. 487– 491.

[32] Byrne, A.T.,et al., *Vascular endothelial growth factor-trap decreases tumor burden, inhibits ascites, and causes dramatic vascular remodeling in an ovarian cancer model.* Clin Cancer Res, 2003. **9**: p.5721–5728.

[33] Cai, H. and Xu, Y., *The role of LPA and YAP signaling in long-term migration of human ovarian cancer cells*. Cell Commun Signal, 2013. **11**: 31.

[34] Campbell, K. S. & Purdy, A. K., *Structure/function of human killer cell immunoglobulin-like receptors: lessons from polymorphisms, evolution, crystal structures and mutations*. Immunology, 2011. **132**: p. 315–325.

[35] Carayannopoulos, L.N., et al., *Cutting edge: murine UL16-binding protein-like transcript 1: a newly described transcript encoding a high-affinity ligand for murine NKG2D*. J Immunol, 2002. **169** (8): p. 4079-83.

[36] Carlsten M., et al., *Primary human tumor cells expressing CD155 impair tumor targeting by down-regulating DNAM-1 on NK cells*. J Immunol, 2009. **183**: p. 4921–30.

[37] Carretero M., et al., *The CD94 and NKG2-A C-type lectins covalently assemble to form a natural killer cell inhibitory receptor for HLA class I molecules*. Eur J Immunol, 1997. **27** (2): p. 563–567.

[38] Cerwenka, A., et al., *Retinoic acid early inducible genes define a ligand family for the activating NKG2D receptor in mice.* Immunity, 2000. **12**(6): p. 721-7.

[39] Cerwenka, A., J.L. Baron, and L.L. Lanier, *Ectopic expression of retinoic acid early inducible-1 gene (RAE-1) permits natural killer cell-mediated rejection of a MHC class I-bearing tumor in vivo.* Proc Natl Acad Sci U S A, 2001. **98** (20): p. 11521-6

[40] Chalupny, N.J., et al., *ULBP4 is a novel ligand for human NKG2D.* Biochem Biophys Res Commun, 2003. **305** (1): p. 129-35.

[41] Champsaur, M. and Lanier, L. L., *Effect of NKG2D ligand expression on host immune responses.* Immunol Rev, 2010. **235**: p. 267–285.

[42] Chan, E., et al., *The Ste20-like kinase Mst2 activates the human large tumor suppressor kinase Lats1*. Oncogene, 2005. **24**: p. 2076-2086.

[43] Chang, Y., et al., *Activated Hippo signal pathway inhibits cell proliferation and promotes apoptosis in NK/T cell lymphoma cells.* Cancer med, 2019. **8** (8): p. 3892-3904.

[44] Chauvin, J. M., et al., *TIGIT and PD-1 impair tumor antigen-specific CD8⁺ T cells in melanoma patients.* J Clin Invest, 2015. **125**: p. 2046–2058.

[45] Chen, Z., et al., *Transcriptional enhancer factor 1 disruption by a retroviral gene trap leads to heart defects and embryonic lethality in mice.* Genes Dev, 1994. **8**: p. 2293-2301.

[46] Chitadze, G., et al., *Shedding of endogenous MHC class I-related chain molecules A and B (MICA and MICB) from different human tumor entities: Heterogeneous involvement of the a disintegrin and metalloproteases 10 and 17 (ADAM10 and ADAM17).* Int J Cancer, 2013. **133** (7) p. 1557-1566.

[47] Chong, W.P., et al., *Natural killer cells become tolerogenic after interaction with apoptotic cells.* Eur J Immunol, 2010. **40** (6): p. 1718-27.

[48] Chow, A., Hao, Y. and Yang, X., *Molecular characterization of human homologs of yeast MOB1*. Int J Cancer, 2010. **126**: p. 2079–2089.

[49] Claus, M., et al., *Regulation of NK cell activity by 2B4, NTB-A and CRACC*. Front Biosci, 2008. **13**: p. 956–965.

[50] Clayton, A., et al., *Human tumor-derived exosomes down-modulate NKG2D expression.* J Immunol, 2008. **180**: p. 7249–7258.

[51] Cooper, M.A., Fehniger, T.A. and Caligiuri, M.A. *The biology of human natural killercell subsets*. Trends Immunol, 2001. **22**: p. 633–640.

[52] Cosman, D., et al., *ULBPs, novel MHC class I-related molecules, bind to CMV glycoprotein UL16 and stimulate NK cytotoxicity through the NKG2D receptor.* Immunity, 2001. **14** (2): p. 123-33.

[53] Costello, R.T., et al., *Defective expression and function of natural killer cell-triggering receptors in patients with acute myeloid leukemia.* Blood, 2002. **99**: p. 3661–3667.

[54] Curiel, T.J., et al., *Specific recruitment of regulatory T cells in ovarian carcinoma fosters immune privilege and predicts reduced survival.* Nat Med, 2004. **10** (9): p. 942–949.

[55] Dai, X., et al., *YAP activates the Hippo pathway in a negative feedback loop.* Cell Res, 2015. **25**: **p.** 1175–1178.

[56] Degrandi, D., et al., *The proinflammatory cytokine-induced IRG1 protein associates with mitochondria*. J Interferon Cytokine Res, 2009. **29**: p. 55–67.

[57] Delahaye, N.F., et al., *Alternatively spliced NKp30 isoforms affect the prognosis of gastrointestinal stromal tumors.* Nat Med, 2011. **17**: p. 700–707.

[58] Deng, W., et al., *A shed NKG2D ligand that promotes natural killer cell activation and tumor rejection.* Science, 2015. **348**: p. 136–139.

[59] Diefenbach, A., et al., *Ligands for the murine NKG2D receptor: expression by tumor cells and activation of NK cells and macrophages*. Nat Immunol, 2000. **1**: p. 119–126.

[60] Dong, J., et al. *Elucidation of a universal size-control mechanism in Drosophila and mammals.* Cell, 2007. **130** (6): p. 1120–1133.

[61] Eagle, R.A., et al., *ULBP6/RAET1L is an additional human NKG2D ligand.* Eur J Immunol, 2009. **39** (11): p. 3207-16.

[62] Eagle, R.A., et al., *Cellular expression, trafficking, and function of two isoforms of human ULBP5/RAET1G.* PLoS One, 2009. **4**(2): p. e4503.

[63] El-Sherbiny Y.M., et al., *The requirement for DNAM1, NKG2D, and NKp46 in the natural killer cell-mediated killing of myeloma cells*. Cancer Res, 2007. **67**: p. 8444–9.

[64] Emens, L.A., Kok, M. and Ojalvo, L.S., *Targeting the programmed cell death-1 pathway in breast and ovarian cancer*. Curr Opin Obstet Gynecol, 2016. **28**: p. 142–147.

[65] Fan, Q., et al., *Sphingosine-1-phosphate promotes ovarian cancer cell proliferation by disrupting Hippo signaling.* Oncotarget, 2017. **8** (16): p. 27166–27176.

[66] Felices, M., et al., *IL-15 super-agonist (ALT-803) enhances natural killer (NK) cell function against ovarian cancer.* Gynecol Oncol, 2017. **145**: p. 453–461.

[67] Feng, J., et al., *Verteporfin, a suppressor of YAP-TEAD complex, presents promising antitumor properties on ovarian cancer*. Onco Targets Ther*,* 2016. **9**: p. 5371–5381.

[68] Fernandez-Messina, L., et al., *Differential mechanisms of shedding of the glycosylphosphatidylinositol (GPI)-anchored NKG2D ligands.* J Biol Chem, 2010. **285** (12): p. 8543-51.

[69] Filipovic, I., et al., *Molecular definition of group 1 innate lymphoid cells in the mouse uterus.* Nat Commun, 2018. **9**: 4492.

[70] Finkernagel F., et al., *Dual-platform affinity proteomics identifies links between the recurrence of ovarian carcinoma and proteins released into the tumor microenvironment*. Theranostics, 2019. **9** (22): p. 6601-6617.

[71] Finn, O.J., *Immuno-oncology: understanding the function and dysfunction of the immune system in cancer.* Ann Oncol, 2012. **23** (Suppl 8): p. viii6-9.

[72] Freud, A.G., et al., *Expression of the activating receptor, NKp46 (CD335), in human natural killer and T-cell neoplasia*. Am J Clin Pathol, 2013. **140** (6): p. 853-66.

[73] Gamliel, M., et al. *Trained memory of human uterine NK cells enhances their function in subsequent pregnancies.* Immunity, 2018. **48**: p. 951–962.

[74] Gardiner, C. M., *Killer cell immunoglobulin-like receptors on NK cells: the how, where and why*. Int J Immunogenet, 2008. **35**: p. 1–8.

[75] Garg, A., et al., *Vimentin expressed on Mycobacterium tuberculosis-infected human monocytes is involved in binding to the NKp46 receptor*. J Immunol, 2006. **177** (9): p. 6192-6198.

[76] Geng, J., et al., *The transcriptional coactivator TAZ regulates reciprocal differentiation of TH17 cells and Treg cells.* Nat Immunol, 2017. **18**: p. 800-812.

[77] Gilfillan, S., et al., *NKG2D recruits two distinct adapters to trigger NK cell activation and costimulation*. Nat Immunol, 2002. **3** (12): p. 1150-5.

[78] Gilks C.B. and Prat, J., *Ovarian carcinoma pathology and genetics: recent advances*. Hum Pathol, 2009. **40**: p. 1213–1223.

[79] Gill, S., et al., *Rapid development of exhaustion and down-regulation of eomesodermin limit the antitumor activity of adoptively transferred murine natural killer cells.* Blood, 2012. **119**: p. 5758–5768.

[80] Groh, V., et al., *Tumour-derived soluble MIC ligands impair expression of NKG2D and T-cell activation.* Nature, 2002. **419** (6908): p. 734-738.

[81] Guo, Y., et al., *IL-15 superagonist-mediated immunotoxicity: role of NK cells and IFN-γ.* J Immunol, 2015. **195**: p. 2353–2364.

[82] Hall, C. A., et al., *Hippo pathway effector Yap is an ovarian cancer oncogene.* Cancer Res, 2010. **70**: p. 8517–8525.

[83] Han, B, et al., *Altered NKp30, NKp46, NKG2D, and DNAM-1 Expression on Circulating NK Cells Is Associated with Tumor Progression in Human Gastric Cancer*. J Immunol Res, 2018. **2018**: 6248590.

[84] Han, W., et al., *DNA copy number alterations and expression of relevant genes in triple-negative breast cancer*. Genes Chromosom Cancer, 2008. **47**: p. 490–499.

[85] Hanna, J., et al., *Decidual NK cells regulate key developmental processes at the human fetal-maternal interface*. Nat Med, 2006. **12**: p. 1065–1074.

[86] Hamerman, J.A., Ogasawara, K. and Lanier, L.L., *Cutting edge: Toll-like receptor signaling in macrophages induces ligands for the NKG2D receptor*. J Immunol, 2004. **172**: p. 2001–2005.

[87] Hao, Y., et al., *Tumor suppressor LATS1 is a negative regulator of oncogene YAP*. J Biol Chem, 2008. **283**: p. 5496-5509.

[88] Harvey, K. F., Zhang, X. and Thomas, D. M., *The Hippo pathway and human cancer.* Nature Rev. Cancer, 2013. **13**: p. 246–257.

[89] Hecht, M.L., et al., *Natural cytotoxicity receptors NKp30, NKp44 and NKp46 bind to different heparan sulfate/heparin sequences*. J Proteome Res, 2009. **8**: p. 712–720.

[90] Henriksen, J., et al., *4 Prognostic impact of tumor infiltrating natural killer cells in ovarian carcinoma.* Int J Gynecol Cancer, 2019. **29:** A3.

[91] Hergovich, A., Schmitz, D. and Hemmings, B. A., *The human tumour suppressor LATS1 is activated by human MOB1 at the membrane.* Biochem Biophys Res Commun, 2006. **345** (1): p. 50 –58.

[92] Hoogstad-van Evert, J.S., et al., *Peritoneal NK cells are responsive to IL-15 and percentages are correlated with outcome in advanced ovarian cancer patients*. Oncotarget, 2018. **9**: p. 34810–34820.

[93] Huang, Y.-J., et al., *Ovatodiolide suppresses colon tumorigenesis and prevents polarization of M2 tumor-associated macrophages through YAP oncogenic pathways.* J Hematol Oncol, 2017. **10**: 60

[94] Hughes, T., et al., *Interleukin-1beta selectively expands and sustains interleukin-22+ immature human natural killer cells in secondary lymphoid tissue.* Immunity, 2010. **32**: p. 803-814

[95] Jacobs, I. and Bast, Jr R.C., *The CA 125 tumour-associated antigen: a review of the literature*. Hum Reprod, 1989. **4** (1): p. 1–12.

[96] Janse van Rensburg, H.J., et al., *The Hippo pathway component TAZ promotes immune evasion in human cancer through PD-L1*. Cancer Res, 2018. **78** (6): p. 1457-1470.

[97] Jayson G.C., et al., *Ovarian cancer*. Lancet, 2014. **384**: p. 1376–1388.

[98] Jemal, A., R., et al., *Cancer Statistics, 2009.* CA: Cancer J Clin, 2009. **59** (4): p. 225–49.

[99] Jiao, S., et al., *VGLL4 targets a TCF4–TEAD4 complex to coregulate Wnt and Hippo signalling in colorectal cancer*. Nat Commun, 2017. **8**: 14058.

[100] Jinushi, M., et al., *Impairment of natural killer cell and dendritic cell functions by the soluble form of MHC class I-related chain A in advanced human hepatocellular carcinomas*. J Hepatol, 2005. **43** (6): p. 1013-20.

[101] Johnston, R.J., et al., *The immunoreceptor TIGIT regulates antitumor and antiviral CD8(+) T cell effector function*. Cancer Cell, 2014. **26**: p. 923-937.

[102] Joller, N. et al., *Cutting edge: TIGIT has T cell-intrinsic inhibitory functions.* J Immunol, 2011. **186**: p. 1338–1342.

[103] Karre, K., et al., *Selective rejection of H-2-deficient lymphoma variants suggests alternative immune defence strategy*. Nature, 1986. **319** (6055): p. 675-8.

[104] Kashii, Y., et al., *Constitutive expression and role of the TNF family ligands in apoptotic killing of tumor cells by human NK cells*. J Immunol, 1999. **163** (10): p. 5358-66.

[105] Kearney C.J., et al., *Loss of DNAM-1 ligand expression by acute myeloid leukemia cells renders them resistant to NK cell killing*. Oncoimmunology, 2016. **5** (8): e1196308.

[106] Kim, M.H, et al., *YAP-induced PD-L1 expression drives immune evasion in BRAFi-resistant melanoma.* Cancer Immunol Res, 2018. **6** (3): p. 255-266.

[107] Kim, S., Kim, B., Song, Y.S., *Ascites modulates cancer cell behavior, contributing to tumor heterogeneity in ovarian cancer.* Cancer Sci, 2016. **107**: p. 1173–1178.

[108] Kipps, E., Tan, D.S.P. and Kaye, S.B., *Meeting the challenge of ascites in ovarian cancer: new avenues for therapy and research*. Nat Rev Cancer, 2013. **13**: p. 273–282.

[109] Klapdor, R., et al., *Characterization of a novel third-generation anti-CD24-CAR against ovarian cancer*. Int J Mol Sci, 2019. **20** (3): 660.

[110] Knight, J., et al*., TEAD1 and c-Cbl are novel prostate basal cell markers that correlate with poor clinical outcome in prostate cancer*. Br J Cancer, 2008. **99**: p. 1849–1858.

[111] Krockenberger, M., et al. *Macrophage migration inhibitory factor contributes to the immune escape of ovarian cancer by down-regulating NKG2D.* J Immunol, 2008. **180**: p. 7338–7348.

[112] Lane, D. et al., *Prognostic significance of IL-6 and IL-8 ascites levels in ovarian cancer patients.* BMC Cancer, 2011. **11**: 210

[113] Lanier, L., Yu, G. and Phillips, J., *Co-association of CD3ζ with a receptor (CD16) for IgG Fc on human natural killer cells*. Nature, 1989. **342**: p. 803–805.

[114] Lanier L.L., et al., *Association of DAP12 with activating CD94/NKG2C NK cell receptors*. Immunity, 1998. **8** (6): p 693–701.

[115] Lanier, L. L. *NK cell recognition*. Annu Rev Immunol, 2005. **23**: p. 225–274.

[116] Lazetic S., *Human natural killer cell receptors involved in MHC class I recognition are disulfide-linked heterodimers of CD94 and NKG2 subunits*. J Immunol, 1996.**157** (11): p. 4741–4745.

[117] Lee, B.S., et al., *Hippo effector YAP directly regulates the expression of PD-L1 transcripts in EGFR-TKI-resistant lung adenocarcinoma*. Biochem Biophys Res Commun, 2017. **491** (2): p. 493-499.

[118] Lee, K.M., et al., *2B4 acts as a non-major histocompatibility complex binding inhibitory receptor on mouse natural killer cells.* J Exp Med, 2004. **199**: p. 1245–1254.

[119] Leffers, N., et al., *Prognostic Significance of TumorInfiltrating T-Lymphocytes in Primary and Metastatic Lesions of Advanced Stage Ovarian Cancer.* Cancer Immunol Immunother, 2009. **58** (3): p. 449–459.

[120] Lei, Q.Y., et al., *TAZ promotes cell proliferation and epithelial–mesenchymal transition and is inhibited by the Hippo pathway*. Mol Cell Biol, 2008. **28**: p. 2426–2436.

[121] Lengyel, Ernst, *Ovarian Cancer Development and Metastasis.* Am J Pathol, 2010. **177** (3): p. 1053–1064.

[122] Leung, W., *Infusions of allogeneic natural killer cells as cancer therapy*. Clin Cancer Res, 2014. 20 (13): p. 3390–400.

[123] Levi, I., et al., *Characterization of tumor infiltrating natural killer cell subset.* Oncotarget, 2015. **6**: p. 13835–13843.

[124] Lheureux S., et al., *Epithelial ovarian cancer*. Lancet, 2019. **393** (10177): p. 1240–1253.

[125] Li, T., et al., *Hepatocellular carcinoma-associated fibroblasts trigger NK cell dysfunction via PGE2 and IDO.* Cancer Lett., 2012. **318**: p. 154–161.

[126] Li, Y., et al., *Human iPSC-derived natural killer cells engineered with chimeric antigen receptors enhance anti-tumor activity*. Cell Stem Cell., 2018. **23** (2): p. 181–92.e5

[127] Lian, I., et al., *The role of YAP transcription coactivator in regulating stem cell self-renewal and differentiation*. Genes Dev, 2010. **24**: p. 1106–1118.

[128] Lin, K.C., Park, H.W. and Guan, K.L, *Regulation of the Hippo pathway transcription factor TEAD.* Trends Biochem Sci, 2017. **42** (11): p. 862–872.

[129] Linsley, P. S., et al., *Copy number loss of the interferon gene cluster in melanomas is linked to reduced T cell infiltrate and poor patient prognosis.* PLoS ONE, 2014. **9**: e109760.

[130] Liu, C.C., et al., *Morphologic and functional characterization of perforin-deficient lymphokine-activated killer cells*. J Immunol, 1995. **155** (2): p. 602-608.

[131] Liu, S., et al., *Recruitment of Grb2 and SHIP1 by the ITT-like motif of TIGIT suppresses granule polarization and cytotoxicity of NK cells.* Cell Death Differ, 2013. **20**: p. 456-464.

[132] Liu, X., et al., *Tead and AP1 coordinate transcription and motility.* Cell Rep, 2016. **14** (5): p. 1169-1180.

[133] Liu, Y., et al., *Increased TEAD4 expression and nuclear localization in colorectal cancer promote epithelial–mesenchymal transition and metastasis in a YAP-independent manner.* Oncogene, 2016. **35**: p. 2789–2800.

[134] Ljunggren, H.G. and K. Karre, *In search of the 'missing self': MHC molecules and NK cell recognition*. Immunol Today, 1990. **11** (7): p. 237-44.

[135] Low, H.B.,et al., *Monocyte-derived factors including PLA2G7 induced by macrophage-nasopharyngeal carcinoma cell interaction promote tumor cell invasiveness.* Oncotarget, 2016. **7**: p. 55473–55490.

[136] Lundholm, M., et al., *Prostate tumor-derived exosomes down-regulate NKG2D expression on natural killer cells and CD8+ T cells: mechanism of immune evasion.* PLoS One, 2014. **9** (9): e108925.

[137] Lutgendorf, S. et al., *Social support, psychological distress and natural killer cell activity in ovarian cancer*. J Clin Oncol, 2005. **23**: p. 7105–7113.

[138] Malaise, M., et al., *KLRG1+ NK cells protect T-bet-deficient mice from pulmonary metastatic colorectal carcinoma.* J Immunol, 2014. **192**: p. 1954–1961.

[139] Mamessier E., et al., *Human breast cancer cells enhance self tolerance by promoting evasion from NK cell antitumor immunity*. J Clin Invest, 2011. **121**: p. 3609–22.

[140] Marchetti C., Ledermann J.A. and Benedetti Panici P., *An overview of early investigational therapies for chemoresistant ovarian cancer*. Expert Opin Investig Drugs, 2015. **24**: p. 1163–1183.

[141] Marten, A., et al., *Soluble MIC is elevated in the serum of patients with pancreatic carcinoma diminishing γδ T cell cytotoxicity*. Int J Cancer, 2006. **119** (10): p. 2359-65.

[142] Martinet, L., et al., *PGE2 inhibits Natural-killer and gammadelta T-cell cytotoxicity triggered by NKR and TCR through a cAMP-mediated PKA type I-dependent signaling*. Biochem Pharmacol, 2010. **80** (6): p. 838–845.

[143] Masson D., et al., *Overexpression of the CD155 gene in human colorectal carcinoma.* Gut, 2001. **49**: p. 236–40.

[144] Matsumoto, M., et al., *A novel LPS-inducible C-type lectin is a transcriptional target of NF-IL6 in macrophages.* J Immunol, 1999. **163**: p. 5039–5048

[145] Matsuzaki, J., et al. *Tumor-infiltrating NY-ESO-1-specific CD8⁺ T cells are negatively regulated by LAG-3 and PD-1 in human ovarian cancer*. Proc Natl Acad Sci USA, 2010. **107**: p. 7875–7880.

[146] McCorkle, J.R., et al., *The metastasis suppressor NME1 regulates expression of genes linked to metastasis and patient outcome in melanoma and breast carcinoma.* Cancer Genom Proteom, 2014. **11** (4): p. 175–94.

[147] McNab, F., et al., *Type I interferons in infectious disease.* Nat Rev Immunol, 2015. **15**: p. 87–103.

[148] Mehta, R.S. and Rezvani, K., *Chimeric antigen receptor expressing natural killer cells for the immunotherapy of cancer*. Front Immunol, 2018. **9**: 283.

[149] Michelucci, A., et al. *Immune-responsive gene 1 protein links metabolism to immunity by catalyzing itaconic acid production*. Proc. Natl Acad. Sci. USA, 2013. **110**: p. 7820–7825.

[150] Molfetta, R., et al., *Regulation of NKG2D expression and signaling by endocytosis.* Trends Immunol, 2016. **37** (11): p. 790–802.

[151] Montaldo, E., et al., *Human NK cells at early stages of differentiation produce CXCL8 and express CD161 molecule that functions as an activating receptor.* Blood, 2012. **119**: p. 3987-3996.

[152] Montel, A.H., et al., *Fas-mediated cytotoxicity remains intact in perforin and granzyme B antisense transfectants of a human NK-like cell line*. Cell Immunol, 1995. **165** (2): p. 312-317.

[153] Monticelli, L. A., et al. *Innate lymphoid cells promote lung-tissue homeostasis after infection with influenza virus*. Nature Immunol., 2011. **12**: p. 1045–1054.

[154] Moore K., et al., *Maintenance olaparib in patients with newly diagnosed advanced ovarian cancer.* N Engl J Med, 2018. **379**: p. 2495–2505.

[155] Moretta, A., et al., *Receptors for HLA class-I molecules in human natural killer cells.* Annu Rev Immunol, 1996. **14** : p. 619-48.

[156] Moroishi, T., et al., *The Hippo Pathway Kinases LATS1/2 Suppress Cancer Immunity.* Cell, 2016. **167** (6): p. 1525–1539.

[157] Nakai R., et al., *Overexpression of Necl-5 correlates with unfavorable prognosis in patients with lung adenocarcinoma.* Cancer Sci, 2010. **101**: p. 1326–30.

[158] Nehme, N.T., et al., *MST1 mutations in autosomal recessive primary immunodeficiency characterized by defective naive T-cell survival*. Blood, 2012. **119** (15): p. 3458–3468.

[159] Nersesian, S., et al., *Naturally Killing the Silent Killer: NK Cell-Based Immunotherapy for Ovarian Cancer.* Front. Immunol, 2019. **10**: 1782.

[160] Ni, X., et al., *YAP Is Essential for Treg-Mediated Suppression of Antitumor Immunity.* Cancer Discov, 2018. **8** (8): p. 1026–1043.

[161] Nishiwada S., et al., *Clinical significance of CD155 expression in human pancreatic cancer*. Anticancer Res, 2015. **35**: p. 2287–97.

[162] Pahima, H., Puzzovio, P. G. and Levi-Schaffer, F., *2B4 and CD48: a powerful couple of the immune system*. Clin Immunol, 2019. **204**: p. 64–68.

[163] Pan, J., et al., *Immune responsive gene 1, a novel oncogene, increases the growth and tumorigenicity of glioma.* Oncology Reports, 2014. **32** (5): p.1957-1966.

[164] Parkes, M.D., Halloran, P.F. and Hidalgo, L.G., *Mechanistic sharing between NK cells in ABMR and effector T cells in TCMR*. Am J Transplant, 2018. **18** (1): p. 63- 73.

[165] Patch, A. M., et al., *Whole-genome characterization of chemoresistant ovarian cancer.* Nature, 2015. **521**: p. 489–494.

[166] Pende D., et al., *Identification and molecular characterization of NKp30, a novel triggering receptor involved in natural cytotoxicity mediated by human natural killer cells.* J Exp Med, 1999. **190**: p. 1505–16.

[167] Pesce S., et al. *Identification of a subset of human natural killer cells expressing high levels of programmed death 1: a phenotypic and functional characterization.* J Allergy Clin Immunol, 2017. **139**: p. 335–46.e3.

[168] Pessino, A., et al., *Molecular cloning of NKp46: a novel member of the immunoglobulin superfamily involved in triggering of natural cytotoxicity*. J Exp Med, 1998. **188**: p. 953–960.

[169] Pignata, S., et al., *Chemotherapy in Epithelial Ovarian Cancer.* Cancer Lett, 2011. **303** (2): p. 73-83.

[170] Ploegh H.L., *Viral strategies of immune evasion*. Science, 1998. **280** (5361): p. 248–253.

[171] Pobbati, A.V., et al., *Structural and functional similarity between the Vgll1-TEAD and the YAP-TEAD complexes.* Structure, 2012. **20** (7): p. 1135-1140.

[172] Pogge von Strandmann, E., et al., *A novel bispecific protein (ULBP2-BB4) targeting the NKG2D receptor on natural killer (NK) cells and CD138 activates NK cells and has potent antitumor activity against human multiple myeloma in vitro and in vivo.* Blood, 2006. **107** (5): p. 1955-1962.

[173] Pogge von Strandmann, E., et al., *Human leukocyte antigen-B-associated transcript 3 is released from tumor cells and engages the NKp30 receptor on natural killer cells*. Immunity, 2007. **27** (6): p. 965-74.

[174] Pogge von Strandmann, E., et al., *Tumor-host cell interactions in ovarian cancer: pathways to therapy failure*. Trends Cancer, 2017. **3**: p. 137–148.

[175] Ponti, C., et al., *Role of CREB transcription factor in c-fos activation in natural killer cells.* Eur J Immunol, 2002. **32** (12): p. 3358–3365.

[176] Pujade-Lauraine E., et al., *Bevacizumab combined with chemotherapy for platinum-resistant recurrent ovarian cancer: the AURELIA open-label randomized phase III trial*. J Clin Oncol, 2014; **32**: p. 1302–1308.

[177] Qian, L., et al., *NKG2D ligand RAE1epsilon induces generation and enhances the inhibitor function of myeloid-derived suppressor cells in mice*. J Cell Mol Med, 2017. **21** (9): p. 2046–54.

[178] Ramalho-Santos, M., et al., *"Stemness": transcriptional profiling of embryonic and adult stem cells.* Science, 2002. **298**: p. 597–600.

[179] Raulet, D.H., et al., *Regulation of Ligands for the NKG2D Activating Receptor*. Annu Rev Immunol, 2013. **31**: p. 413–441.

[180] Reinartz, S., et al., *Mixed-polarization phenotype of ascites-associated macrophages in human ovarian carcinoma: Correlation of CD163*

expression, cytokine levels and early relapse. Int J Cancer, 2014. **134**: p. 32-42.

[181] Reinartz, S., et al., *A transcriptome-based global map of signaling pathways in the ovarian cancer microenvironment associated with clinical outcome.* Genome Biol, 2016. **17**: 108

[182] Reinartz, S., et al., *Cell type-selective pathways and clinical associations of lysophosphatidic acid biosynthesis and signaling in the ovarian cancer microenvironment.* Mol Oncol, 2019. **13**: p.185–201.

[183] Reiners, K.S., et al., *Rescue of impaired NK cell activity in hodgkin lymphoma with bispecific antibodies in vitro and in patients*. Mol Ther, 2013. **21** (4): p. 895-903.

[184] Reiners, K.S., et al., *Soluble ligands for NK cell receptors promote evasion of chronic lymphocytic leukemia cells from NK cell anti-tumor activity*. Blood, 2013. **121** (18): p. 3658-65.

[185] Robinson, T.O. and Schluns, K.S., *The potential and promise of IL-15 in immuno-oncogenic therapies.* Immunol Lett, 2017. **190**: p. 159–168.

[186] Rosental, B., et al., *Proliferating cell nuclear antigen is a novel inhibitory ligand for the natural cytotoxicity receptor NKp44*. J Immunol, 2011. **187** (11): p. 5693-702.

[187] Salih H.R., Rammensee H.G. and Steinle A., *Cutting edge: down-regulation of MICA on human tumours by proteolytic shedding.* J Immunol, 2002. **169**: p. 4098–102.

[188] Salih, H.R., Goehlsdorf, D. and Steinle, A., *Release of MICB molecules by tumor cells: mechanism and soluble MICB in sera of cancer patients.* Hum Immunol, 2006. **67** (3): p. 188-95.

[189] Santin, A.D., et al., *Secretion of Vascular Endothelial Growth Factor in Ovarian Cancer.* Eur.J.Gynaecol.Oncol, 1999. **20** (3): p. 177-181.

[190] Sarkar, S., et al., *PRKCI promotes immune suppression in ovarian cancer.* Genes Dev., 2017. **31**: p. 1109-1121.

[191] Sekiya, T., et al., *The nuclear orphan receptor Nr4a2 induces Foxp3 and regulates differentiation of CD4⁺ T cells.* Nat Commun, 2011. **2**: 269.

[192] Shen, F. *et al., CEMIP promotes ovarian cancer development and progression via the PI3K/AKT signaling pathway.* Biomed Pharmacother, 2019*.* **114***:* 108787*.*

[193] Shi, L. et al. *Granzyme B (GraB) autonomously crosses the cell membrane and perforin initiates apoptosis and GraB nuclear localization*. J Exp Med, 1997. **185**: p. 855–866.

[194] Shi, Z., et al*., DNA-binding mechanism of the Hippo pathway transcription factor TEAD4.* Oncogene, 2017. **36**: p. 4362-4369.

[195] Shibuya A., et al., *DNAM-1, a novel adhesion molecule involved in the cytolytic function of T lymphocytes.* Immunity, 1996. **4**: p. 573–81.

[196] Shield, K., et al., *Multicellular spheroids in ovarian cancer metastases: biology and pathology.* Gynecol Oncol, 2009. **113** (1): p. 143-148.

[197] Simhadri, V.R., et al., *Dendritic cells release HLA-B-associated transcript-3 positive exosomes to regulate natural killer function.* PLoS One, 2008. **3** (10): p. e3377.

[198] Simonetta, F., Pradier, A., Roosnek, E., *T-bet and eomesodermin in NK cell development, maturation, and function.* Front Immunol, 2016. **7**: 241.

[199] Sivori S., et al. *p46, a novel natural killer cell–specific surface molecule that mediates cell activation.* J Exp Med, 1997. **186**: p. 1129–36.

[200] Sivori S., et al., *2B4 functions as a co-receptor in human natural killer cell activation*. Eur J Immunol, 2000. **30**: p. 787-793.

[201] Solomon, B.L. and Garrido-Laguna, I., *TIGIT: a novel immunotherapy target moving from bench to bedside*. Cancer Immunol Immunother, 2018. **67: p.** 1659–1667.

[202] Song, H., et al., *Soluble ULBP suppresses natural killer cell activity via down-regulating NKG2D expression.* Cell Immunol, 2006. **239** (1): p. 22-30.

[203] Spits, H., et al., *Innate lymphoid cells — a proposal for uniform nomenclature*. Nat Rev Immunol, 2013. **13**: p. 145–149.

[204] Stanietsky, N., et al*., The interaction of TIGIT with PVR and PVRL2 inhibits human NK cell cytotoxicity.* Proc Natl Acad Sci USA, 2009. **106**: p. 17858-17863.

[205] Steinhardt, A. A., et al. *Expression of Yes-associated protein in common solid tumors*. Hum Pathol, 2008. **39**: p. 1582–1589.

[206] Stewart C.A., et al., *Recognition of peptide-MHC class I complexes by activating killer immunoglobulin-like receptors*. Proc Natl Acad Sci USA, 2005. **102** (37): p. 13224–13229.

[207] Stojanovic, A., Correia, M.P. and Cerwenka, A., *The NKG2D/NKG2DL axis in the crosstalk between lymphoid and myeloid cells in health and disease.* Front Immunol, 2018. **9**: 827.

[208] Sun C., et al. *High NKG2A expression contributes to NK cell exhaustion and predicts a poor prognosis of patients with liver cancer.* Oncoimmunology, 2017. **6** (1): e1264562.

[209] Tahara-Hanaoka S., et al., 2004. *Functional characterization of DNAM-1 (CD226) interaction with its ligands PVR (CD155) and nectin-2 (PRR-2/CD112)*. Int Immunol, 2004. **16**: p. 533–38.

[210] Tang, R., et al., *WW domain binding protein 5 induces multidrug resistance of small cell lung cancer under the regulation of miR-335 through the Hippo pathway*. Br J Cancer, 2016. **115** (2): p. 243–51.

[211] Thaventhiran, J.E., et al., *Activation of the Hippo pathway by CTLA-4 regulates the expression of Blimp-1 in the CD8+ T cell.* Proc Natl Acad Sci USA, 2012. **109** (33): E2223–E2229.

[212] Thill, M., et al., *Expression of vitamin D receptor (VDR), cyclooxygenase-2 (COX-2) and 15-hydroxyprostaglandin dehydrogenase (15-PGDH) in benign and malignant ovarian tissue and 25-hydroxycholecalciferol (25(OH2)D3) and prostaglandin E2 (PGE2) serum level in ovarian cancer patients.* J Steroid Biochem Mol Biol, 2010. **121**: p. 387–390.

[213] Trotta, R., et al., *TGF-beta utilizes SMAD3 to inhibit CD16-mediated IFN-gamma production and antibody-dependent cellular cytotoxicity in human NK cells.* J Immunol, 2008. **181**: p. 3784–3792.

[214] Upshaw, J., et al., *NKG2D-mediated signaling requires a DAP10-bound Grb2-Vav1 intermediate and phosphatidylinositol-3-kinase in human natural killer cells.* Nat Immunol, 2006. **7**: p. 524–532.

[215] Vance R.E., Jamieson A.M., Raulet D.H., *Recognition of the class Ib molecule Qa-1(b) by putative activating receptors CD94/NKG2C and CD94/NKG2E on mouse natural killer cells.* J Exp Med, 1999. **190** (12): p. 1801–1812.

[216] Varelas, X., et al., *TAZ controls Smad nucleocytoplasmic shuttling and regulates human embryonic stem-cell self-renewal.* Nature Cell Biol, 2008. **10**: p. 837–848.

[217] Viaud, S. et al., *Dendritic cell-derived exosomes promote natural killer cell activation and proliferation: a role for NKG2D ligands and IL-15Rα.* PLoS ONE, 2009. **4**: e4942.

[218] Vitale M., et al., *NKp44, a novel triggering surface molecule specifically expressed by activated natural killer cells, is involved in non-major histocompatibility complex-restricted tumor cell lysis.* J Exp Med, 1998. **187**: p. 2065–72.

[219] Vivier, E., et al., *Functions of natural killer cells.* Nat Immunol, 2008. **9** (5): p. 503-10.

[220] Vivier, E., et al., *Targeting natural killer cells and natural killer T cells in cancer.* Nat Rev Immunol, 2012. **12** (4): p. 239-52.

[221] Vyas, M., et al., *Soluble NKG2D ligands in the ovarian cancer microenvironment are associated with an adverse clinical outcome and decreased memory effector T cells independent of NKG2D downregulation*. Oncoimmunology, 2017. **6** (9): e1339854.

[222] Waldhauer, I., et al., *Tumor-associated MICA is shed by ADAM proteases.* Cancer Res, 2008. **68** (15): p. 6368-76.

[223] Wang, C., et al., *The interplay between TEAD4 and KLF5 promotes breast cancer partially through inhibiting the transcription of p27Kip1*. Oncotarget, 2015. **6**: p. 17685–17697.

[224] Wang, G., et al., *Targeting YAP-Dependent MDSC Infiltration Impairs Tumor Progression.* Cancer Discov, 2016. **6**: p. 80–95.

[225] Wang, S., et al., *YAP antagonizes innate antiviral immunity and is targeted for lysosomal degradation through IKKε-mediated phosphorylation*. Nat Immunol, 2017. **18**: p. 733–743.

[226] Wang, W., et al., *Tumor-released Galectin-3, a soluble inhibitory ligand of human NKp30, plays an important role in tumor escape from NK cell attack*. J Biol Chem, 2014. **289** (48): p. 33311-9.

[227] Wang, W., et al., *NK Cell-Mediated Antibody-Dependent Cellular Cytotoxicity in Cancer Immunotherapy*. Front Immunol, 2015. **6**: 368.

[228] Weiner-Gorzel, K., et al. *Overexpression of the microRNA miR-433 promotes resistance to paclitaxel through the induction of cellular senescence in ovarian cancer cells.* Cancer Med, 2015. **4**: p. 745-758.

[229] Weiss, J. M., et al., *Itaconic acid mediates crosstalk between macrophage metabolism and peritoneal tumors.* J Clin Invest, 2018. **128**: p. 3794–3805.

[230] Wherry EJ. *T cell exhaustion.* Nat Immunol, 2011. **12**: p. 492–499.

[231] Wilson, E. B., et al. *Human tumour immune evasion via TGF-β blocks NK cell activation but not survival allowing therapeutic restoration of anti-tumour activity*. PLoS ONE, 2011. **6**: e22842.

[232] Worzfeld, T., et al., *The unique molecular and cellular microenvironment of ovarian cancer.* Front Oncol, 2017. **7**: 24.

[233] Wu J., et al., *An activating immunoreceptor complex formed by NKG2D and DAP10*. Science, 1999. **285** (5428): p. 730–732.

[234] Xiao, G., et al., *Soluble NKG2D ligand promotes MDSC expansion and skews macrophage to the alternatively activated phenotype*. J Hematol Oncol, 2015. **8**: 13.

[235] Xu, L., et al. *Increased Tim-3 expression in peripheral NK cells predicts a poorer prognosis and Tim-3 blockade improves NK cell-mediated cytotoxicity in human lung adenocarcinoma.* Int Immunopharmacol, 2015. **29**: p. 635–641.

[236] Xu, M. Z., et al., *Yes-associated protein is an independent prognostic marker in hepatocellular carcinoma.* Cancer, 2009. **115**: p. 4576–4585.

[237] Yagi, R., et al., *Transcription factor TEAD4 specifies the trophectoderm lineage at the beginning of mammalian development.* Development, 2007. **134**: p. 3827-3836.

[238] Yang, D., et al., *Integrated analyses identify a master microRNA regulatory network for the mesenchymal subtype in serous ovarian cancer*. Cancer Cell, 2013. **23**: p. 186–199.

[239] Yasuda, K., et al., *Enhanced cytotoxic T-cell function and inhibition of tumor progression by Mst1 deficiency.* FEBS Lett, 2016. **590** (1): p. 68–75.

[240] Ye, J., et al., *The nuclear factor YY1 suppresses the human gamma interferon promoter through two mechanisms: inhibition of AP1 binding and activation of a silencer element.* Mol Cell Biol, 1996. **16**: p. 4744-4753.

[241] Yokoyama, W.M. and W.E. Seaman, *The Ly-49 and NKR-P1 gene families encoding lectin-like receptors on natural killer cells: the NK gene complex*. Annu Rev Immunol, 1993. **11**: p. 613-35.

[242] Yu, X., et al., *The surface protein TIGIT suppresses T cell activation by promoting the generation of mature immunoregulatory dendritic cells.* Nat Immunol, 2009. **10**: p. 48-57

[243] Zamai, L., et al., *Natural killer (NK) cell–mediated cytotoxicity: differential use of TRAIL and Fas ligand by immature and mature primary human NK cells*. J Exp Med, 1998. **188** (12): p. 2375-2380.

[244] Zhan, N., Dong, W.G. and Wang, J., *The clinical significance of vascular endothelial growth factor in malignant ascites*. Tumor Biol, 2016. **37**: p. 3719–3725.

[245] Zhang, J., et al*., YAP-dependent induction of amphiregulin identifies a non-cell-autonomous component of the Hippo pathway*. Nat Cell Biol, 2009. **11**: p. 1444–1450.

[246] Zhang, L., et al., *Intratumoral T cells, recurrence, and survival in epithelial ovarian cancer.* N Engl J Med, 2003. **348** (3): p. 203-213.

[247] Zhang, Q., et al., *Blockade of the checkpoint receptor TIGIT prevents NK cell exhaustion and elicits potent anti-tumor immunity.* Nat Immunol, 2018. **19**: p. 723–732.

[248] Zhang, W., et al., *VGLL4 functions as a new tumor suppressor in lung cancer by negatively regulating the YAP-TEAD transcriptional complex.* Cell Res, 2014. **24**: p .331–343.

[249] Zhang, W., et al., *TEAD4 overexpression promotes epithelial-mesenchymal transition and associates with aggressiveness and adverse prognosis in head neck squamous cell carcinoma.* Cancer Cell Int, 2018. **18**: 178

[250] Zhang, X., et al., *The Hippo pathway transcriptional co-activator, YAP, is an ovarian cancer oncogene.* Oncogene, 2011. **30**: p. 2810–2822.

[251] Zhao, B., et al., *Inactivation of YAP oncoprotein by the Hippo pathway is involved in cell contact inhibition and tissue growth control*. Genes Dev, 2007. **21**: p. 2747–2761.

[252] Zhao, B., et al., *TEAD mediates YAP-dependent gene induction and growth control.* Genes Dev, 2008. **22**: p. 1962–1971.

[253] Zhao, B., et al., *A coordinated phosphorylation by Lats and CK1 regulates YAP stability through SCF(beta-TRCP).* Genes Dev, 2010. **24**: p. 72-85.

[254] Zhao, B., et al., *Angiomotin is a novel Hippo pathway component that inhibits YAP oncoprotein.* Genes Dev, 2011. **25**: p. 51–63.

[255] Zhou, Z., et al., *Macrophages help NK cells to attack tumor cells by stimulatory NKG2D ligand but protect themselves from NK killing by inhibitory ligand Qa-1*. PLoS One, 2012. **7** (5): e36928.

[256] Zou, S., et al., *Changing age distribution of the blood donor population in the US*. Transfusion, 2008. **48** (2): p. 251-257.

List of Figures

List of Tables

Abbreviations

7-AAD	7-aminoactinomycin D
AB	Antibody
ADCC	Antibody-dependent cell-mediated cytotoxicity
AF647	Alexa Fluor 647
AICL	Activation-induced C-type lectin
AML	Acute myeloid leukemia
AMOTL2	Angiomotin-like protein 2
aNKs	Activated NK cells
APAF1	Apoptotic peptidase activating factor 1
APC	Allophycocyanin
AREG	Amphiregulin
Asc	Ascites
BAG6	BCL2- associated athanogene 6
BB515	Brilliant Blue 515
BCL2	B-cell lymphoma 2
BID	BH3-interacting domain death agonist
BSA	Bovine serum albumin
BV421	Brilliant Violet 421
CAR	Chimeric antigen receptor
CCL2	CC-chemokine ligand 2
CD	Cluster of Differentiation
cDNA	Complementary DNA
ChIP	Chromatin immunoprecipitation
Crossl.	Crosslinking
CST	Cell Signaling Technology
Ct	Threshold cycle
CTGF	Connective tissue growth factor
CTLs	Cytotoxic T cells

CXCL	C-X-C motif chemokine ligand
CXCR2	C-X-C motif chemokine receptor 2
Cy	Cyanine
d0	Day 0
DAP	DNAX-activation protein
DC	Dendritic cell
DNA	Deoxyribonucleic acid
DNAM-1	DNAX accessory molecule-1
dNK cells	Decidual NK cells
E:T	Effector : Target
ELISA	Enzyme Linked Immunosorbent Assay
EOC	Epithelial ovarian cancer
EP	E-prostanoid
ERK	Extracellular signal-regulated kinase
EV	Extracellular vesicle
FACS	Fluorescence-activated cell sorting (flow cytometry)
FBS	Fetal Bovine Serum
Fc	Fragment crystallizable
FC	Fold change
FDA	US Food and Drug Administration
FDR	False discovery rate
FITC	Fluorescein isothiocyanate
for (primers)	Forward (primers)
FOXO1	Forkhead box O1
FoxP3	Forkhead box P3
GAPDH	Glyceraldehyde 3-phosphate dehydrogenase
GPCR	G protein-coupled receptor
Grb2	Growth factor receptor bound protein 2
GVHD	Graft-versus-host disease

H60	Histocompatibility 60
H	Human
HD	Healthy donor
HGSOC	High-grade serous ovarian cancer
HLA	Human leukocyte antigen
HNSCC	Head and neck squamous cell carcinoma
HRP	Horseradish peroxidase
IDO	Indoleamine 2,3-dioxygenase
IFNγ	Interferon gamma
IGFBP-5	Insulin-like growth factor binding protein-5
IgG	Immunoglobulin G
IKKε	Inhibitor of nuclear factor κ-B kinase subunit epsilon
IL	Interleukin
ILC2	Type 2 innate lymphoid cell
Inh.	Inhibitor
IRF3	Interferon regulatory factor 3
ITAM	Tyrosine-based activating motif
ITIM	Tyrosine-based inhibitory motif
KIR	Killer cell immunoglobulin-like receptor
LAMP-1	Lysosomal-associated membrane protein-1
LATS	Large tumor suppressor
LPA	Lysophosphatidic acid
LPAR	LPA receptor
LPS	Lipopolysaccharide
LRS	Leukoreduction system
MACS	Magnetic-activated cell sorting
MCA	3′-methylcholanthrene
MDM	Monocyte-derived macrophage
MDSC	Myeloid-derived suppressor cell

MeOH	Methanol
MFI	Mean fluorescence intensity
MHC	Major histocompatibility complex
MIC	Major histocompatibility complex class I-related chain
MIF	Macrophage migration inhibitory factor
Min	Minutes
MIP-1β	Macrophage inflammatory protein 1 beta
MLL5	Mixed lineage leukemia 5
mNKG2D-L	Membrane-bound NKG2D ligand
MOB1	MOB kinase activator 1
mRNA	Messenger RNA
MST	Mammalian STE20-like protein kinase
MULT-1	Murine UL16 binding protein-like transcript
NCR	Natural cytotoxicity receptor
NK cells	Natural Killer cells
NKG2	NK group 2 member
NKG2D-L	NKG2D ligand
NKp	Natural killer cell protein
NKTCL	Natural killer T-cell lymphoma
Ns	Not significant
OC	Ovarian carcinoma
P17	Peptide 17
P/S	Penicillin/streptomycin
PBMCs	Peripheral blood mononuclear cells
PBL	Peripheral blood lymphocytes
PBS	Phosphate buffered saline
PCs	Peritoneal cells
PCNA	Proliferating cell nuclear antigen
PCR	Polymerase chain reaction

PD-1	Programmed death receptor 1
PD-L1	Programmed death-ligand 1
PE	Phycoerythrin
PerCP	Peridinin-Chlorophyll-protein
PGE2	Prostaglandin E2
PI3K	Phosphatidylinositol-4,5-bisphosphate 3- kinase
PMA	Phorbol 12-myristate 13-acetate
Poly I:C	polyriboinosinic-polyribocytidilic acid
PRKCI	Protein kinase C iota
PVR	Polio virus receptor
qRT-PCR	Quantitative real time PCR
RAE-1	Retinoic acid early inducible gene 1
RBC	Red blood cell
rev (primers)	Reverse (primers)
RFS	Relapse-free survival
RIPA	Radioimmunoprecipitation assay buffer
RNA	Ribonucleic acid
rNKs	Resting NK cells
RPL30	60S ribosomal protein L27
S1P	Sphingosine1-phosphate
S1PR	S1P receptor
S2 cells	Schneider 2 cells
SAV1	Salvador homologue 1
SCLC	Small cell lung cancer
SD	Standard deviation
SDS	Sodium dodecyl sulfate
Seq	Sequencing
SH2	Src Homology 2
sMICA	Soluble MICA

sNKG2D-L	Soluble NKG2D ligand
SRC1	Steroid receptor coactivator 1
STAT3	Signal transducer and activator of transcription 3
sULBP2	Soluble ULBP2
SYK	Spleen tyrosine kinase
T cell	Thymus derived lymphocyte
TCR	T cell receptor
T-bet	T-box transcription factor 21
TAM	Tumor-associated macrophage
TANK	Tumor-associated NK cell
TAZ	Transcriptional co-activator with PDZ-binding motif
TBK1	TANK-binding kinase 1
TBS-T	Tris-buffered saline with Tween 20
TCF4	Transcription factor 4
TEAD	TEA domain transcription factor
TGFβ	Transforming growth factor beta
TIGIT	T cell immunoglobulin and ITIM domain
TIM-3	T cell immunoglobulin- and mucin-domain-containing molecule-3
TLR	Toll-like receptor
TME	Tumor microenvironment
TNFα	Tumor necrosis factor alpha
TPM	Transcripts per million reads
TRAIL	TNF-related apoptosis-inducing ligand
T_{regs}	T regulatory cells
TSLP	Thymic stromal lymphopoietin
TSS	Transcription start site
ULBP	UL16 binding proteins
VAV	Vav guanine nucleotide exchange factor
VEGF	Vascular endothelial growth factor

VGLL	Vestigial-like
w/o	Without
WB	Western Blot
WBP5	WW domain binding protein 5
WT	Wild type
YAP	Yes-associated protein
YY1	Yin yang 1
ZAP70	ζ-chain-associated protein kinase 70

Appendix

Table S1: Normalized Ct values of *MICA*.

Shown are the normalized Ct values of *MICA* of each donor and each treatment used in Fig. 1E. The mean *RPL27* Ct of all donors and all treatments was calculated and added to the Δ Ct values (*MICA* - *RPL27*) of each condition. The mean *RPL27* Ct value was 20,93.

donors	**untreated**	**+ 24 h LPS**	**+ 48 h LPS**	**+ 72 h LPS**
Sp1 22.11.16	28,64	27,23	26,83	27,40
Sp2 22.11.16	28,08	27,07	27,00	27,17
Sp1 24.11.16	28,26	27,27	26,83	27,60
Sp2 24.11.16	31,63	31,15	30,98	31,78
Sp1 04.01.17	27,73	27,03	26,98	26,81
Sp2 04.01.17	28,88	27,80	27,53	27,90
Sp3 04.01.17	34,26	33,26	33,51	33,01

Table S2: Normalized Ct values of *MICB.*

Shown are the normalized Ct values of *MICB* of each donor and each treatment used in Fig. 1F. The mean *RPL27* Ct of all donors and all treatments was calculated and added to the Δ Ct values (*MICB* - *RPL27*) of each condition. The mean *RPL27* Ct value was 20,93.

donors	**untreated**	**+ 24 h LPS**	**+ 48 h LPS**	**+ 72 h LPS**
Sp1 22.11.16	29,19	27,11	27,18	27,16
Sp2 22.11.16	28,54	27,37	27,43	28,05
Sp1 24.11.16	30,10	28,23	27,92	28,74
Sp2 24.11.16	29,40	28,89	28,37	29,04
Sp1 04.01.17	31,03	29,73	30,33	29,55
Sp2 04.01.17	31,53	29,39	30,18	30,47
Sp3 04.01.17	30,95	28,87	30,45	30,03

Table S3: Normalized Ct values of *ULBP2.*

Shown are the normalized Ct values of *ULBP2* of each donor and each treatment used in Fig. 1G. The mean *RPL27* Ct of all donors and all treatments was calculated and added to the Δ Ct values (*ULBP2* - *RPL27*) of each condition. The mean *RPL27* Ct value was 20,93.

donors	**untreated**	**+ 24 h LPS**	**+ 48 h LPS**	**+ 72 h LPS**
Sp1 22.11.16	32,82	32,57	32,11	32,05
Sp2 22.11.16	31,16	30,85	30,52	30,72

Sp1 24.11.16	32,28	31,42	31,02	31,26
Sp2 24.11.16	32,41	32,01	31,57	31,57
Sp1 04.01.17	33,95	32,27	32,53	37,78
Sp2 04.01.17	30,02	30,04	30,00	30,97
Sp3 04.01.17	33,49	33,22	35,73	38,84

Table S4: TPM values of mULBP2 target genes.

	Sp1 20.02.19 NKs			
Genes	IL-2 + IL-15	sULBP2	S2 WT cells	S2 ULBP2 cells
CCR6	9,7	8,98	8,41	2,26
CD69	258,97	239,64	527,58	1379,12
EGR1	17,62	20,72	12,45	51,46
FOS	4,68	4,74	7,42	19,02
NR4A2	10,98	8	29,15	99,47
RAET1L	4,15	4,35	2,81	709,8
TNF	201,6	202,8	122	456,56
TNFRSF9	21,5	16,08	30,52	65,11
TNFSF9	2,7	3,11	2,7	16,55
ULBP2	11,76	10,97	9,44	319,16
	Sp1 07.06.19 NKs			
Genes	IL-2 + IL-15	sULBP2	S2 WT cells	S2 ULBP2 cells
CCR6	9,67	9,89	13,38	7,4
CD69	155,35	161,49	270,12	905,77
EGR1	11,97	11,48	7,02	38,87
FOS	2,6	2,95	4,5	16,85
NR4A2	5,64	5,22	7,92	37,59
RAET1L	3,69	2,63	4,62	267,3
TNF	166,11	127,85	173,65	448,89
TNFRSF9	9,23	6,01	6,75	20,9
TNFSF9	1,41	1,66	0,69	7,32
ULBP2	9,07	7,16	9,31	129,43
	Sp1 24.06.19 NKs			
genes	IL-2 + IL-15	sULBP2	S2 WT cells	S2 ULBP2 cells
CCR6	3,7	3,31	3,17	1,54

CD69	269,86	362,79	265,68	331,87
EGR1	17,79	18,1	6,87	22,2
FOS	4,57	5,73	5,67	10,58
NR4A2	15,94	20,05	18,46	25,98
RAET1L	4,97	4,8	5,76	1369,11
TNF	195,68	276,67	133,49	168,26
TNFRSF9	37,85	52,58	45,92	56,53
TNFSF9	7,41	10,96	1,58	5,25
ULBP2	11,9	14,25	11,62	604,46

Table S5: Log fold change of mULBP2 target genes.

	Sp1 20.02.19 NKs		**Sp1 07.06.19 NKs**		**Sp1 24.06.19 NKs**	
genes	sULBP2	S2 ULBP2 cells	sULBP2	S2 ULBP2 cells	sULBP2	S2 ULBP2 cells
CCR6	-0,11	-1,89	-0,16	-1,04	0,03	-0,85
CD69	-0,11	1,39	0,43	0,32	0,06	1,75
EGR1	0,23	2,05	0,02	1,69	-0,06	2,47
FOS	0,02	1,36	0,33	0,90	0,18	1,90
NR4A2	-0,46	1,77	0,33	0,49	-0,11	2,25
RAET1L	0,07	7,98	-0,05	7,89	-0,49	5,85
TNF	0,01	1,90	0,50	0,33	-0,38	1,37
TNFRSF9	-0,42	1,09	0,47	0,30	-0,62	1,63
TNFSF9	0,20	2,61	0,56	1,73	0,24	3,39
ULBP2	-0,10	5,08	0,26	5,70	-0,34	3,80

Table S6: TPM values of sULBP2 target genes.

	Sp1 20.02.19 NKs			
genes	IL-2 + IL-15	sULBP2	S2 WT cells	S2 ULBP2 cells
ACOD1	0,00	0,09	0,00	0,00
AQP9	0,00	0,13	0,00	0,00
CEMIP	0,02	0,05	0,00	0,00
CLEC4E	0,00	0,09	0,00	0,00
CXCL8	0,00	0,40	0,00	1,25
DSC1	0,03	0,32	0,15	0,00
FRMD4A	0,00	0,07	0,00	0,00
HHIPL1	0,00	0,07	0,00	0,10

IL1B	0,00	0,38	0,00	0,40
INHBA	0,00	0,03	0,00	0,12
NXPH4	0,22	0,54	1,05	0,45
PLA2G7	0,00	0,19	0,00	0,00
	Sp1 07.06.19 NKs			
genes	IL-2 + IL-15	sULBP2	S2 WT cells	S2 ULBP2 cells
ACOD1	0,06	0,71	0,26	0,34
AQP9	0,08	0,19	0,18	0,00
CEMIP	0,02	0,06	0,15	0,00
CLEC4E	0,00	0,11	0,00	0,00
CXCL8	0,25	0,72	1,43	1,14
DSC1	0,00	0,25	0,00	0,00
FRMD4A	0,01	0,09	0,05	0,07
HHIPL1	0,02	0,11	0,00	0,10
IL1B	0,00	1,03	0,00	0,73
INHBA	0,00	0,11	0,09	0,23
NXPH4	2,75	28,26	3,13	3,73
PLA2G7	0,12	0,52	0,28	0,00
	Sp1 24.06.19 NKs			
genes	IL-2 + IL-15	sULBP2	S2 WT cells	S2 ULBP2 cells
ACOD1	1,56	11,11	1,19	0,44
AQP9	0,82	2,96	0,84	1,56
CEMIP	0,36	1,32	0,68	0,50
CLEC4E	0,13	2,02	0,77	0,43
CXCL8	3,54	16,79	5,25	6,30
DSC1	0,00	0,02	0,00	0,00
FRMD4A	0,01	0,06	0,08	0,00
HHIPL1	0,01	0,12	0,00	0,00
IL1B	2,07	24,81	7,12	1,85
INHBA	4,32	12,06	11,01	11,03
NXPH4	0,97	2,20	28,16	24,84
PLA2G7	2,10	5,88	2,98	1,41

Table S7: Log fold change of sULBP2 target genes.

	Sp1 20.02.19 NKs		Sp1 07.06.19 NKs		Sp1 24.06.19 NKs	
Genes	sULBP2	S2 ULBP2 cells	sULBP2	S2 ULBP2 cells	sULBP2	S2 ULBP2 cells
ACOD1	3,32	0,00	2,83	-1,42	3,45	0,39
AQP9	3,78	0,00	1,83	0,88	1,19	-4,28
CEMIP	1,18	0,00	1,86	-0,43	1,48	-3,99
CLEC4E	3,28	0,00	3,86	-0,84	3,53	0,00
CXCL8	5,35	6,98	2,24	0,26	1,51	-0,33
DSC1	3,03	-3,98	1,66	0,00	4,69	0,00
FRMD4A	2,97	0,00	2,01	-3,09	2,32	0,34
HHIPL1	3,08	3,52	2,51	0,00	2,18	3,40
IL1B	5,28	5,35	3,58	-1,93	6,70	6,20
INHBA	1,99	3,75	1,48	0,00	3,56	1,31
NXPH4	1,29	-1,19	1,18	-0,18	3,36	0,25
PLA2G7	4,34	0,00	1,48	-1,07	2,04	-4,85

Verzeichnis der akademischen Lehrer

Meine akademischen Lehrenden waren in Bonn:

Bakker, Bartels, Bartolomaeus, Bleckmann, Dahl, Deppenmeier, Dörmann, Fakoussa, Filippou, Fürst, Galinski, Heinzel, Herzog, Hoch, Hofmann, Höhfeld, Kirch, Knoop, Koch, Lobin, Menzel, Mogdans, Mutke, Quandt, Schlüssel, Schreiber, von der Emde, Weigend, Welter, Witke

Meine akademischen Lehrenden waren in Marburg:

Adhikary, J.-W. Bartsch, Bauer, Brehm, Brendel, Buchholz, Burchert, Exner, Garn, Greene, Grosse, Kinscherf, Lauth, Mandic, Müller, Müller-Brüsselbach, Pankuweit, Reinartz, Schmeck, Schnare, Slater, Stiewe, Suske, Timmesfeld, Timofeev, Wanzel, Worzfeld

Danksagung

Mein besonderer Dank geht an Prof. Dr. Elke Pogge von Strandmann, die mich nun schon seit vielen Jahren begleitet, mir ein spannendes Thema für meine Promotion ermöglicht hat und mich bei dem Erstellen dieser Arbeit unterstützt hat. Vielen vielen Dank für die ganzen Möglichkeiten und Chancen, die du mir geboten hast! Vielen Dank für alles, was du mir beigebrachst hast, für die Motivation, für den Freiraum und für die produktiven Gespräche! Ich habe dir sehr viel zu verdanken und durch dich habe ich unglaublich viel gelernt!

An dieser Stelle möchte ich mich ganz herzlich bei den gesamten Kollegen des dritten Stockwerks des ZTI bedanken. Vielen Dank für die interessanten Gespräche, sowieso die Tipps und Hinweise, die mir geholfen haben, meine Arbeit anzufertigen. Durch euch hatte ich jedes Mal ein Lächeln im Gesicht, wenn ich über den Flur gegangen bin! Ein Dankeschön geht an Kathrin, die mir von Anfang an zur Seite stand und mich sowohl experimentell unterstützt hat, als auch immer ein offenes Ohr für mich hatte. Vielen Dank Reem für die vielen motivierenden Gespräche! Danke Viviane für deine wissenschaftlichen Ratschläge, besonders beim Erstellen dieser Arbeit. Danke Sonja für die vielen Gespräche und vielen Dank an Annika, die mich selbst in ihrer Elternzeit unterstützt und motiviert hat! Vielen Dank an Margitta für die Unterstützung bei der Blutaufarbeitung und herzlichen Dank an die gesamte AG Reinartz für die Unterstützung bei der Aufarbeitung der Patienten-Proben!

Als Nächstes möchte ich mich bei PD Dr. Till Adhikary bedanken. Vielen vielen Dank, dass deine Tür für mich immer offenstand! Danke für die unzähligen Gespräche, für die Unterstützung, die wertvollen Ratschläge und deine motivierenden Worte. Ich habe von dir sehr viel gelernt!

Zum Schluss möchte ich mich noch bei meiner Familie - besonders bei meiner Mutter - und meinen Freunden bedanken, die mich während der ganzen Zeit immer unterstützt haben. Sie haben mich ermutigt, an mich selbst zu glauben und nie aufzugeben.